TÉCNICO LISBOA

Technical and Economic Feasibility of Hydrogen Production Integrated into Waste-to-Energy Plants: the CTRSU case-study

Diansambo Zola Miguel Masembo

Thesis to obtain the Master of Science Degree in

Energy Engineering and Management

Supervisors: Prof. Ana Filipa da Silva Ferreira
Eng. Diana Fonseca Tomázio

Examination Committee

Chairperson: Prof. Duarte de Mesquita e Sousa
Supervisor: Prof. Ana Filipa da Silva Ferreira
Member of the Committee: Prof. Paulo Sérgio Duque de Brito

September 2022

Declaration

I declare that this document is an original work of my own authorship and that it fulfills all the requirements of the Code of Conduct and Good Practices of the Universidade de Lisboa.

Acknowledgements

First and above all, I would like to thank my Lord Jesus Christ, in whom, all the treasures of wisdom and knowledge abide, for the opportunity, the strength and the capacity to undertake this project and complete it satisfactorily.

I would certainly take great pleasure in acknowledging my gratitude to Valorsul and to Diana Tomázio for proposing me such an important project to work on, and for providing me with the necessary data and important guidance during the execution of this project.

I would also like to thank Prof. Ana Filipa for readily accepting the challenge of supervising my work, and taking great interest in assessing the progress of the work at different stages.

I am specially grateful to Cornerstone Bible College for showing support and for allowing me to complete my thesis defence while attending their institution.

Special thanks also to all friends and family for the encouragement and direct support along the master's degree program and during the thesis writing phase.

Resumo

A gestão de resíduos, além de ser um elemento essencial no desenvolvimento sustentável de qualquer localidade do mundo, também contribui significativamente na produção global de energia renovável quando é integrada com recuperação energética. No entanto, com as flutuações dos níveis de demanda, as centrais de energia sem tecnologias de armazenamento tendem a ficar em posição desvantajosa, pois a energia excedente pode ser desperdiçada quando a demanda é menor que a produção. Visto que o hidrogénio é considerado atualmente como uma das principais alternativas para enfrentar o problema do armazenamento de energia para apoiar a transição energética para fontes renováveis, nesta tese, são estudados dois cenários de produção de hidrogénio em uma central de tratamento de resíduos sólidos com valorização de energia. O cenário 1 considera a conversão da energia total produzida na central em hidrogénio, enquanto o cenário 2 considera apenas um terço da energia total. Em ambos os cenários são avaliadas duas tecnologias de eletrólise da água, nomeadamente eletrólise alcalina e células electrolisadoras de óxido sólido. A partir do estudo, sugere-se que produzir hidrogénio com um terço da eletricidade total é sempre mais rentável do que vender toda a eletricidade à rede. Além disso, produzir hidrogénio no cenário 1 é mais rentável do que vender toda a eletricidade à rede quando o preço da eletricidade é inferior a 90 €/MWh e mais rentável do que o cenário 2 quando o preço da eletricidade é inferior a 80 €/MWh, portanto, a partir deste preço o cenário 2 se torna o mais rentável. Em ambos os casos, a tecnologia SOEC é a mais lucrativa no cenário 1 e a eletrólise alcalina no cenário 2.

Palavras-chave: hidrogénio, eletrólise da água, alcalina, SOEC, conversão de resíduos em energia

Abstract

Waste management, apart from being an essential element in the sustainable development of any location in the world, also contributes significantly to the global renewable energy production levels when it is integrated with energy recovery. However, with the changes in demand levels, plants without energy storage technologies tend to be in a disadvantageous position as surplus power can be often wasted when the demand is lower than the supply. Since hydrogen is currently regarded as one of the main alternatives to tackle the problem of energy storage to support the energy transition into renewable sources, in this thesis, two scenarios of hydrogen production in a waste-to-energy plant are studied. Scenario 1 considers the conversion of the total energy produced at the plant into hydrogen, while scenario 2 considers only one-third of the total energy. In both scenarios, two water electrolysis technologies are assessed, namely alkaline electrolysis and SOEC. From the study, it is suggested that producing hydrogen with one-third of total electricity is always more profitable than selling all electricity to the grid. Moreover, producing hydrogen in scenario 1 is more profitable than selling all the electricity to the grid when the electricity price is lower than 90 C/MWh and more profitable than in scenario 2 when the electricity price is lower than 80 C/MWh, therefore, from this price onwards, scenario 2 becomes the most profitable one. In both situations, SOEC technology is the most profitable one in scenario 1 and alkaline electrolysis in scenario 2.

Keywords: green hydrogen, water electrolysis, alkaline, SOEC, waste-to-energy

Contents

1. Introduction 1
1.1. Motivation 1
1.2. Objectives 7
1.3. Thesis Outline 8
2. Hydrogen – An Energy Carrier 9
2.1. Water Electrolysis for Hydrogen Production 10
2.2. Storage Methods 19
3. Literature Review on Water Electrolysis Technologies 25
3.1. Water Electrolysis Costs 25
3.2. Technological Developments of Water Electrolysis 33
4. Waste-to-Energy for MSW treatment 38
4.1. Incineration of MSW 38
4.2. Characteristics of the CTRSU 41
5. Scenarios for Hydrogen Production in CTRSU 43
5.1. Scenario 1: Hydrogen Production Using the Total Energy from CTRSU 43
5.2. Scenario 2: Hydrogen Production Using One-third of Total Energy from CTRSU 52
5.3. Oxygen Selling Option 56
6. Results and Discussion 57
6.1. Hydrogen Production Cost 57
6.2. Selling Profits 60
6.3. Economic Feasibility of the Project 63
7. Concluding Remarks 71
7.1. Remarks for the Future 72
8. References 74

List of Figures

Figure 1 – Global shares of waste production by region [1]. 1
Figure 2 - Amount of waste production by region [1]. 1
Figure 3 - Waste management pathways [5]. 2
Figure 4 – EU waste hierarchy concept [8]. 3
Figure 5 - WtE incineration plants in Portugal [11]. 3
Figure 6 - Production of municipal waste (MW) in mainland Portugal, total and per capita [12]. 4
Figure 7 - Municipal waste per management operation in mainland Portugal, in 2020 [12]. 4
Figure 8 - Electricity produced from municipal waste in Portugal [13]. 5
Figure 9 - Variation of daily electricity prices (€/MWh) in the Portuguese market from January 2019 to July 2022 [15]. 6
Figure 10 – Thesis outline. 8
Figure 11 - Applications of Hydrogen ($H2$) in the United States energy system [19]. 9
Figure 12 - Illustration of an electrochemical cell. [27] 11
Figure 13 - Characteristics of the main electrolysis technologies. [28] 13
Figure 14 - A schematic flow diagram of alkaline water electrolysis [32]. 14
Figure 15 - Detailed process flow chart of alkaline water electrolysis [29]. 15
Figure 16 - Working principle of a PEM electrolysis cell [38]. 17
Figure 17 – Process flow chart of a PEM hydrogen production unit [29]. 17
Figure 18 - Solid oxide electrolysis cell principle for H2 production from water [38]. 18
Figure 19 - Electric, thermal and total energy demand for H2O electrolysis as a function of temperature [43]. 19
Figure 20 - Hydrogen density under different temperatures and pressure. [44] 20
Figure 21 - Hydrogen storage technologies categorisation [46]. 21
Figure 22 - Compilation of past and expected Alkaline (top) and PEM (bottom) electrolysis plant costs in €/kW. [66] 26
Figure 23 - CAPEX data comparison of PEM and Alkaline technologies as a function of power input (Data for Alkaline systems are based on a single stack of 2.13 MW consisting of 230 cells, 2.6 $m2$ in size. The change in slope for Alkaline electrolysers corresponds to the use of multi-stack systems). [66] 27
Figure 24 - CAPEX reduction when using multi-stack systems, both for PEM (a) and Alkaline (b) electrolysers. [66] 28
Figure 25 - Breakdown of the total installed costs for 1 GW green hydrogen plant based on Alkaline technology. [68] 30

Figure 26 - Breakdown of the total installed costs for 1 GW green hydrogen plant based on PEM technology. [68] 31
Figure 27 - Relative impact of R&D funding and production scale-up (R&D, RD&D) on capital costs. [69] 32
Figure 28 - Breakdown of the total installed costs of hydrogen plant based on SOEC technology. [70] 33
Figure 29 - Predominant MSW treatments in EU [87]. 38
Figure 30 - Flowchart schematic of a WtE incineration plant [89]. 39
Figure 31 – Example of a MSW incinerator scheme in urban areas in Japan [92]. 40
Figure 32 - a) System based on bleeding condensing turbine (b) System based on backpressure turbine [88]. 41
Figure 33 - Process flowchart of A3880 electrolysis system [99]. 44
Figure 34 – 3D Plant set up of A3880 [99]. 44
Figure 35 - Topsoe SOEC unit process model [108]. 48
Figure 36 - SUNFIRE-HYLINK SOEC representation [111]. 54
Figure 37 - Hydrogen production costs, scenario 1: a) alkaline case; b) SOEC case 58
Figure 38 - Hydrogen production costs, scenario 2: a) alkaline case; b) soec case. 59
Figure 39 - Hydrogen production costs in all scenario cases. 60
Figure 40 - Profits and specific costs of hydrogen production, scenario 1: alkaline case. 61
Figure 41 - Profits and specific costs of hydrogen production, scenario 1: SOEC case. 61
Figure 42 - Profits and specific costs of hydrogen production, scenario 1: alkaline case 62
Figure 43 - Profits and specific costs of hydrogen production, scenario 2: SOEC case 62
Figure 44 - Comparison of Profits between the two scenarios. 63
Figure 45 – LCOH scenario 1: a) alkaline case; b) SOEC case 65
Figure 46 – LCOH scenario 2: a) alkaline case; b) SOEC case. 65
Figure 47 – LCOH curves from all scenarios and cases. 66
Figure 48 – NPV scenario 1: a) alkaline case; b) SOEC case. 67
Figure 49 - NPV scenario 2: a) alkaline case; b) SOEC case. 67
Figure 50 – NPV from all scenarios and cases. 68
Figure 51 – IRR scenario 1: a) alkaline case; b) SOEC case. 69
Figure 52 – IRR scenario 2: a) alkaline case; b) SOEC case. 69
Figure 53 – Comparison of all IRR values. 70

List of Tables

Table 1 - Physical properties of hydrogen [20]. 10
Table 2 - Current state of SOFC and SOEC technology [83]. 36
Table 3 – Energy production data at CTRSU from the year 2019 [97]. 43
Table 4 - Key specifications of the A3880 [99]. 45
Table 5 - Production and consumption rates. 46
Table 6 - Capital and operational costs rates for scenario 1: alkaline case. 47
Table 7 - CAPEX and OPEX for the A3880 system with 17 stack modules. 48
Table 8 - Key specifications of the Topsoe SOEC electrolyser system [108]. 49
Table 9 – SOEC system characteristics sized according to CTRSU energy specifications. 49
Table 10 - Steam and energy usage ratio for SOEC. 50
Table 11 - Production rates for scenario 1, SOEC case. 50
Table 12 - Capital and operational costs rates for scenario 1: SOEC case. 51
Table 13 - CAPEX and OPEX for the Topsoe SOEC. 51
Table 14 – Energy values for scenario 2. 52
Table 15 - Production and consumption rates for scenario 2: alkaline case. 52
Table 16 - CAPEX and OPEX for the A3880 system with 6 stack modules. 53
Table 17 - Key specifications of the SUNFIRE-HYLINK SOEC electrolyser system [111]. 54
Table 18 – SOEC system characteristics sized according to CTRSU energy specifications. 54
Table 19 - Steam and energy usage ratio for SOEC, scenario 2. 55
Table 20 - Production rates for scenario 2, SOEC case. 55
Table 21 - CAPEX and OPEX for the SUNFIRE-HYLINK SOEC. 55
Table 22 - Capital and operational costs rates for O_2 liquefaction and storage. 56

List of Abbreviations

AC	Alternating Current
CAPEX	Capital Expenditure
CHP	Combined Heat and Power
CTRSU	Centro de Tratamento de Resíduos Sólidos Urbanos
DC	Direct Current
EU	European Union
GHG	Greenhouse Gas
H2	Hydrogen
HHV	Higher Heating Value
HTGR	High-Temperature Gas-cooled Reactor
IEA	International Energy Agency
IRC	Imposto sobre Pessoas Colectivas
IRENA	International Renewable Energy Agency
IRR	Internal Rate of Return
KOH	Potassium Hydroxide
LCOH	Levelised Cost of Hydrogen
LFL	Lower Flammable Limit
LHV	Lower Heating Value
MIBEL	Mercado Ibérico de Electricidade
MSW	Municipal Solid Waste
MW	Municipal Waste
NASA	The National Aeronautics and Space Administration
NGNP	Next Generation Nuclear Plant
NPV	Net Present Value
NTP	Normal Temperature and Pressure
O2	Oxygen
OPEX	Operational Expenditure
PEM	Proton Exchange Membrane
PLC	Programmable Logic Controller
SCC	Secondary Combustion Chamber
SMR	Steam Methane Reforming
SOEC	Solid Oxide Electrolysis Cell
SOFC	Solid Oxide Fuel Cell

STP Standard Temperature and Pressure

UFL Upper Flammable Limits

USD United States Dollar

1. Introduction

1.1. Motivation

Waste production is a general phenomenon that can be observed in every part of the world. Its degree of generation may vary according to different factors such as urbanisation, economic development, and population growth [1]. Waste generation is also proportional to the level of participation of the countries and cities in the global trades and the creation of more products and services. Therefore, regions that combine high levels of urbanisation, economic development and population growth tend to have higher global share percentages of waste generation, as shown in the data recorded in 2018 by the World Bank Group, regarding the global production of municipal solid waste (MSW) (Figure 1 and Figure 2).

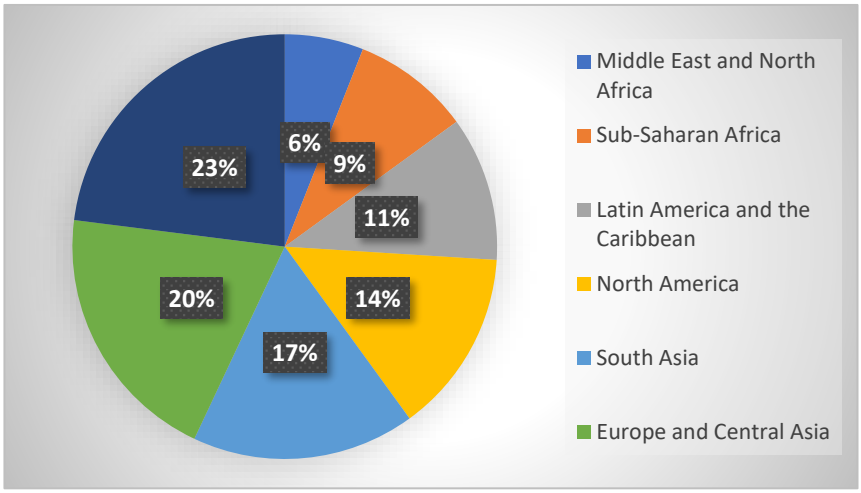

Figure 1 – Global shares of waste production by region *[1]*.

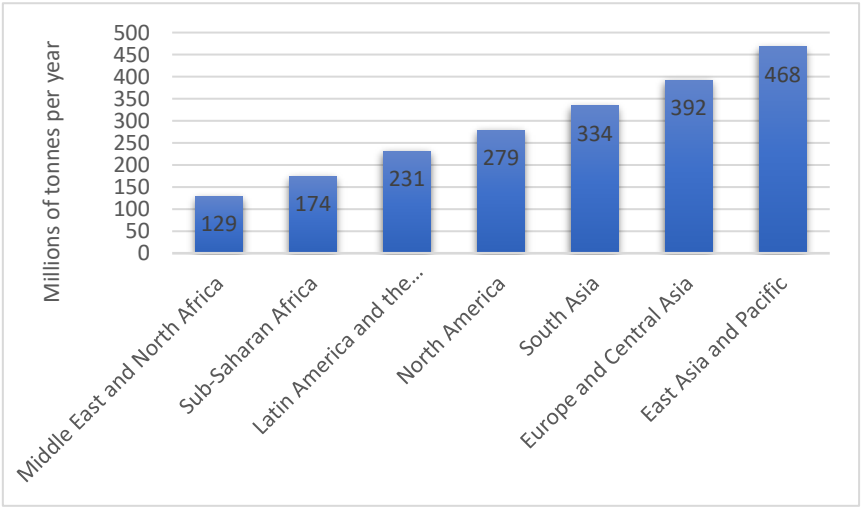

Figure 2 - Amount of waste production by region *[1]*.

In many parts of the world, MSW is disposed in open dumps (unloading of waste in the ground), controlled landfills (grounding the waste without soil sealing), or sanitary landfills (confinement and compaction of waste with consequent reduction of area and volume) [2], but these alternatives are causes of soil, water, and air pollution. Most recent research studies have been looking into waste valorisation options such as methods to turn waste into energy, fuels, and other value-added products to tackle MSW management challenges related to reducing pollution emissions, achieving technical and financial feasibility, and moving towards a circular economy [3], [4]. Three main MSW management pathways are currently considered, including disposal, energy recovery, and finally recycling.

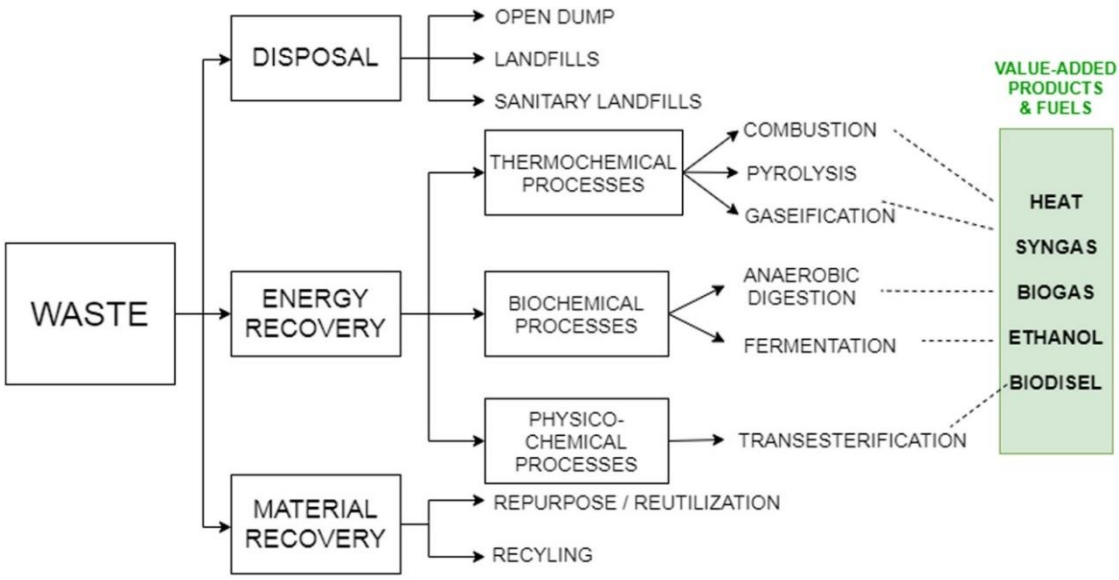

Figure 3 - Waste management pathways *[5]*.

Waste-to-energy (WtE) process, as a renewable energy source, is estimated a contribute significantly to the sustainable management of MSW globally. It is expected that a reduction of around 10–15% in the global GHG emissions can be reached through improved solid waste management (recycling, waste diversion from landfill and energy recovery from waste) [6].

The EU has enacted comprehensive legislation with goals and targets to improve waste management while also lowering GHG emissions and negative health and environmental impacts. The concept of a hierarchy of waste management options, which includes a legally binding prioritisation of waste management activities, has been developed in the EU. Essentially, waste prevention is the most desirable option, followed by material recovery and recycling (metal, glass, paper recycling, or organic waste composting), energy recovery from waste (through incineration, or digestion of

biodegradable wastes), and finally disposal (landfilling), with no material or energy recovery as the least desirable option [7].

Figure 4 – EU waste hierarchy concept *[8]*.

MSW Management in Portugal

Europe is estimated to have 582 WtE plants, with Germany, France and UK being at the leading front [9], while Portugal has three plants distributed along the country [10].

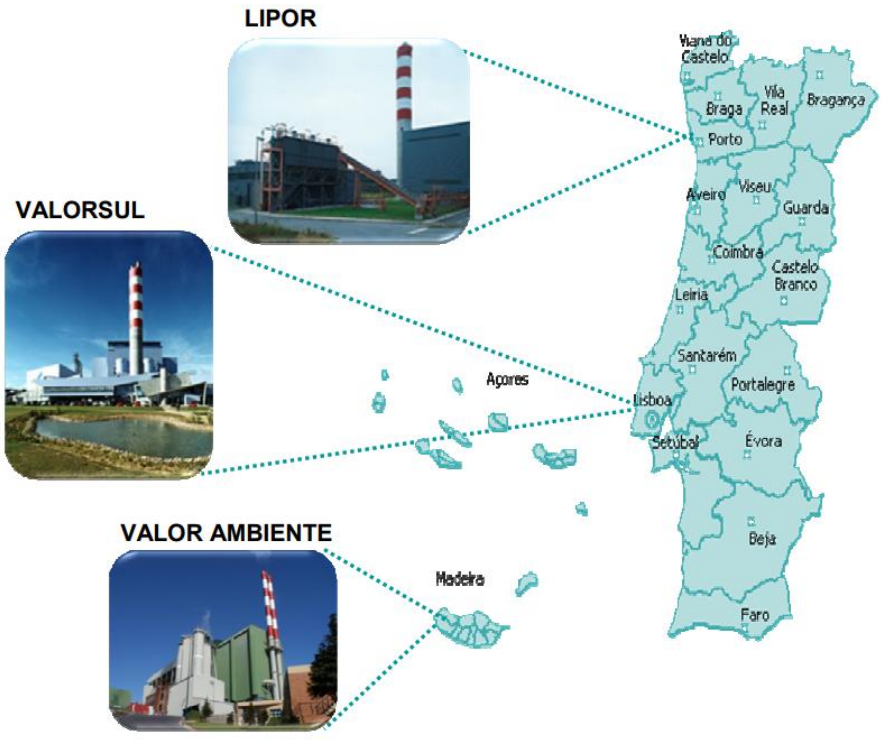

Figure 5 - WtE incineration plants in Portugal *[11]*.

In 2020, the total production of municipal waste (MW) registered in mainland Portugal was around 5.01 million tonnes (more 0.1% than in 2019) which points to an annual capitation of 512 kg/(inhab.year), i.e. a daily MW production of 1.40 kg per inhabitant. These values show a stabilisation in MW production compared to 2019, turning the growth trend seen since 2014, although, these values may be affected by the situation of the pandemic that started in March 2020, leading to lower consumption by Portuguese families, since the imposition of lockdowns [12].

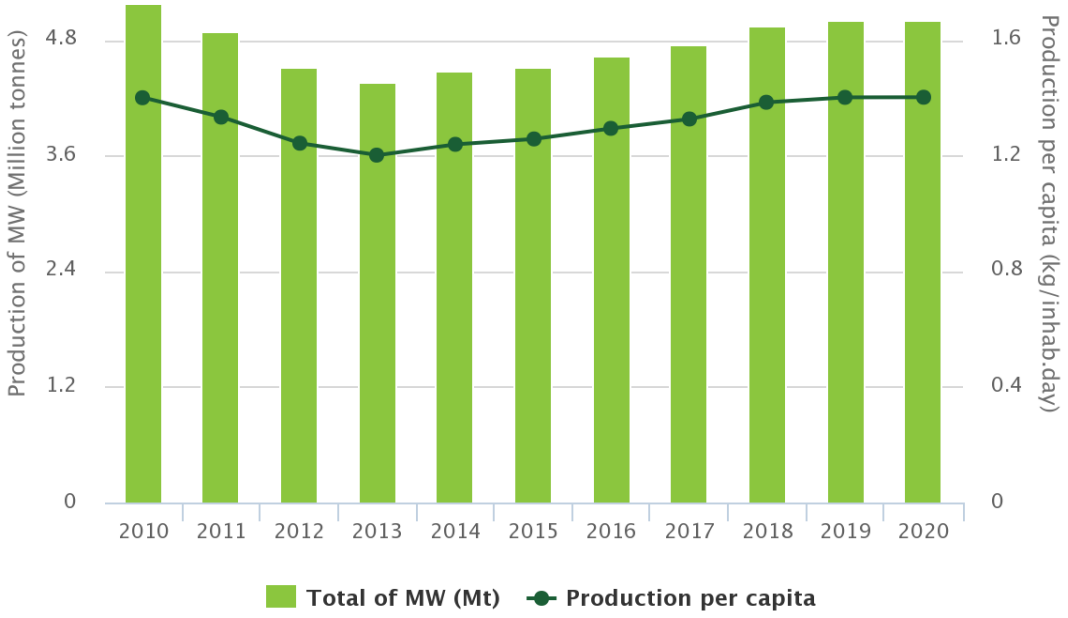

Figure 6 - Production of municipal waste (MW) in mainland Portugal, total and per capita *[12]*.

Of the total MW generated in 2020, in the Portugal mainland, about 41% was sent to landfill and 19% was directed for energy recovery and other fractions for different types of waste treatments.

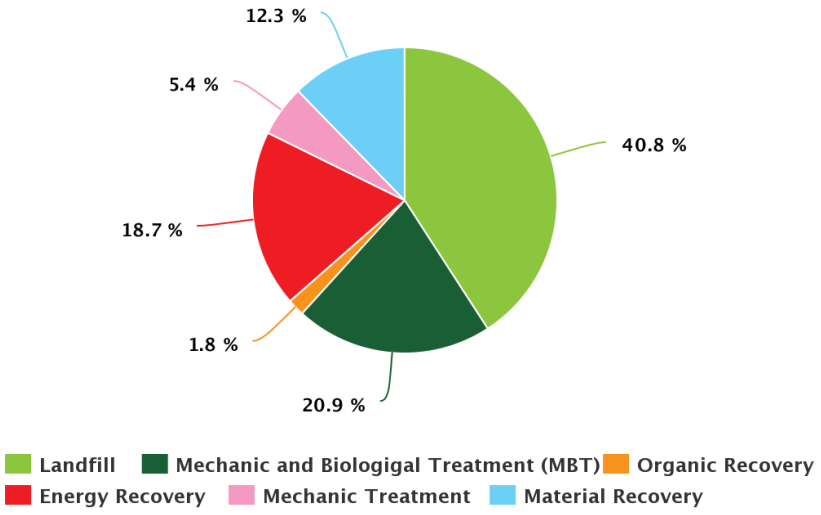

Figure 7 - Municipal waste per management operation in mainland Portugal, in 2020 *[12]*.

According to the data from IEA (International Energy Agency), in 2020, around 325 GWh of electricity was produced from the conversion of MSW into energy in Portugal. Figure 8 indicates significant growth in production level in 2020 compared to the past 20 years.

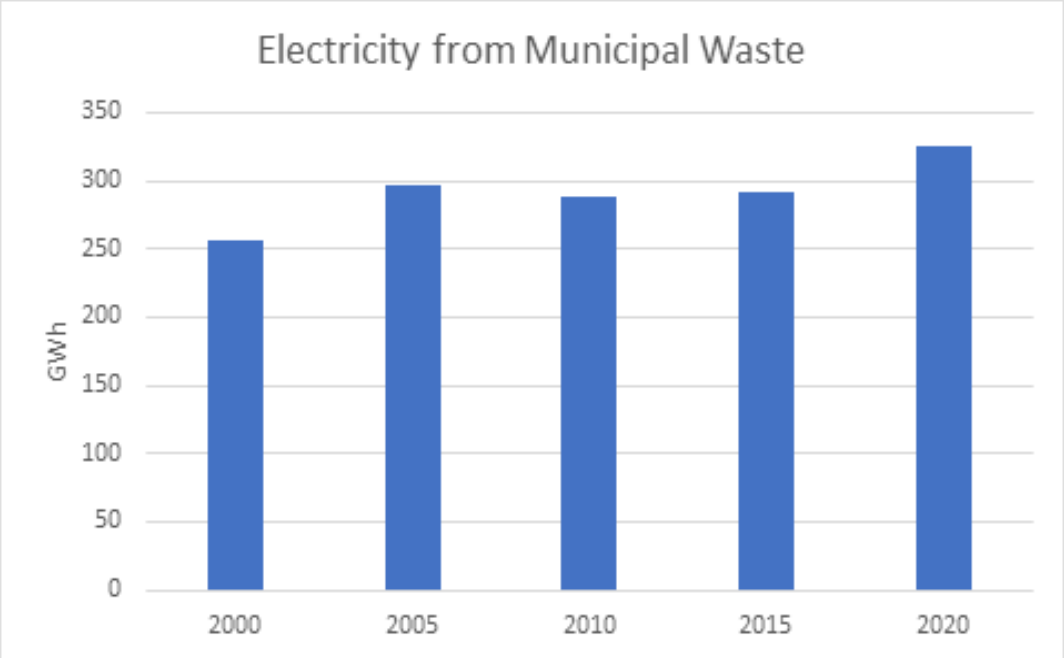

Figure 8 - Electricity produced from municipal waste in Portugal *[13]*.

Electricity in MIBEL

The Iberian Electricity Market, also known as MIBEL, was created in 2007 to integrate both the Portuguese and the Spanish electrical systems, creating a legal, economic and regulatory convergence of the two markets to allow electricity trading between entities in Spain or Portugal [14].

In MIBEL, electricity is traded on the daily market, which aims to operate the transactions by submitting bids and sales by all market players for 24 hours the next day, since energy prices are set for the following day, every day at noon.

Nevertheless, electricity prices can be volatile to several factors, such as the rise or fall of fossil fuels prices, CO_2 prices, or even natural events such as lack of rain that may affect hydroelectricity production as well as political conflicts that affect the global or regional trading of energy commodities.

Figure 9 - Variation of daily electricity prices (€/MWh) in the Portuguese market from January 2019 to July 2022 *[15]*.

Towards the end of the year 2021, the prices increased due to the situation of conflict between Russia and Ukraine, which directly affected the supply of natural gas and other resources to the EU market.

Because of the frequent fluctuations of electricity prices, energy producers such as WtE plants ought to look at energy storage alternatives to ensure the technical and economical sustainability of their businesses, considering scenarios when the prices are low and/or high in the market.

Several types of energy storage are currently being studied in the literature for electrical energy storage [16] such as:

- Mechanical energy storage: flywheel, pumped hydro, gravity, compressed air.
- Chemical energy storage: hydrogen, biofuel, biodiesel.
- Electrochemical energy storage: supercapacitor, batteries.
- Superconducting magnetic energy storage.
- Cryogenic energy storage: liquid air energy storage.

Amongst the chemical storage options, hydrogen is currently highly rated, as it is transportable, highly versatile, efficient, a clean energy carrier, and has a high energy density [16].

The Portuguese government published a draft of the National Strategy for Hydrogen (EN-H_2) in 2020, based on the path and discussion regarding the National Energy and Climate Plan 2021-2030 (PNEC 2030) [17]. This strategy seeks to promote the gradual introduction of hydrogen as a sustainable framework, as part of a broader strategy of transition to a decarbonized economy.

Simultaneously, it claims to provide a solid framework as well as short, medium, and long-term visions to all corporates and promoters of hydrogen projects [17]. EN-H_2 establishes the following strategy:

POWER-TO-GAS (P2G): Hydrogen may be directly injected into the natural gas grid or converted into synthetic methane via a methanation process.

POWER-TO-MOBILITY (P2M): Hydrogen is transported or locally produced to provide vehicle filling stations, with a particular focus on heavy transportation, railway (on non-electrified lines), taxis, fleets of companies and shared mobility, and ships.

POWER-TO-INDUSTRY (P2I): To reduce GHG emissions, natural gas is replaced by hydrogen in the industrial sector, namely in those that use high temperatures (e.g.: steel and cement industry).

POWER-TO-POWER (P2P): Stored hydrogen obtained from the excess of renewable electricity can be reconverted again to electricity using fuel cells or gas plant turbines properly adapted and converted for this purpose.

POWER-TO-SYNFUEL (P2FUEL): The production of fuels could be decarbonized, replacing them with synthetic fuels of renewable origin.

In this thesis work, a technical and economic analysis will be carried out to assess the feasibility of producing hydrogen gas from electricity at the WtE plant of Valorsul in Lisbon, Portugal.

1.2. Objectives

The main objectives of this feasibility study are the following:

- Investigate the state-of-the-art CAPEX values for low-temperature and high-temperature water electrolysis technologies, and their technological development state through a literature review.
- Understand the working principle of the main water electrolysis technologies for hydrogen production, their advantages and downsides, and applicability.
- Understand the current state of municipal solid waste management with energy recovery as well as the functional characteristics of the waste-to-energy plant (CTRSU) run by Valorsul, in Lisbon, Portugal.
- Assess the feasibility of producing hydrogen from the energy produced at CTRSU in different case scenarios.

1.3. Thesis Outline

The diagram in Figure 10 – Thesis outline Figure 10 provides an illustrative guideline to facilitate the comprehension of this thesis work. Chapters are shown connected by arrow, and the main elements addressed in the chapters are mentioned in their respective attached box.

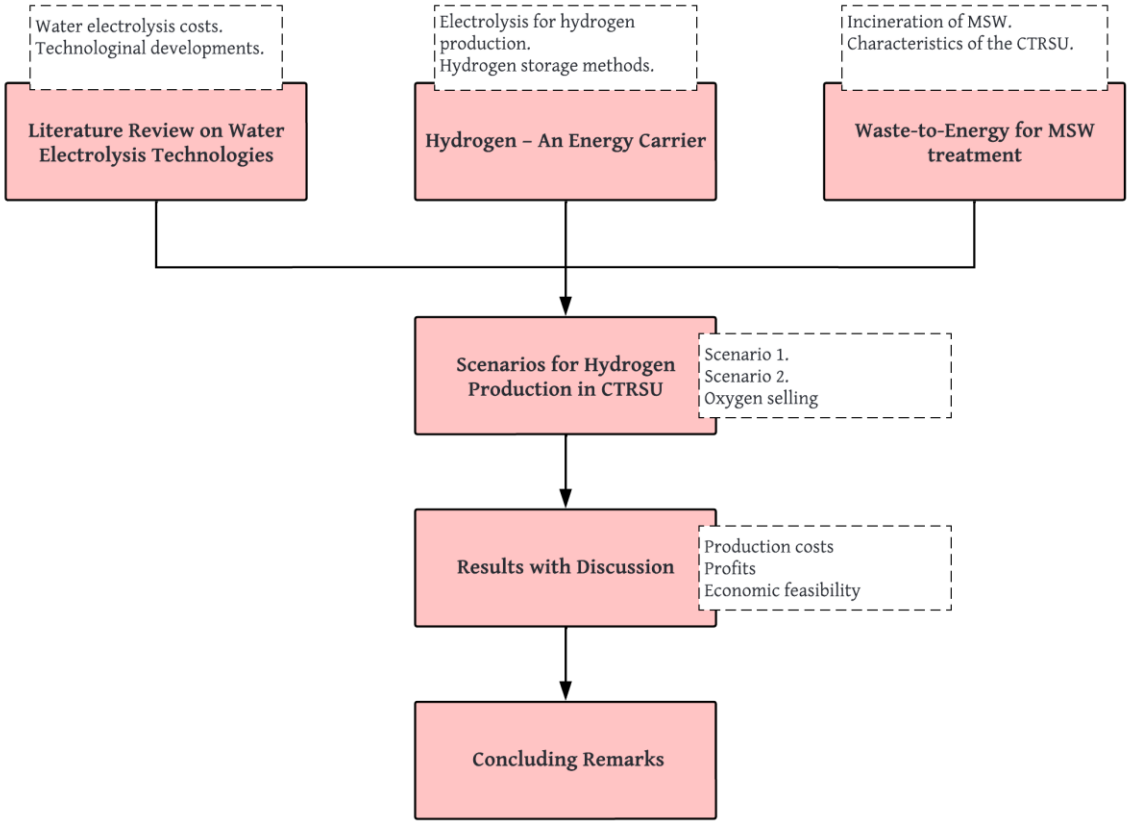

Figure 10 – Thesis outline.

2. Hydrogen – An Energy Carrier

Hydrogen is not a source of energy, but rather a versatile energy carrier with a high heating value. Although hydrogen is abundant in nature, energy is required to produce pure hydrogen. It offers a wide range of end-use applications and the potential to reduce CO_2 emissions in the energy sector, hence minimizing global warming [18].

Hydrogen can be used to balance the electricity network during peak times and store surplus electric energy by generating hydrogen gas to be used in various applications, as shown in Figure *11*.

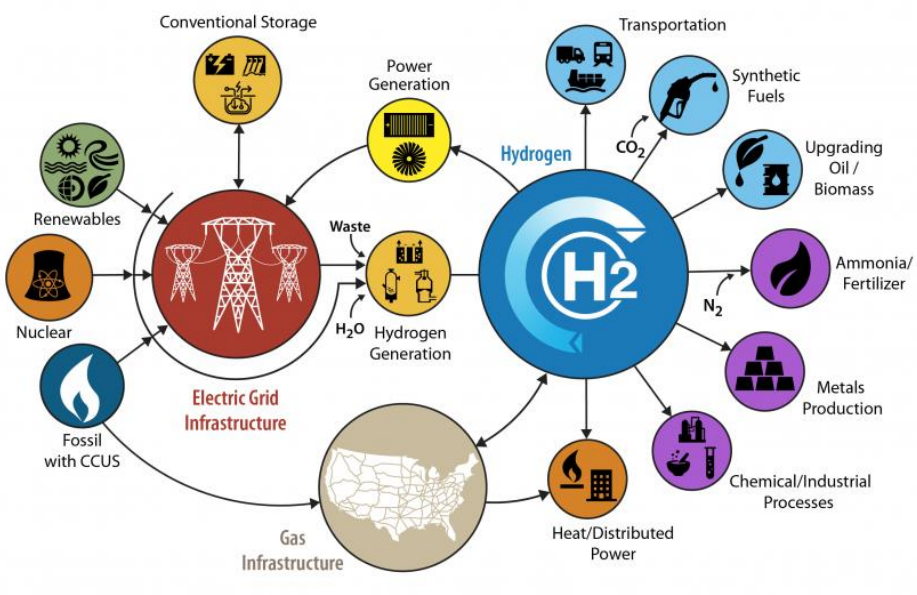

Figure 11 - Applications of Hydrogen (H_2) in the United States energy system *[19]*.

At standard temperature and pressure, hydrogen is a colourless, odourless, and tasteless non-toxic gas (STP, 273.15 K and 1 atm). Hydrogen has a high energy content, with a higher heating value (HHV) of 142 $\mathrm{MJ/kg}$ and a lower heating value (LHV) of 120 $\mathrm{MJ/kg}$ (LHV). The molar enthalpy of water vaporization (44.01 $\mathrm{kJ/mol}$) is the difference between high and low heating values [20]. Table *1* shows the important physical properties of hydrogen.

Hydrogen has a wide flammability range in air, ranging from 4 to 74%, but as long as it is kept in a well-ventilated area, there is no danger of exceeding this limit [21]. However, as the temperature rises, so do the limits. Furthermore, for stoichiometric hydrogen in air, the autoignition temperature is relatively high (773-850 K) [22]. The temperature of autoignition varies in the literature because it is affected by system factors. Because of its low density, hydrogen is safe because it does not collect near the ground but also, in the event of a leak, dissipates quickly in the air [20].

Table 1 - Physical properties of hydrogen *[20]*.

Heating Values	HHV: 142 $\mathrm{MJ/kg}$ (39.4 $\mathrm{kWh/kg}$) LHV: 120.0 $\mathrm{MJ/kg}$ (33.3 $\mathrm{kWh/kg}$)
Density	0.0899 $\mathrm{kg/m^3}$
Boiling point	20.27 K
Melting point	13.99 K
Lower and upper flammability limits	LFL: 4%; UFL: 75%
Autoignition temperature	773 - 850 K [22]

When pressure and temperature change, a special property of hydrogen, the negative Joule-Thomson coefficient, must be considered. In contrast to normal air, hydrogen heats up when it expands. Only below 202 K does hydrogen exhibit a typical Joule-Thomson effect [23].

2.1. Water Electrolysis for Hydrogen Production

For decades, electrochemical hydrogen production has been studied extensively, mostly due to the potential to reduce environmental impact, meet distributed demand, lower hydrogen costs, and improve public perception. These methods, which are an alternative to steam methane reforming for hydrogen production, have regained popularity in recent years. Renewable energy sources account for around 5% of total hydrogen generation [24].

Electrolysis is the process of splitting water into hydrogen and oxygen using electricity. This reaction takes place in a cell unit known as an electrolyser. Electrolysers can range in size from small, appliance-sized equipment suitable for small-scale distributed hydrogen production to large-scale, central production facilities that could be directly connected to renewable or other non-GHG-emitting forms of electricity production [25].

The splitting happens in two partial reactions that occur at the two electrodes – cathode (-) and anode (+) – in the electrolysis cell. Electrolysers, also known as stacks, are made of several interconnected electrolysis cells. [26] At a certain applied voltage, known as critical voltage, hydrogen gas is produced at the negatively biased electrode and oxygen gas is produced at the positively biased electrode. The current that passes through the electrochemical cell determines the quantity of gases produced per unit of time [27].

Since there is always a certain percentage of ionic species found in water, $\mathrm{H^+}$and $\mathrm{OH^-}$ are represented in the equilibrium equation:

$$H_2O(l) \rightleftarrows H^+(aq) + OH^-(aq)$$

The electrolysis of water can produce oxygen and hydrogen gas at noble metal electrodes:

positive electrode (anode): $4OH^- \leftrightarrow H_2O(l) + O_2 + 4e^-$

negative electrode (cathode): $2H^+(aq) + 2e^- \leftrightarrow H_2(g)$

The reactions at the electrode interface differ slightly depending on whether the water is acidic or basic. Because there are no side reactions in water electrolysis that could produce undesirable byproducts, the net balance is:

$$2H_2O \rightarrow (4e^-) \rightarrow O_2 + 2H_2$$

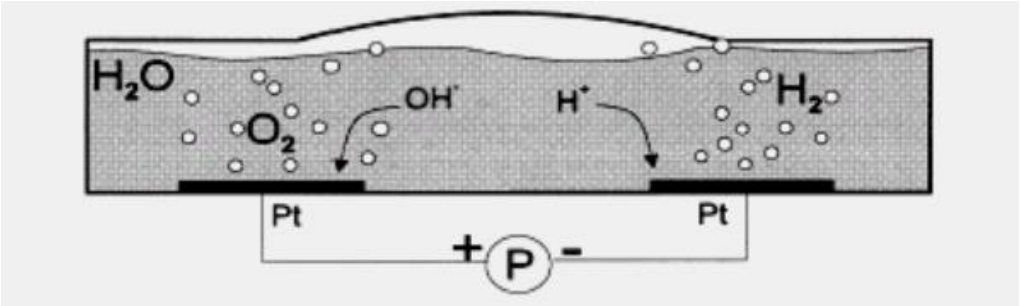

Figure 12 - Illustration of an electrochemical cell. *[27]*

Under standard conditions (P, T constant), the minimum necessary cell voltage for the start-up of electrolysis, E°_{cell}, is given by the equation:

$$E^\circ_{cell} = \frac{-\Delta G^\circ}{nF} \quad (1)$$

Where ΔG° is the change in Gibbs free energy under standard conditions, and n is the number of electrons transferred. Because the change in the cell volume is smaller than the change in pressure, the conditions in a closed electrochemical cell differ slightly from standard conditions, open cell $(P, T) = \text{constant}$ to closed cell $(V, T) = \text{constant}$. Hence, instead of ΔG°, ΔA° – free energy (Helmholtz) is used.

The voltage required for an electron to break through the Helmholtz energy barrier is as follows:

$$E^{\circ}_{cell} = \frac{-\Delta A^{\circ}}{nF} \quad (2)$$

$$\Delta A^{\circ} = \Delta H^{\circ} - TR\Delta n - T\Delta S^{\circ} \quad (3)$$

To initiate a reaction, an (extra) energy barrier known as activation energy, E_{act}, must be overcome. The controlling agent of the reaction rate, r, is the number of molecules able to overcome this barrier, and it is given by the statistical Maxwell-Boltzman relation, which has an exponential behaviour: $r \sim r_o \exp(-E_{act}/RT)$. Therefore, the activation energy represents the rate at which a reaction occurs.

The following equation defines the maximum possible efficiency of an ideal closed electrochemical cell:

$$\varepsilon_{max} = \frac{\Delta H^{\circ}}{\Delta A^{\circ}} = -\frac{\Delta H^{\circ}}{nFE^{\circ}_{cell}} \quad (4)$$

However, in reality, the efficiency of an electrochemical cell is determined by:

$$\varepsilon_{real} = -\frac{\Delta H^{\circ}}{nF\Delta E^{\circ}_{elec}} \quad (5)$$

Where ΔE°_{elec} is the voltage to drive the electrochemical cell at current, I:

$$\Delta E^{\circ}_{elec} = \Delta A^{\circ} + IR + \Sigma\eta \quad (6)$$

Where R denotes the total ohmic series resistance in the cell, which includes external circuit resistance, electrolyte, electrodes, and membrane material; and $\Sigma\eta$ is the sum of the overpotentials (activation overpotential at the two electrodes, and the concentration overpotential due to the mass transport of the gaseous products away from the anode and cathode surfaces).

Charge equalisation occurs between the two partial reactions via ion conduction through an electrolyte (which is an electrically conductive substance). A membrane is also required to separate

the two reactions spatially and prevent the product gases from mixing. In different electrolysis technologies, the ion charge and the type of electrolyte differ [26].

Various electrochemical technologies can be used to produce hydrogen, including proton exchange membrane (PEM), Alkaline, and a high-temperature electrolysis process, Solid Oxide Electrolysis Cells (SOEC) [26].

These systems use various materials and operating conditions, but the operating principles are the same. Low and high-temperature water electrolysis are also possible based on different operating temperatures [28].

	Low Temperature Electrolysis			High Temperature Electrolysis		
	Alkaline (OH^-) electrolysis		Proton Exchange (H^+) electrolysis	Oxygen ion(O^{2-}) electrolysis		
	Liquid	Polymer Electrolyte Membrane		Solid Oxide Electrolysis (SOE)		
	Conventional	Solid alkaline	H^+ - PEM	H^+ - SOE	O^{2-} - SOE	Co-electrolysis
Operation principles	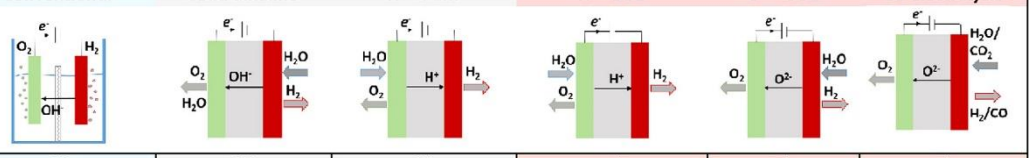					
Charge carrier	OH^-	OH^-	H^+	H^+	O^{2-}	O^{2-}
Temperature	20-80°C	20-200°C	20-200°C	500-1000°C	500-1000°C	750-900°C
Electrolyte	liquid	solid (polymeric)	solid (polymeric)	solid (ceramic)	solid (ceramic)	solid (ceramic)
Anodic Reaction (OER)	$4OH^- \rightarrow 2H_2O + O_2 + 4e^-$	$4OH^- \rightarrow 2H_2O + O_2 + 4e^-$	$2H_2O \rightarrow 4H^+ + O_2 + 4e^-$	$2H_2O \rightarrow 4H^+ + 4e^- + O_2$	$O^{2-} \rightarrow {}^1/_2O_2 + 2e^-$	$O^{2-} \rightarrow {}^1/_2O_2 + 2e^-$
Anodes	Ni > Co > Fe (oxides) Perovskites: $Ba_{0.5}Sr_{0.5}Co_{0.8}Fe_{0.2}O_{3-\delta}$, $LaCoO_3$	Ni-based	IrO_2, RuO_2, $Ir_xRu_{1-x}O_2$ Supports: TiO_2, ITO, TiC	Perovskites with protonic-electronic conductivity	$La_xSr_{1-x}MnO_3$ + Y-Stabilized ZrO_2 (LSM-YSZ)	$La_xSr_{1-x}MnO_3$ + Y-Stabilized ZrO_2 (LSM-YSZ)
Cathodic Reaction (HER)	$2H_2O + 4e^- \rightarrow 4OH^- + 2H_2$	$2H_2O + 4e^- \rightarrow 4OH^- + 2H_2$	$4H^+ + 4e^- \rightarrow 2H_2$	$4H^+ + 4e^- \rightarrow 2H_2$	$H_2O + 2e^- \rightarrow H_2 + O^{2-}$	$H_2O + 2e^- \rightarrow H_2 + O^{2-}$ $CO_2 + 2e^- \rightarrow CO + O^{2-}$
Cathodes	Ni alloys	Ni, Ni-Fe, $NiFe_2O_4$	Pt/C MoS_2	Ni-cermets	Ni-YSZ Subst. $LaCrO_3$	Ni-YSZ perovskites
Efficiency	59-70%		65-82%	up to 100%	up to 100%	-
Applicability	commercial	laboratory scale	near-term commercialization	laboratory scale	demonstration	laboratory scale
Advantages	low capital cost, relatively stable, mature technology	combination of alkaline and H^+-PEM electrolysis	compact design, fast response/start-up, high-purity H_2	enhanced kinetics, thermodynamics: lower energy demands, low capital cost		+ direct production of syngas
Disadvantages	corrosive electrolyte, gas permeation, slow dynamics	low OH^- conductivity in polymeric membranes	high cost polymeric membranes; acidic: noble metals	mechanically unstable electrodes (cracking), safety issues: improper sealing		
Challenges	Improve durability/reliability; and Oxygen Evolution	Improve electrolyte	Reduce noble-metal utilization	microstructural changes in the electrodes: delamination, blocking of TPBs, passivation		C deposition, microstructural change electrodes

Figure 13 - Characteristics of the main electrolysis technologies. *[28]*

Alkaline Water Electrolysis

Alkaline water electrolysis works at a low temperature (60–80 °C), with KOH and/or NaOH aqueous solution as the electrolyte, and the electrolyte concentration ranges from 20% to 30% [28]. The diaphragm in an alkaline electrolyser is made of asbestos, and the electrode is made of nickel materials [29]. The generated hydrogen is approximately 99% pure; nevertheless, an alkali fog in the gas must be removed, which is most often carried out through desorption [28]. The operating

current density of an alkaline electrolyser is between $200\ \mathrm{mA/cm^2}$ and $400\ \mathrm{mA/cm^2}$ with the working pressure around 3.2MPa [29], and the power consumption for H_2 production is around $4.5 - 5.5\ \mathrm{kWh/Nm^3}$ with a 60% efficiency [28]. The pressure between the anode and cathode sides must be balanced to prevent hydrogen/oxygen from penetrating the porous asbestos diaphragm and risking an explosion [28].

Furthermore, alkaline electrolysers take a long time to start up and have a slow loading response [28]. Alkaline electrolysers are difficult to adapt to the variable nature of renewable energy sources because of the lengthy start-up preparation [30]. As a result, alkaline electrolysers are normally applied with a constant power source.

Alkaline Electrolysis System

The electrolyte is pumped through an electrolysis stack, which produces product gases. While natural convection can be a cost-effective option, covering the electrode surface with gas can elevate the required cell voltage and thus increase operational costs [31]. Furthermore, most alkaline water electrolyser systems include temperature control for the electrolyte to ensure that it stays within a safe temperature range [32].

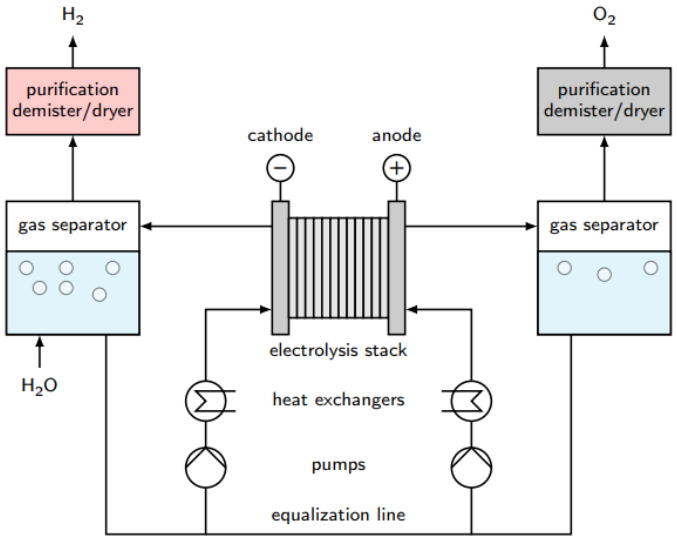

Figure 14 - A schematic flow diagram of alkaline water electrolysis *[32]*.

Adjacent gas separators divide phases, and the liquid phase returns to the electrolysis stack. Heat exchangers maintain the optimal temperature, and the product gases can then be purified [32]. After leaving the electrolysis cell, the two-phase mixtures of liquid electrolyte and product gas pass through gas separators. The phase separation is usually achieved in large tanks with a long residence time. Before being purified to the desired level, the product gas is demisted and dried [33].

The liquid electrolyte is reinjected to the electrolysis stack from the gas separator. Since the product gases are soluble in the electrolyte solution, mixing the two electrolyte cycles results in gas impurities and losses. A partially separated electrolyte cycle with an equalisation line for liquid level balancing of both vessels can be used as an alternative [34], [35]. The electrolyte concentration will rise on the cathodic side due to water consumption and fall on the anodic side due to water production with separated electrolyte cycles. As a result, mixing the electrolyte is required on occasion to maintain optimal electrolyte conductivity [32].

The alkaline water hydrogen production unit is made up of three major components: an alkaline water hydrogen production system, a control cabinet, and a rectifier cabinet. An alkaline water hydrogen generator consists of an alkaline electrolyser, a hydrogen separator, an oxygen separator, a gas cooler, a lye circulating pump, a lye cooler, a water storage tank, an alkali tank, control valves, and other components.

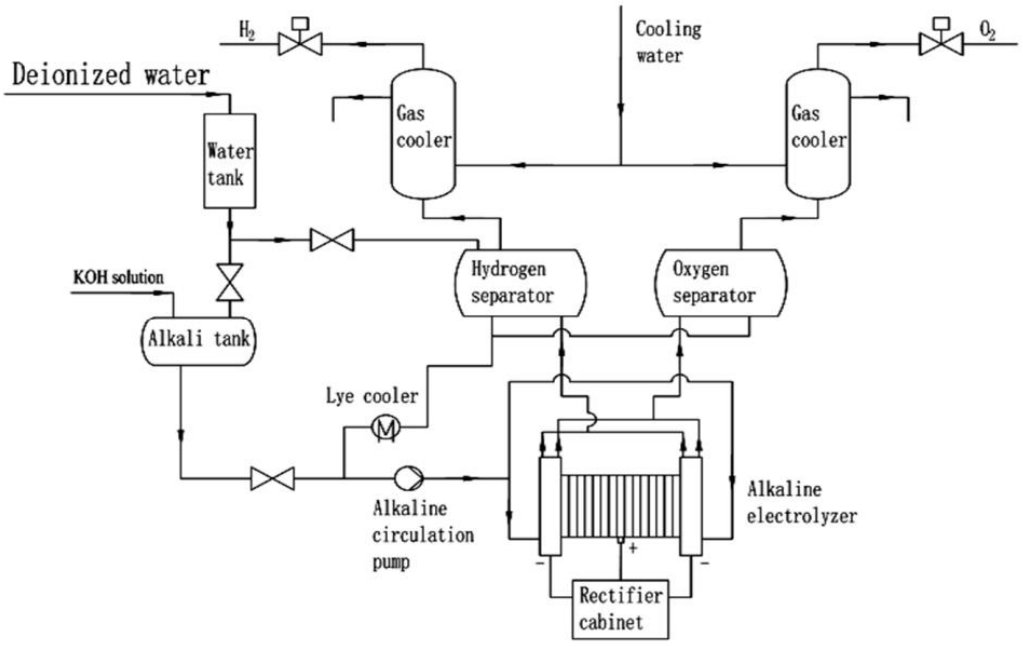

Figure 15 - Detailed process flow chart of alkaline water electrolysis *[29]*.

Once the equipment is started, the electrolyte is mixed thoroughly in the alkali tank before being pumped into the electrolytic tank and entering the entire hydrogen production system. The lye inlet valve is closed, and the power is turned on once the liquid in the separator reaches the specified liquid level. After the alkali solution has been electrolyzed in the alkaline electrolyser, the hydrogen separator and the oxygen separator are introduced in a gas-liquid mixed state from the hydrogen side of the electrolyser and the oxygen side outlet, respectively. The gas is discharged after it has

been cooled from the upper part of the separator. The liquid circulates after merging into the bottom of the separator.

Because water is reduced during electrolysis, it is necessary to refill water into the hydrogen separator regularly. Simultaneously, the specific gravity of the alkali solution must be checked regularly, and the alkali solution must be refilled. Because the alkaline electrolyser can only operate at the same pressure, the hydrogen generator must be gradually pressurized to the set pressure by the regulating valve at the start, resulting in a 1-hour start-up time [29].

PEM Electrolysis

PEM electrolysers, developed for the first time by General Electric in the 1960s, are more expensive than alkaline electrolysers and, due to their recent introduction to the market, have less developed technology [21]. These electrolysers were developed for both the needs of the civil industry and for use in specialised applications (spacecraft, submarines, etc.) [36].

PEM electrolysis is based on proton exchange membrane fuel cell technology. Proton exchange membranes, which conduct protons through the membrane, are used to replace asbestos. Notably, the gas permeability of a PEM is much lower than that of asbestos. PEM electrolysers are more environmentally friendly because the generated gas does not contain an alkaline fog. Moreover, the fast response, high efficiency, compact design, and high output pressure make PEM electrolysis a promising hydrogen production technology [28].

The electrolyte, typically Nafion® or Fumapem®, is a thin polymeric membrane between the electrodes that is gas-tight and thin enough (ranging from 20 to 300 µm in thickness) to provide high proton conductivity, low gas crossover, compact system design, and high-pressure operation [37]. It has a cross-linked structure and an acid character given the presence of sulfonic acid (SO_3H) functional groups. These functional groups cause the proton (H^+) exchange mechanism across the membrane [38].

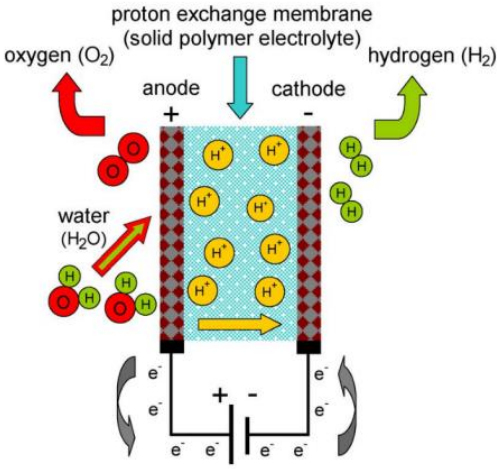

Figure 16 - Working principle of a PEM electrolysis cell *[38]*.

The PEM hydrogen production unit consists of a DC power supply, a control system, and a PEM hydrogen production system. The PEM hydrogen production system is simpler than the alkaline water system because the gas after-treatment device is smaller, no special alkali tank is required, and the water tank can also serve as an oxygen separator [29].

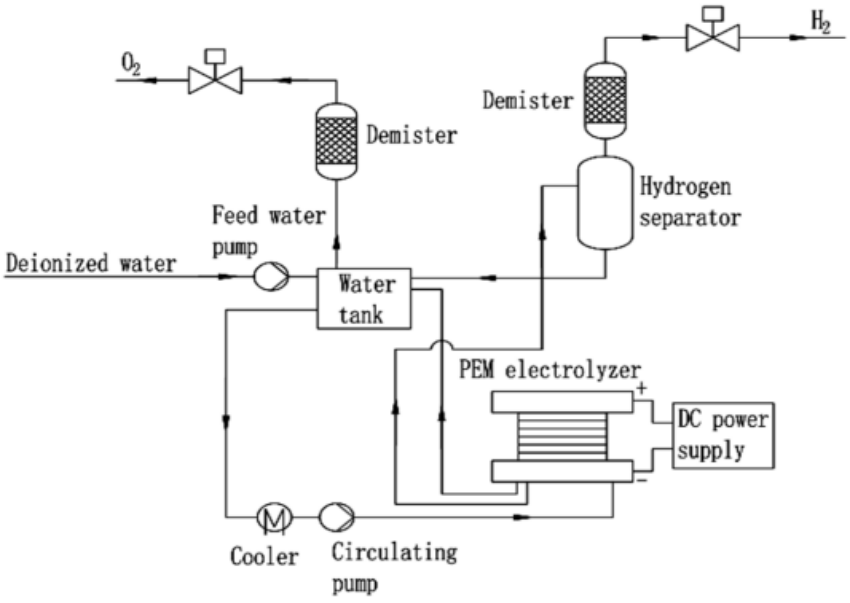

Figure 17 – Process flow chart of a PEM hydrogen production unit *[29]*.

When the equipment is started turning on, the water in the water tank is replenished to the specified liquid level, the circulation pump is activated, and the water level of the hydrogen separator is observed to reach the defined position. The DC power source is turned on after the liquid level in the water tank and the hydrogen separator has been stabilized, and the PEM electrolytic cell begins to electrolyze. Oxygen and water are separated in the water tank, and the

oxygen is discharged after passing through a molecular sieve. The hydrogen separator receives hydrogen and a small amount of water, and the hydrogen gas is passed through the molecular sieve for further treatment. When the water in the hydrogen separator reaches a certain liquid level, some of it flows into the water tank.

Because electrolysis reduces moisture during operation, the amount of water replenishment must be controlled. Furthermore, the PEM electrolyser can be operated under differential pressure. It does not need to be gradually regulated like hydrogen by alkaline water when starting. The pressure of the regulating valve can be directly set to the defined pressure, and the equipment can be stabilised in 15 minutes [29].

Despite its lower level of technological and commercial maturity, PEM-based electrolysis systems have a few advantages over traditional water-alkaline electrolysers, including environmental cleanliness, significantly smaller mass-volume characteristics and power costs, and, most importantly, a high degree of gas purity, the ability to obtain compressed gases directly in the installation, and an increased level of safety [39].

Solid Oxide Electrolysis

Solid Oxide Electrolysis Cells operate at high temperatures and can significantly reduce the power required to split water into hydrogen, increasing power-to-hydrogen efficiency (up to >95% HHV H2) [40].

In a solid oxide electrolysis cell (SOEC), water supplied at the cathode side is reduced into H_2 and O_2 ions. By oxidation on the anode side, the latter eventually crosses the electrolyte to form O_2 [41].

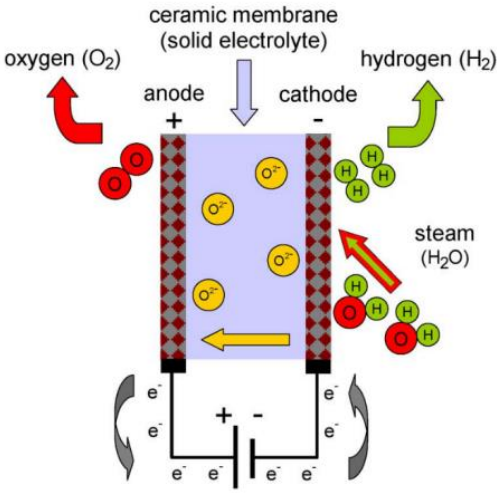

Figure 18 - Solid oxide electrolysis cell principle for H2 production from water *[38]*.

The formula for the total energy demand (ΔH) is ΔH = ΔG + TΔS, where ΔG stands for the electrical energy demand and TΔS for the heat energy demand [42]. With the use of ZrO_3 doped with 8-mol% Y_2O_3 as the electrolyte, anions transfer in the SOEC at high temperatures. Solid oxide is chemically and thermally stable [28].

Figure 19 shows steam electrolysis thermodynamic data at a steam pressure of 1 atm. When water transitions from the liquid to the gas phase, the total energy demand (ΔH) of the reaction drops significantly above 100 °C and then remains almost constant. With thermal energy compensation (TΔS), the electrical energy demand (ΔG) decreases significantly [42].

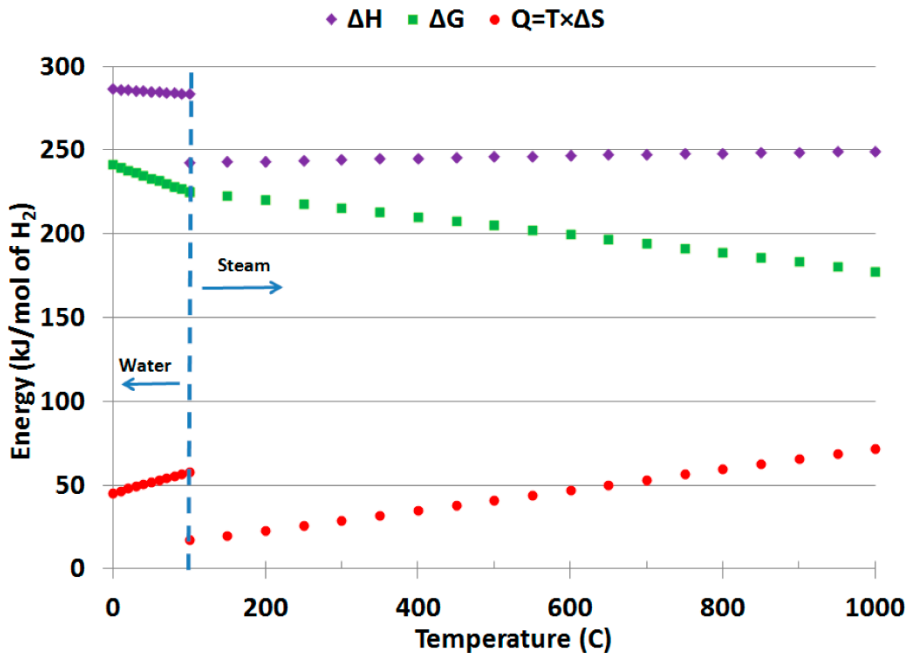

Figure 19 - Electric, thermal and total energy demand for H2O electrolysis as a function of temperature *[43]*.

As a result, SOECs operating at high temperatures can result in lower costs for hydrogen production with less electricity consumption, especially when the required heat energy can be obtained from external sources such as waste heat from high-temperature industries [42]. Hence, this technology is very appealing when a high-temperature source is available (nuclear energy sector, geothermal energy, etc).

2.2. Storage Methods

In STP conditions, hydrogen is a very light gas with a density of 0.0899 kg/m^3 which complicates hydrogen storage, and hydrogen is typically pressurized or liquefied to store reasonable amounts of energy [21]. Figure 20 shows the relationship of hydrogen density with respect to temperature and

pressure. Temperature and pressure zones for pressurized, liquefied, and cryo-compressed storage. For example, compressing hydrogen to 700 bar at 293 K raises its density to 40 $\mathrm{kg/m^3}$.

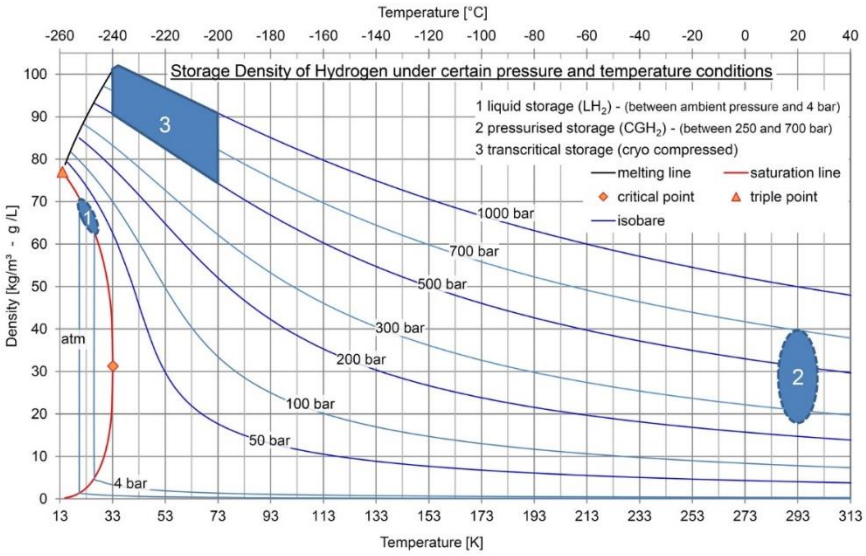

Figure 20 - Hydrogen density under different temperatures and pressure. *[44]*

Innovative hydrogen storage methods research is being conducted on a larger scale to develop materials that are safe, reliable, compact, and cost-effective. Hydrogen, like any other product, must be packaged, transported, stored, and transferred from the point of production to the point of final use [45]. Hence, for hydrogen storage to be economically viable, its storage density must be increased. There are several methods for storing hydrogen at high density. All these methods, however, require the use of some input energy in the form of work, heat, or, in some cases, hydrogen-binding materials [46].

There are three major categories of hydrogen storage technologies: 1) hydrogen may be stored as a gas or a liquid in pure, molecular form without any significant physical or chemical bonding to other materials; 2) molecular hydrogen may be adsorbed onto or into a material, held by relatively weak physical van der Waals bonds; 3) atomic hydrogen may be chemically bonded (absorbed) [46]. Furthermore, the storage technologies based on chemical bonding can be divided into two subcategories: metal hydrides and chemical hydrides – metal hydrides, as the name implies, contain metal atoms. In this case, hydrogen can be bonded to a metal atom directly (elemental metal hydrides and intermetallic hydrides) or as part of a complex ion that is bonded to a metal atom (complex metal hydrides) [46]. Chemical hydrides, on the other hand, are made up entirely of non-metallic elements, typically some combination of carbon, nitrogen, boron, oxygen, and hydrogen [46]. Figure *21* shows the categorisation of the different storage methods.

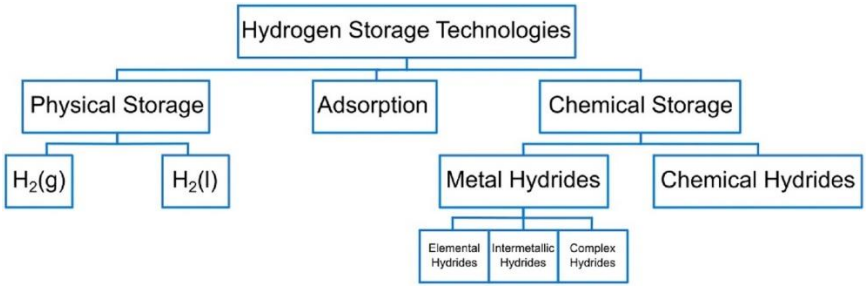

Figure 21 - Hydrogen storage technologies categorisation *[46]*.

Hydrogen storage in pure and molecular form is possible in both gas and liquid phases. These are the only forms of hydrogen storage that are currently used on a large scale [47], [48]. Liquid hydrogen storage in the space industry, as well as large salt cavity storages in Texas, USA, and Teesside, UK, are notable examples [47], [49].

Hydrogen gas storage

A compressed hydrogen gas storage system consists of two major components: the storage compartment(s) and the compressors required to achieve the storage pressure.

Large amounts of gaseous hydrogen are typically not stored at pressures greater than 100 bar in aboveground vessels and 200 bar in underground storage due to material properties and operating costs [50]. The achievable hydrogen storage densities are limited by the storage pressures: at 100 bar and 20 °C, the density of hydrogen gas is approximately 7.8 $\mathrm{kg/m^3}$. Because of the low hydrogen density, large storage-specific volumes are required, resulting in high investment costs. A lower storage pressure, on the other hand, requires less compression work and, as a result, lower operating costs [51], [52].

This method is advantageous for fuel storage because it can be stored in a smaller space while retaining its energy effectiveness [53]. When the pressure of the gas is increased, energy density by volume gets improved. Although the technology is simple, the process is volumetrically and gravimetrically inefficient [54].

Liquid hydrogen

Pure hydrogen can be compressed, but it can also be liquefied to increase density (condensation). The benefit of liquefaction is that very high hydrogen storage densities can already be reached at atmospheric pressure; saturated liquid hydrogen has a density of 70 $\mathrm{kg/m^3}$ at 1 bar [55].

Slush hydrogen also referred to as liquid hydrogen, is colourless and non-corrosive at 20 K. To store concentrated forms of hydrogen, liquid hydrogen must be kept in a cryogenic environment [45]. Because of its high density, liquid hydrogen has primarily been considered a hydrogen distribution medium [56].

The energy-intensive liquefaction process is the main issue for the storage of liquid hydrogen. Due to hydrogen's extremely low boiling point (-253 °C at 1 bar) and the fact that hydrogen gas does not cool down during throttling processes (adiabatic, isenthalpic expansion) for temperatures above about -73 °C, the liquefaction of hydrogen requires a significant input of energy. Precooling is required for the latter issue during the liquefaction process, most frequently by the evaporation of liquid nitrogen [57].

After the hydrogen has been liquefied, it must be able to be stored to reduce evaporation. The evaporation of liquid hydrogen constitutes not only a loss of the energy spent liquefying the hydrogen but also, eventually, a loss of hydrogen. This is because the evaporated gas must be vented because of the pressure build-up inside the storage vessel. Boil-off is the term for this gradual loss of stored hydrogen; it is frequently expressed as the percentage of stored hydrogen lost each day, or the boil-off rate. Making tanks spherical reduces the surface-to-volume ratio, which in turn reduces heat transfer from the environment to the liquid hydrogen inside, and advanced insulation reduces heat transfer through the tank walls. This reduces the boil-off rate [46].

Boil-off is less of an issue in applications where the liquefaction plant and liquid hydrogen storage are close together. In such cases, cold boil-off gas from the storage vessel(s) could be injected back into the liquefaction process at a later stage using an ejector [58]. Because the storage's boil-off gas is already close to the boiling point, reliquefaction is accomplished at a low additional cost. If reliquefaction is not an option, the boil-off gas can be used in downstream applications [46].

Although the technology appears to be very promising because it is gravimetrically and volumetrically efficient, more research has been ongoing to overcome issues such as hydrogen uptake and release, high hydrogen liquefaction rate that causes significant energy loss, hydrogen boil-off, and tank cost [59].

Adsorption of hydrogen

Adsorption-based hydrogen storage takes advantage of physical van der Waals bonding between molecular hydrogen and a material with a large specific surface area. Because of the weakness of the van der Waals bonding, low temperatures and high pressures are usually required to achieve

significant hydrogen storage densities through adsorption. Liquid nitrogen (boiling point: -196 °C) is by far the most used refrigerant for hydrogen adsorption [60]. The hydrogen pressure applied is usually 10-100 bar, but it varies based on the adsorbent and the specific application [60]. Higher pressures are not desirable beyond a certain threshold because the presence of the adsorbent may no longer improve the hydrogen storage capacity compared to if pressurized gas was stored in the same vessel, due to the space occupied by the adsorbent [61].

In comparison to compressed gaseous or liquid hydrogen storage, there is not much experience with the implementation of adsorbent-based hydrogen storage; most developed adsorption-based storage vessels have so far only been on the laboratory scale [46]. Certain activated carbons and metal-organic frameworks (MOFs) have achieved excess hydrogen adsorption of 8-10% (wt.) hydrogen at 196 °C, making them the most successful adsorbents [62]. However, given the low density of most used adsorbents and the need for additives to enhance effective heat conductivity, the volumetric hydrogen storage density is affected and achieving a vessel-level deliverable hydrogen storage capacity of much higher than 40-50 $\mathrm{kg/m^3}$ at 196 °C is likely difficult using presently available adsorbents [63].

Metal hydrides

Metal hydrides are well-known for their extraordinary ability to absorb hydrogen [64]. Hydrogen is chemically bonded in metal hydrides and these bonds are far stronger than the physical bonds in hydrogen adsorption [46]. As a result, more energy is required to release the chemically bonded hydrogen. On the other side, the stronger bonding allows hydrogen to be stored at high density even at ambient temperatures [65].

The release of hydrogen from metal hydrides can be accomplished in two ways: by heating (thermolysis) or by reaction with water (hydrolysis) [46]. These approaches are opposed: thermolysis is endothermic, whereas hydrolysis is exothermic; thermolysis is reversible in some cases, whereas hydrolysis is irreversible; thermolysis occurs in the solid phase, whereas hydrolysis normally occurs in solution; and thermolysis requires elevated temperatures (around 120–200 °C [45]), whereas hydrolysis may be spontaneous at room temperature [61]. Although a wide range of metal hydrides have been developed and studied for thermolysis-based storage, only a few have been successfully applied for hydrolysis [46].

Hydrides have serious limitations because they react badly when exposed to moist air, are difficult to handle and recycle because they cause skin or eye irritation, and cause impurities to be absorbed

into the tank during hydrogen uptake [45]. This reduces tank lifetime because impurities occupy the spaces inside the metal that were previously occupied by hydrogen [45].

Chemical hydrides

Similar to metal hydrides, chemical hydrides bond hydrogen chemically. However, because chemical hydrides are composed of lighter elements, their properties differ significantly from those of metal hydrides. The most significant difference is that chemical hydrides are typically liquids under normal conditions, simplifying transport and storage as well as heat and mass transfer during dehydrogenation and hydrogenation processes [46].

Many of the chemical hydrides proposed for hydrogen storage, such as methanol, ammonia, and formic acid, are currently bulk chemicals produced from natural gas, meaning that the utility of these chemicals extends beyond hydrogen storage [46]. Since these chemicals are already broadly produced, it is beneficial that much of the infrastructure required for their production, handling, and transportation is already existent. Furthermore, producing these bulk chemicals with hydrogen derived from water electrolysis rather than natural gas reforming is not only ideal for storing hydrogen but also a means of reducing fossil fuel utilisation in the production of bulk chemicals [46].

3. Literature Review on Water Electrolysis Technologies

Hydrogen is currently regarded among the main technologies that will enable future large-scale and long-term storage of electricity production via the mature concept of Power-to-Gas. The direct electrochemical splitting of water into hydrogen and oxygen ($2H_2O \rightarrow 2H_2 + O_2$) underpins this type of chemical storage, making use of various electrical energy sources, such as renewables. Several encouraging works and reports on the technological and economic viability of the Power-to-Gas concept have recently been published focusing on ongoing or completed large-scale demonstration projects, particularly in Europe. Based on the global ambitious scenarios for electricity from renewable sources, a large amount of "green and clean" H_2 can be assumed to become readily accessible in the market shortly. Therefore, water electrolysis is currently being viewed as the only viable path forward for large-scale production of CO_2-free H_2, although steam methane reforming (SMR) is still the dominant technology in H_2 production nowadays, however, it presents the downside of CO_2 emissions ($CH_4 + 2H_2O \rightleftharpoons 4H_2 + CO_2$), allowing water electrolysis to eventually become directly competitive.

Water electrolysis technologies can reasonably be categorised into two groups based on their operating water temperature, namely low-temperature (below 100°C) and high-temperature (500°C-800°C). There are two main low-temperature technologies widely considered in actual literature, Alkaline Electrolysis and PEM, with Alkaline systems being in a higher stage of technological and commercial maturity. On the other side, high-temperature electrolysis is solely represented by the Solid Oxide Electrolysis technology which is still in the laboratory experimental stage.

3.1. Water Electrolysis Costs

Low-Temperature Water Electrolysis

Proost (2019) [66] presents a compilation of capital costs (CAPEX) data for water electrolysers and a summary of their impact on renewable energy prices, studying two main water electrolysis technologies, namely Alkaline and PEM [66]. The author points out the lack of operational costs (OPEX) data available in the literature for large-scale operating electrolysers such as depreciation and interest on capital investment, utilities and feedstock costs, manpower and maintenance, making CAPEX the main factor in economic analysis, although, the production cost of H_2 via water electrolysis nowadays is dominated by the cost of electricity which can still be referred to as the dominant OPEX parameter.

Figure 22 shows that in the 1990s, the range of CAPEX estimations for alkaline and PEM technology was 870–2350 €/kW and 310–4750 €/kW, respectively. Simultaneously, projections for future investment costs by 2030 are reported to be in the range of 790–910 €/kW and 400–960 €/kW, respectively.

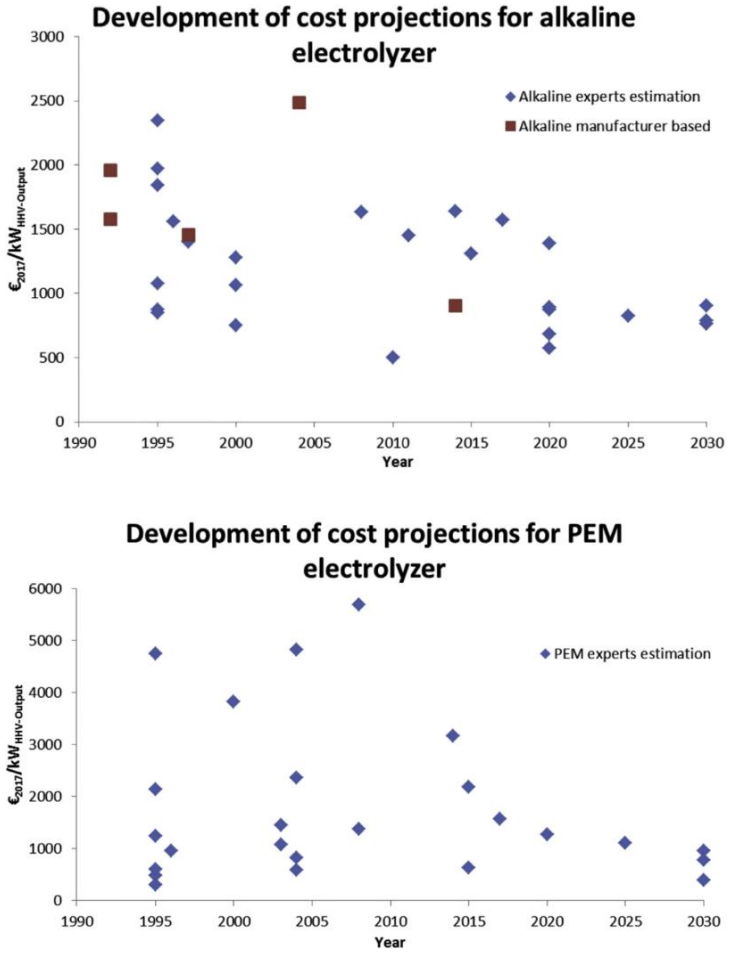

Figure 22 - Compilation of past and expected Alkaline (top) and PEM (bottom) electrolysis plant costs in €/kW. *[66]*

According to the short- and long-term estimations indicated in the expert elicitation study on the future cost and performance of water electrolysers, capital costs for Alkaline technologies were expected to be between 800 and 1300 €/kW by 2020, and between 1000 and 1950 €/kW for PEM technologies (all 50th percentile estimates, at current R&D funding and without production scale-up). The same report estimates that by 2030, these costs will be only slightly lower than in 2020, falling into the 700–1000 €/kW and 850–1650 €/kW ranges for Alkaline and PEM, respectively.

A relevant notice is also observed in the CAPEX comparison attempt between PEM and Alkaline water electrolysis technologies, using data collected from TASK 33 [67] for PEM and exclusively verified data with the electrolyser manufacturers to include components such as:

- Transformer(s), rectifier(s), control panel with PLC.
- Water demineraliser/deioniser.
- Electrolyser stack(s).
- Gas analysers, separators and separating vessels.
- Scrubber or gas purifier system & recirculating pump.
- Dry piston compressor @ 15 bar (note that PEM systems are typically self-pressurising up to 20/50 bar).

In this comparison, an overall system energy consumption of 4.8 $\mathrm{kWh/Nm^3}$ was considered for Alkaline data as indicated by the manufacturer. Noting that the electrolyser itself runs at 4.4 $\mathrm{kWh/Nm^3}$ (DC power), based on a $\mathrm{H_2}$ Higher Heating Value (HHV) of 3.54 $\mathrm{kWh/Nm^3}$ [20], the efficiency of the electrolyser is found at 80%, whilst the system would be running at 74% efficiency (at the specified discharge pressure level of 15 bar) [66].

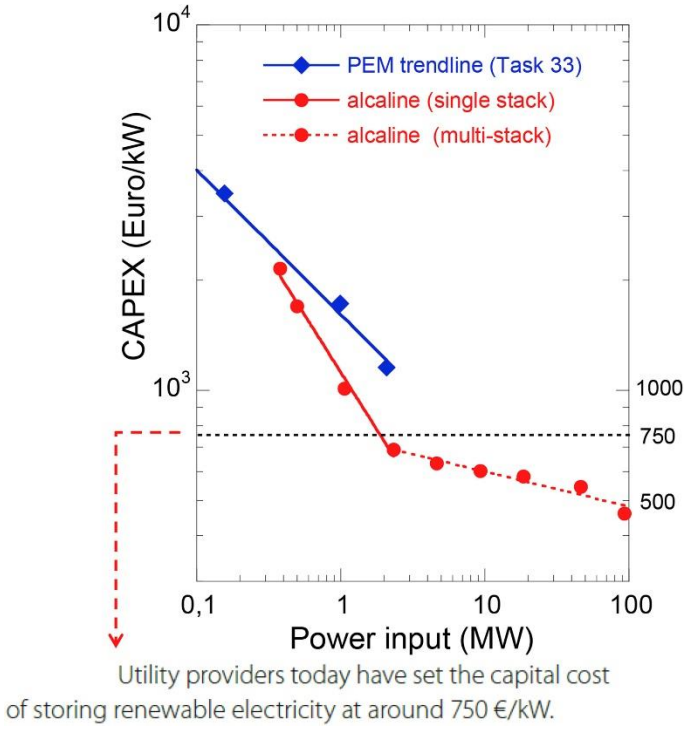

Figure 23 - CAPEX data comparison of PEM and Alkaline technologies as a function of power input (Data for Alkaline systems are based on a single stack of 2.13 MW consisting of 230 cells, 2.6 m^2 in size. The change in slope for Alkaline electrolysers corresponds to the use of multi-stack systems). *[66]*

The comparison in Figure 23 clearly shows that, for single stack systems, Alkaline electrolysers are far more vulnerable to CAPEX reduction when scaling than PEM. Particularly, for Alkaline systems, a CAPEX of 750 €/kW, regarded by utility providers to be the capital cost for storing renewable

electricity, was already attainable for a single stack 2 MW system in 2019. For PEM, such a critical CAPEX value should be achievable for 5 MW systems, necessitating the use of multi-stack systems.

Regarding the usage of the multi-stack system, Figure 24 provides some insights for further reduction in CAPEX using multi-stack systems for both PEM (a) and Alkaline (b) electrolysers. It can be seen that, in comparison to single-stack systems, the further reduction in CAPEX when scaling for a multi-stack PEM design is much more prevalent (on a relative scale) than for Alkaline. However, it should be remarked that life cycle issues of electrolysers and electrodes were not considered in the above CAPEX estimates. Evidently, with the durability element of Alkaline stacks still strongly favoured in current state-of-the-art Alkaline vs. PEM technologies, including such lifetime (and thus OPEX) aspects in the calculation can be estimated to somewhat flatten out the projected difference in CAPEX reduction between Alkaline and PEM for multi-stack systems.

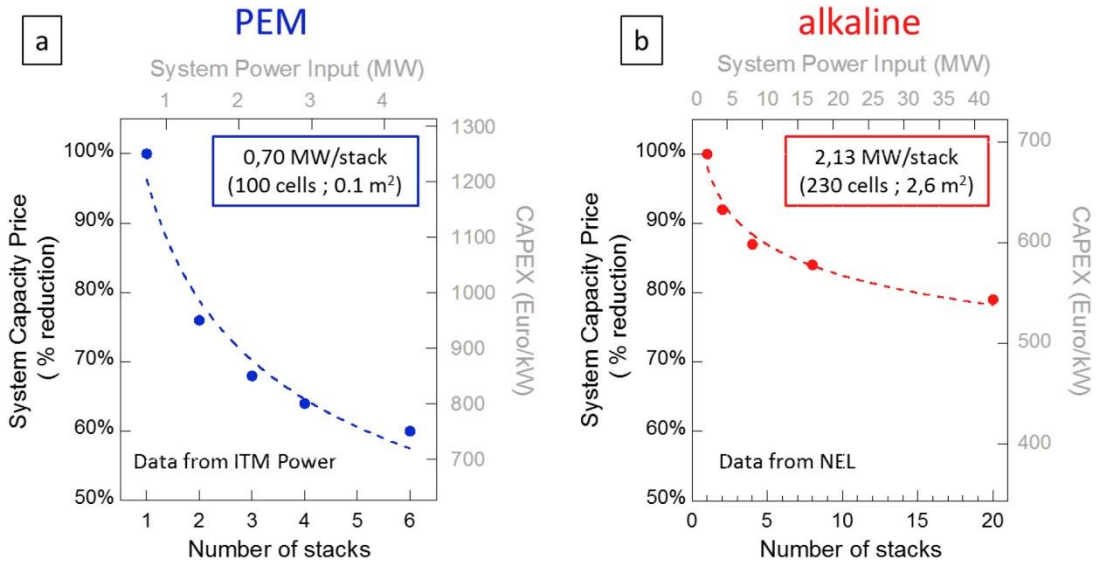

Figure 24 - CAPEX reduction when using multi-stack systems, both for PEM (a) and Alkaline (b) electrolysers. *[66]*

Furthermore, CAPEX values as low as 400 €/kW are currently projected by NEL, a company leader in the electrolysis market, for Alkaline systems scaling up to 100 MW [66]. The latter is derived from an intelligent engineering design of a 40-stack system. Further to that, the manufacturer claims that it would be very feasible to deliver hydrogen at 100 bar for roughly the same CAPEX value as the hydrogen pressure of 15 bar considered the default for Alkaline systems in Figure 23 and Figure 24. This would greatly enhance their Power-to-Gas and energy storage business cases, where high pressures are indeed required.

At this stage, the study concluded that a CAPEX of 750 €/kW for Alkaline systems, which is considered critical for storage purposes, is already achievable today for a single stack, 2.13 MW

system. The CAPEX values are projected to be on the order of 400 €/kW, but this will require further scaling up to 100 MW. For PEM, such values of CAPEX near 750 €/kW are achievable for 5 MW systems, needing multi-stack systems.

Based on the CAPEX data (for Alkaline and PEM systems) compiled by Proost (2019), the production cost of H_2 around 3 €/kW was estimated to be very realistic by 2020.

By 2030, the EU hopes to have installed at least 40 gigawatts (GW) of renewable hydrogen electrolysers, generating up to 10 million tonnes of renewable hydrogen. This necessitates the scaling up of water electrolysis technology. The current state-of-the-art is at a scale of 10 MW, but GW-scale green hydrogen plants are required. [68]

The Netherlands Case

The Institute for Sustainable Process Technology (ISPT) presents a report as part of the Hydrohub GigaWatt Scale Electrolyser project [68], which seeks to reduce capital expenditures (CAPEX) and convey conceptual designs (blueprints) for GW water electrolysis infrastructures in the Netherlands' five major industrial clusters. The first part of the project consists of an assessment of the economics of a 1GW green hydrogen plant to be built in the Netherlands, in 2020, taking into account Alkaline and PEM electrolysers.

The total cost estimations were produced based on common principles in the chemical industry-defining scopes such as heat and material balance, drawings and sized equipment lists to estimate the capital expenditures for the equipment supply. Additionally, costs for installation, mounting and erection on site were considered as well as indirect costs and contingency using multipliers. The financial investment decisions would then be based on the total installed costs, which breakdown is as follow:

- **Direct costs**

  This includes all costs associated with the supply of the scope items mentioned above, as well as installation, mounting, and erection on-site, including interconnecting piping and all materials and services from contractors and suppliers.

- **Indirect costs**

  These include, amongst others, expenses for engineering, project management, construction supervision and management, and commissioning are just a few examples. Over direct costs, 10% allowances have been applied to cover (known) uncertainties, such as changes in material quantities and prices.

- **Indirect owner costs**

  This includes costs for the owner's project management, site supervisory teams, operator training, as well as insurances, grid fees, electricity consumption, and land lease during construction, commissioning, and start-up. Because no price escalations are factored in, the estimate is based on a 2020 cost level.

- **Contingencies**

  Because not all equipment, materials, and installation are detailed in engineering deliverables during the feasibility phase, the project definition is still at a low level. It is a standard engineering principle to include a contingency to cover risks (such as delays) and unknown scope, which result in higher costs. A percentage of 30% of the base estimate was applied based on the achieved project definition of the study.

The total installed costs of a 1 GW green hydrogen plant are estimated to be 1400 €/kW for an Alkaline plant and 1800 €/kW for a PEM plant. In terms of hydrogen production, the estimated total installation costs for Alkaline would be 3100 €/(kg/day) and 4400 €/(kg/day) for PEM technology. The latter numbers are preferred because they are based on the amount of hydrogen produced rather than the amount of electricity input. In these values, the difference between Alkaline and PEM is greater than the difference in CAPEX due to the current higher efficiency of Alkaline technology.

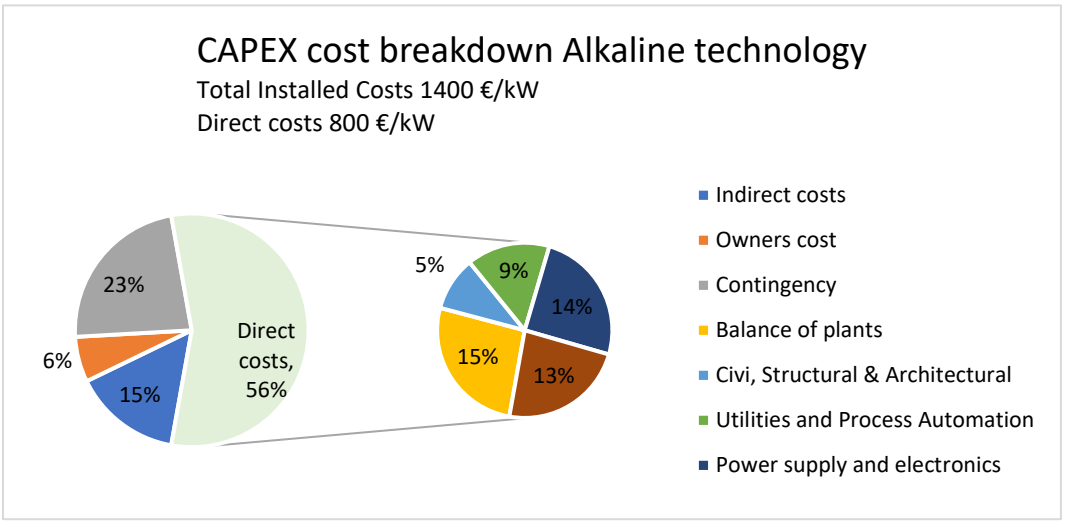

Figure 25 - Breakdown of the total installed costs for 1 GW green hydrogen plant based on Alkaline technology. *[68]*

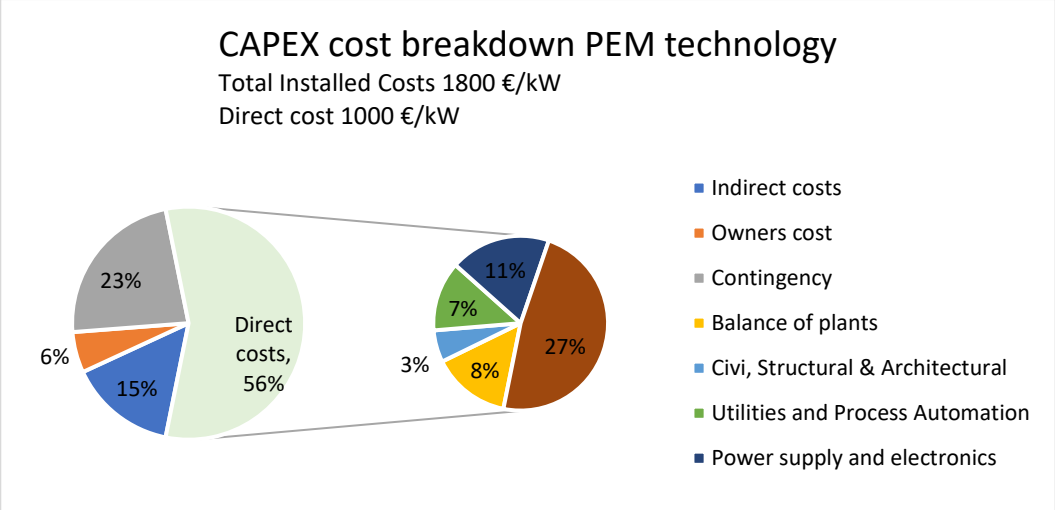

Figure 26 - Breakdown of the total installed costs for 1 GW green hydrogen plant based on PEM technology. *[68]*

The total installed costs are broken down further in Figure *25* and Figure *26*. The figures show that, in addition to the stacks, the power supply and electronics, as well as the balance of the plant, all make a significant contribution to direct costs. The capital expenditures necessary for each of these parts in Alkaline technology are the same as for the electrolysis equipment. Utilities and civil costs also play a significant role. Because of the higher stack costs, the contribution of electrolysis equipment is substantially higher in PEM technology.

Conclusively, the report demonstrates the significance of considering indirect and owner costs, which account for roughly a quarter of total costs. Additionally, the CAPEX estimates in this study for system supply (and installation) are in the ballpark with the above reference numbers based on a similar scope of supply.

High-Temperature Water Electrolysis

The expert elicitation study from Schmidt et al. (2017) presents expert views on future CAPEX, lifetime and efficiency of electrolysis technologies, including SOEC, which was estimated to be quite expensive at 3000 – 5000 €/kW for the year 2020. Experts expect that for 2030, PEM and SOEC will be the dominant water electrolysis technologies with SOEC presenting the highest relative cost reduction by 2030 with a cost range estimated at 1050 – 4250 €/kW.

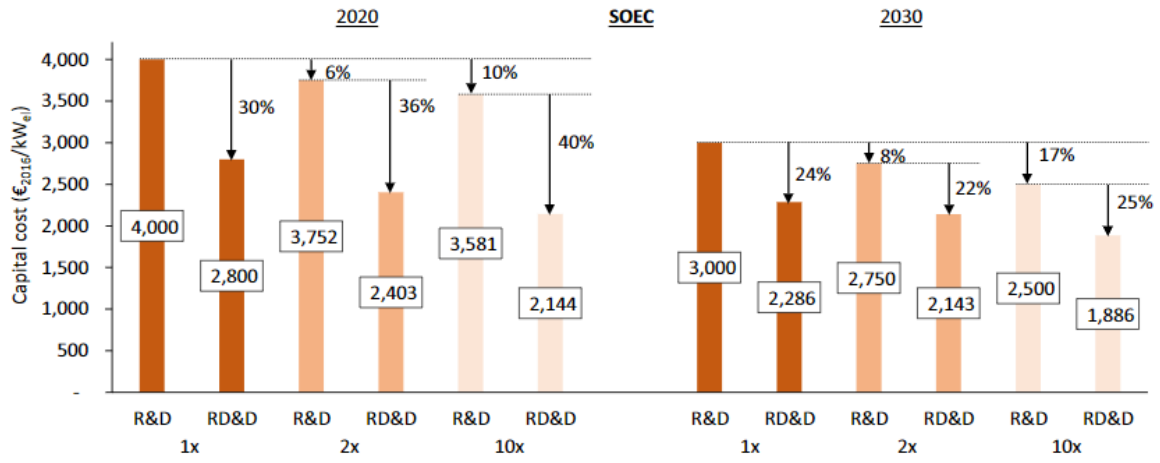

Figure 27 - Relative impact of R&D funding and production scale-up (R&D, RD&D) on capital costs. *[69]*

Figure 27 demonstrates the relative impacts of increased R&D funding and production scale-up based on the experts' estimates' median percentage reductions. The cost impact of production scale-up at current funding (RD&D, 1x) is 30% by 2020 and 24% by 2030.

Schmidt et al. (2017) [69] found that production scale-up is most important for technologies that have not yet been commercialized, with cost reduction potentials of 30-40% by 2020 (RD&D). It would imply that learning in production during the early stages of SOEC development has a larger marginal effect on cost reduction than commercial Alkaline and PEM systems, where production developments have already been partially exploited. This argument would be based on the learning curve theory (Wright, 1936, cited by Schmidt et al., 2017), which states that every doubling of cumulative produced capacity results in a constant relative cost reduction, justifying the early-stage technologies experiencing higher cost reductions than mature ones.

NGNP Project Case

McKellar et al. (2010) present an economic analysis of a high-temperature gas-cooled reactor (HTGR) powered high-temperature hydrogen production plant as part of a study conducted by the Next Generation Nuclear Plant (NGNP) Project to assess the incorporation of high-temperature gas-cooled reactor (HTGR) technology with conventional chemical processes. The NGNP Project is being carried out under the direction of the United States Department of Energy (DOE) to fulfil a key national demand defined in the National Energy Policy to promote reliance on safe, clean, and affordable nuclear energy, as well as to establish a greenhouse-gas-free technology for hydrogen production. [70]

The capital installed costs for the High-Temperature Electrolysis (HTE) process assumed hydrogen production from a 600 MW high-temperature gas reactor with an outlet temperature of 900 °C. The

costs are in 2006 dollars; however, the assessment was performed using 2009 dollars, thus, the Chemical Engineering Plant Cost Index (CEPCI) was used to adjust costs to 2009 dollars.

The economic modelling calculations reached a best estimate capital cost scenario of 2000 USD/kW without considering the reactor and power cycle costs. The total installed costs breakdown is shown in Figure 28.

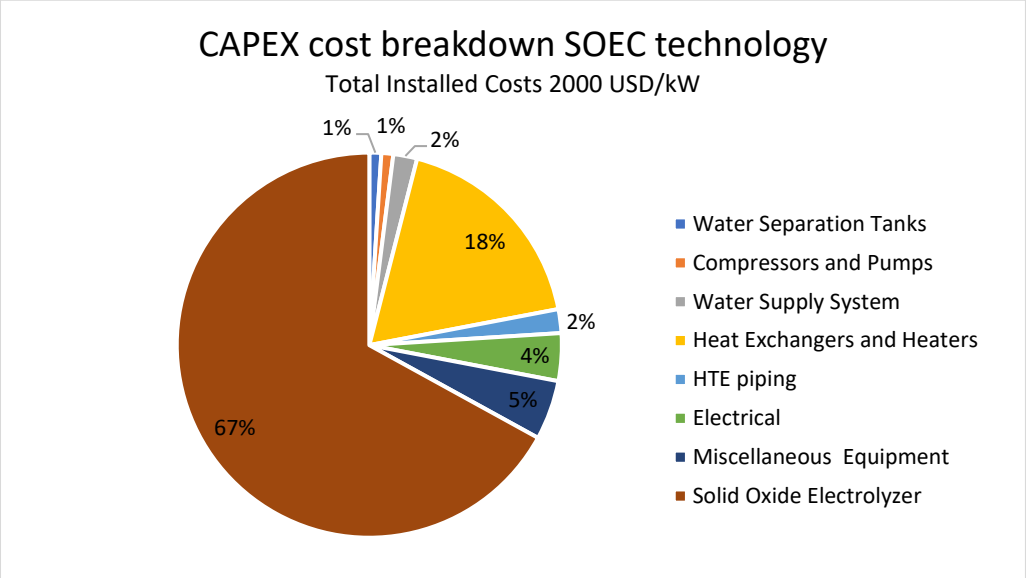

Figure 28 - Breakdown of the total installed costs of hydrogen plant based on SOEC technology. *[70]*

The total capital investment of the HTE connected to a 600 MW_t HTGR is determined by multiplying the installed power cycle and HTE costs by a 10% engineering fee and an 18% contingency fee. The HTE total capital investment also includes cooling towers and support capital like water, piping, instrument and controls, electrical systems and buildings and structures.

3.2. Technological Developments of Water Electrolysis

Alkaline Water Electrolysis

According to the hydrogen production introductory review presented by Navarro et al. (2015) presented in Compendium of Hydrogen Energy, Alkaline water electrolysis is known as the main process for water splitting reaction. The advancement of this technology was accelerated due to the military utilisation of hydrogen isotopes. Nowadays, several companies in Norway are reported to be developing Alkaline electrolysers with industrial production capacity in the range of 5-500 $m^3\ H_2/h$ for electrolytic production of hydrogen.

At atmospheric pressure, NEL electrolysers deliver 50–485 $\mathrm{m^3\ H_2/h}$ with energy consumption ranging from 4.1–4.3 $\mathrm{kWh/H_2\ Nm^3}$ at current densities up to 0.3 $\mathrm{A/cm^2}$. The purity of hydrogen can reach 99.9%, the operating temperature is 353 K, and the electrolyte solution is 25% KOH. On the other side, The Hydrogenics Corporation produces electrolysers with hydrogen capacities of up to 120 $\mathrm{m^3\ H_2/h}$ at 20 bar output pressure, $\mathrm{H_2}$ purity of 99.9% and $\mathrm{O_2}$ purity of 99.5%, and specific energy consumption of 4.8–4.9 $\mathrm{kWh/m^3H_2}$including plant infrastructure energy requirements. [71]

Alkaline water electrolysers can be designed and manufactured for various applications. Electric power generator cooling in power plants, semiconductor industry, flat-panel computers and television screen producing units, and glass plants and metallurgical industries are the main gas-consuming industries. Food processing, laboratory applications, heat treatments, meteorology, and welding industries are among the other industrial applications. As a mature technology, many industrial Alkaline electrolysers can produce up to 650 $\mathrm{m^3\ H_2/h}$ are installed for different applications.

Nevertheless, Millet and Grigoriev (2013) argue that Alkaline electrolyser cells present significant challenges as they can hardly operate at very low current densities. This is a constraint in terms of the flexibility required for load-following operation with renewable energy sources. Major material research efforts are focused on the development of advanced diaphragms with adapted electrode materials. The most efficient diaphragms are made of asbestos, which is illegal in many countries. The replacement of asbestos with composite ceramic/polymer materials has been proposed but there is still room for improvement. Equally, investigations have been ongoing to develop new electrocatalysts by studying the electrocatalytic properties of some transition metal macrocycles.

In terms of performance, Millet and Grigoriev (2013) claim that higher efficiencies can be achieved using advanced Alkaline electrolysers. Over the last few decades, prototypes capable of delivering up to 25 $\mathrm{m^3\ H_2/h}$ have been developed. These units are designed to operate at high current densities (1.25 $\mathrm{A/cm^2}$), at 393 K, and 5–40 bar of operating pressure. At 363 K, the electrical power consumption (at 0.2 $\mathrm{A/cm^2}$) is 3.81 $\mathrm{kWh/m^3H_2}$, while at 393 K, it is slightly lower at 3.65 $\mathrm{kWh/m^3H_2}$. [72]

PEM Technology

Proton exchange membranes (PEMs) are widely used in fuel cells and electrolysers to generate electricity and hydrogen. PEMs are also used to separate the anode and the cathode. Because of their high ionic conductivity, thermostability, mechanical strength, chemical stability, and durability

at low temperatures and high relative humidity, Nafion™ and Nafion™-based membranes are the most popular PEMs [73]. The benefits of PEM electrolysers include their ability to operate at high current densities with high voltage and to produce very pure hydrogen gas (up to 99.995% purity) [74]. On the other hand, Nafion™ has two major drawbacks: a time-consuming synthesis procedure and poor proton conductivity at high temperatures in low humidity conditions [75]. Furthermore, the main barriers to using Nafion™ membranes are their exorbitant price, the unsafe membrane synthesis process, and the fact that ionic conductivity declines when the operating temperature is higher than 90 °C under low relative humidity [76].

Significant progress in catalyst and membrane materials, as well as the labour-intensive manufacturing process, are required for PEM water electrolysis to be cost-effective for widespread use in renewable energy systems [77]. The state-of-the-art anode catalyst in conventional PEMs is iridium oxide (IrOx) or mixed oxide with ruthenium [78]. IrOx loadings of 1 to 3 $\mathrm{mg/cm^2}$ are common for commercial electrode catalysts [79]. This level of catalyst loading is insufficient to meet energy market long-term cost targets [80]. Moreover, using current electrolysis technology, translating catalyst development from the lab to the megawatt scale remains difficult in terms of catalyst cost and stability [81].

Solid Oxide Electrolysis

In contrast to SOFC technology that is already on the market, the solid oxide electrolysis operation is attempting to be competitive and replace the widely used low-temperature systems. The most recent results are quite encouraging, as the estimated SOEC energy consumption is around 3.7 $\mathrm{kWh/Nm^3}$ ($\mathrm{H_2}$), which is significantly lower than Alkaline and PEM [82].

According to [83], unlike other cell technologies, SOCs have only recently emerged as promising solutions due to their high efficiency and low material costs, since research initially focused primarily on the fuel cell mode, which has already seen commercial stationary applications, while large-scale prototype plants are being built to produce hydrogen or other useful fuels via SOECs. Regarding the reversible operation, some issues must be addressed before these cells can compete in the energy market; most notably, improvements in thermal management strategies should be implemented to reduce potential stresses caused by switching from electrolysis to fuel cell mode and vice-versa. Furthermore, [83] also state that a fundamental step is the evaluation of the delay caused by the switch between two operations and the resulting time required to return to steady-state conditions.

The EU project names HELMETH developed a SOEC unit thermally coupled with a downstream methanation reactor to optimize internal heat exchange [84]. The system has a 10 $\mathrm{kW_{el}}$ power

capacity and energy consumption of 3.37 $\mathrm{kWh/Nm^3}$. Since the global conversion efficiency of renewable electricity to methane is greater than 85%, this application is more convenient than basic steam electrolysis. This improved performance can also be obtained by using a pressurized system at around 10–15 bar; however, a proper strategy must be implemented to minimize the internal pressure gradient, which causes dangerous mechanical stresses [83].

Based on various tested and operational systems, Table 2 summarizes the current state of SOFC and SOEC technology.

Table 2 - Current state of SOFC and SOEC technology *[83]*.

	SOFC	**SOEC**
Power Capacity	From few $\mathrm{kW_{el}}$ for the automotive sector to 1 $\mathrm{MW_{el}}$ for stationary power plants.	From applications lower than 1 $\mathrm{kW_{el}}$ to 200 $\mathrm{kW_{el}}$, as the highest tested size.
Inlet Requirements	Gas feeding: pure hydrogen, syngas, natural gas, liquid natural gas.	Average energy consumption: 3.70 $\mathrm{kWh/Nm^3}$ ($\mathrm{H_2}$), 3.44 $\mathrm{kWh/Nm^3}$ (CO).
Outcomes	Electricity, heat, hot-exhausted gases (mainly steam).	Several chemicals including hydrogen, oxygen, carbon monoxide and syngas.
Global Process Efficiency	88–90%	80–90%
Applications	Residential co-generator, industrial-scale power plant, auxiliary power unit.	Power to Gas/Liquid, seasonal energy storage, oxygen extractor.

Current Applicability

Some prototypes are being used to evaluate the effective reaching efficiency of reversible solid oxide applications, as reported in [82]. In 2015, the Southern California Edison power grid was connected to the world's first fully integrated rSOC system. The electrolyser, powered by renewable energy, produced hydrogen with feeding water provided by a co-located steam source, but seawater was also tested after a desalination step. $\mathrm{H_2}$ was compressed and stored in a commercial gas storage tube at a cost of approximately 25-30 €/kWh. The system switched into fuel cell mode in a matter of minutes to provide the requested supplementary power during peak hours. Final tests were carried out at the US Navy base on the Hawaiian island of Oahu, connecting the system to the islanded microgrid [85]. Two 100 $\mathrm{kW_{el}}$ modules guaranteed a hydrogen production of 50 $\mathrm{Nm^3/h}$ with a system efficiency of more than 80%, whereas the SOFC size was 50 $\mathrm{kW_{el}}$ with a performance of 60%. The obtained round-trip energy efficiency was approximately 45%.

Solid oxide cell technology combined with renewable sources was recently installed in a German steelwork as part of the GrInHy project. It is composed of six modules, each with 48 stacks, ensuring a high level of system flexibility. The electrolysis mode, which has a nominal capacity of 150 $\mathrm{kW_{el}}$, can produce 40 $\mathrm{Nm^3/h}$ of hydrogen and has an 84% system efficiency, however, it can be overloaded to 200 $\mathrm{kW_{el}}$, making it the largest SOEC application in the world. The plant also operates in a reversible mode, changing to fuel cell mode when electricity demand peaks. The same unit is fed by process gases with a high hydrogen purity level or by natural gas directly, resulting in an efficiency of 50%.

Despite promising demonstrations at the laboratory level, according to [83], there are still issues to be resolved before rSOC can be commercially launched. Aside from a basic understanding of cell behaviour and degradation when switching from fuel cell to electrolysis mode, the balance of the plant needs careful optimization, with a focus on thermal management due to different operation sequences, as well as reactant storage to reduce overall system size. The integration of renewable energy sources is an interesting application for lowering external energy costs; however, it is still necessary to investigate how to connect the rSOC unit to existing grids to minimize energy losses and always meet user demand, thus selecting the most appropriate plant size.

4. Waste-to-Energy for MSW treatment

WtE technologies are any waste treatment processes that generate energy in the form of electricity, heat, or transport fuels from a waste source [86].

These technologies apply to a variety of waste types, ranging from semi-solid (e.g., thickened sludge from effluent treatment plants) to liquid (e.g., domestic sewage) and gaseous (e.g., refinery gases) [86]. The most common application, by far, is the processing of (MSW) [87]. Incineration in a combined heat and power (CHP) plant is the most well-known WtE technology for MSW processing [86].

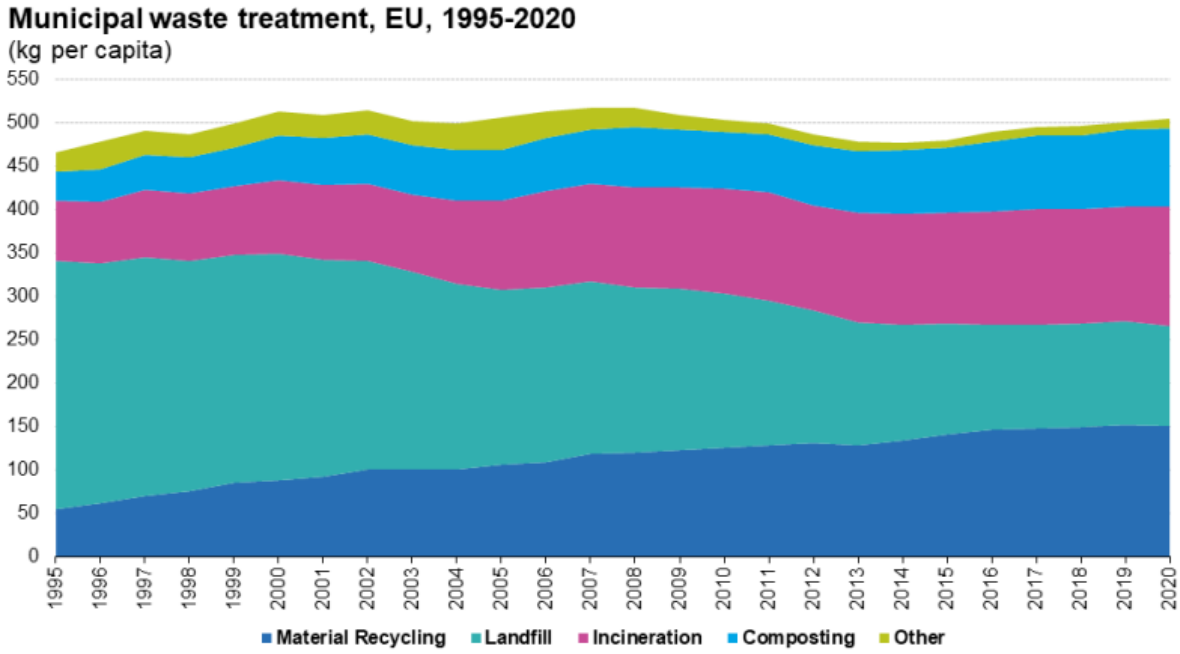

Figure 29 - Predominant MSW treatments in EU *[87]*.

4.1. Incineration of MSW

Waste incineration occurs when there is an excess of oxygen (complete oxidation). In the case of solid municipal waste, for example, incineration can reduce its initial volume by 90% and weight by 75% [88].

The components of a system of a WtE incineration project are similar to the ones in general thermal power generation plants, such as thermal and ash handling systems, water supply, water treatment systems, etc [89]. A waste leachate treatment system is also taken into consideration to manage the waste leachate produced during storage [90].

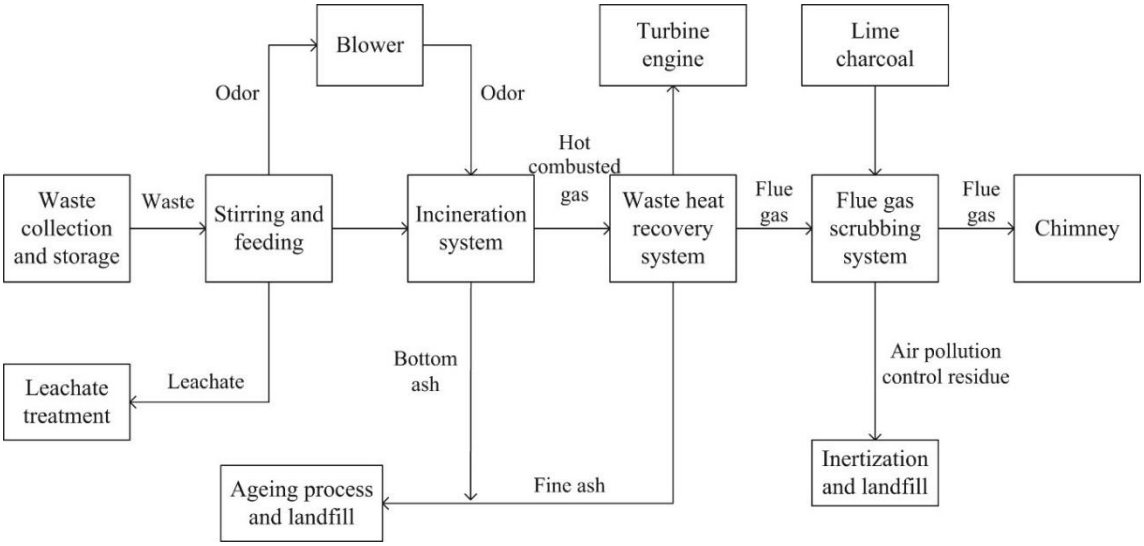

Figure 30 - Flowchart schematic of a WtE incineration plant *[89]*.

The specific technological solution of an incineration plant can undergo numerous modifications depending on the investor's needs and the type of waste incinerated [88]. Currently, mostly incineration plants designed for the incineration of municipal solid waste or hazardous and industrial waste are in operation [88]. Aside from these two types of the most common incineration plants, there are numerous specialised units, which include, for example, incineration plants for industrial sediments, such as those used in pulp and paper production [91].

MSW technologies underwent a rapid development process that produced the complex systems existent nowadays. The waste is thermally decomposed, and its energy is used with little impact on the environment. Under European conditions, MSW is a fuel with a heating capacity ranging from 7.2 to 14.9 GJ/t [88].

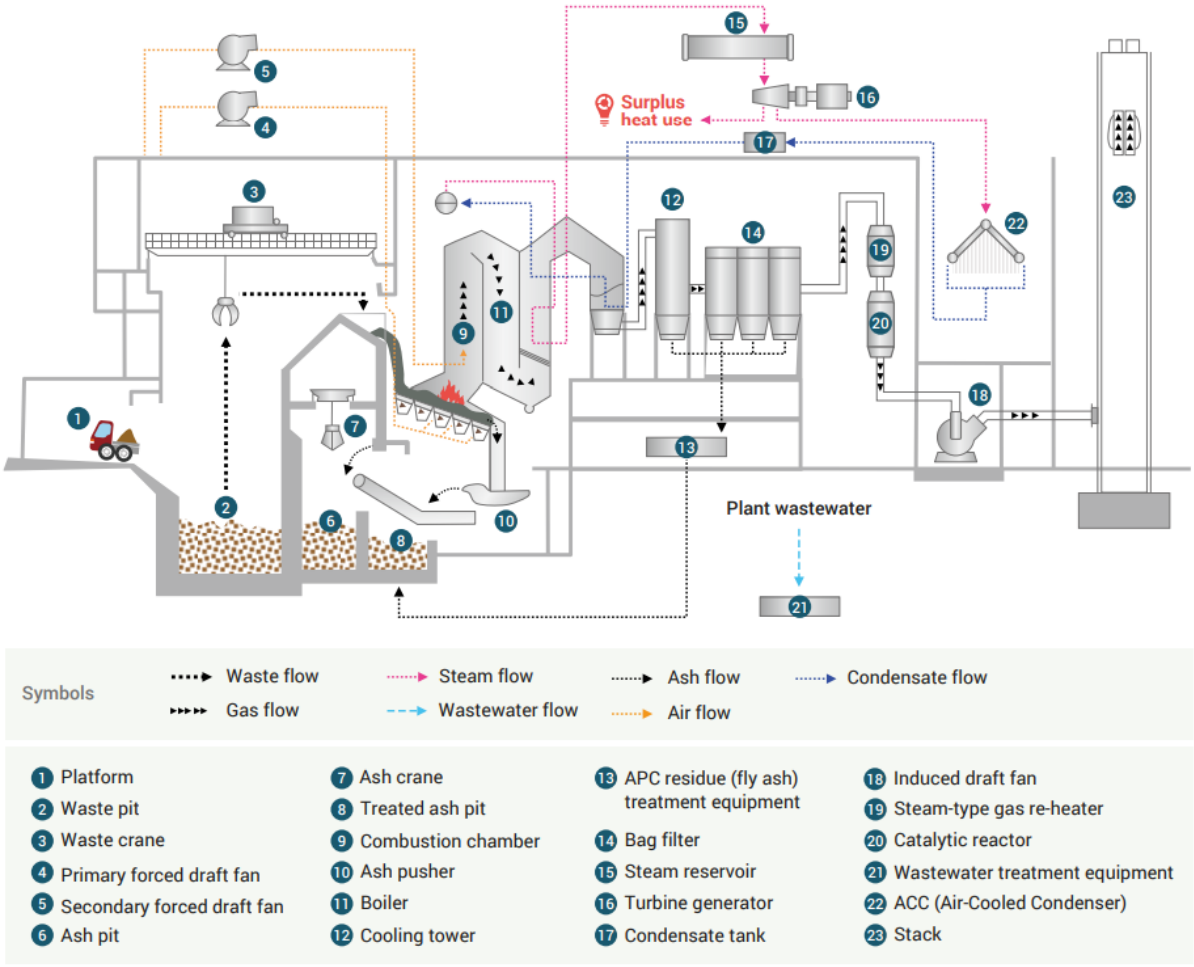

Figure 31 – Example of a MSW incinerator scheme in urban areas in Japan *[92]*.

In the initial stage of the incineration, the flammable components of the waste come to incineration and to evolving nearly all the heat contained in the combustibles of the waste [88]. This occurs in combustion chambers with moving grate, rotary kilns and incineration in fluidised bed can be utilised [88]. The fluidised bed technology requires that MSW have a certain particle size range; therefore, some preliminary modification or waste separation is required in this case.

The thermal decomposition and oxidation of combustible substances are completed in the burning out part - secondary combustion chamber (SCC), which constitutes the second combustion stage [88]. A properly constructed device allows the flue gas to stay in the area of high temperatures for the necessary time for the decomposition of even the most stable compounds in the flue gas [88]. The walls of the secondary combustion chamber frequently have a built-in tubular heat exchange system from the boiler's evaporating part, which attaches the thermal block to the released heat utilisation system [93], where the flue gas is led into, before reaching the flue gas cleaning system [88].

Energy Production from Incineration of MSW

The heat recovery system of a WtE plant is often made of air pre-heaters, steam generators or different types of heaters that are used to cool down the temperature of the flue gas generated, as other forms of energy, are produced from the heat [88]. This energy production has a significant positive impact on the economics of the plant.

In the case of cogeneration of power and heat, a bleeding condensing turbine or a backpressure turbine may be used.

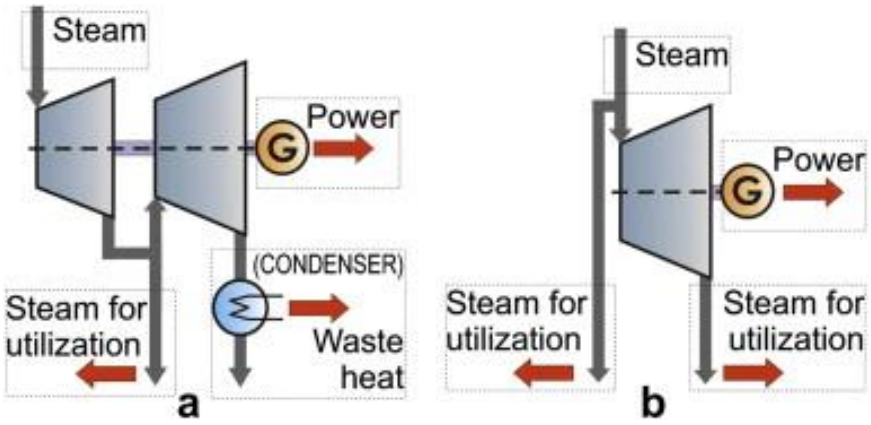

Figure 32 - a) System based on bleeding condensing turbine (b) System based on backpressure turbine *[88]*.

According to [88], a heat recovery system ought to be designed in such a way that the power production reaches between 0.3 to 0.7 $\mathrm{MWh_{el}/t}$ of incinerated waste. The lower limit can be achieved by using a backpressure turbine, such as in a cogeneration system with maximal heat supply into the hot water system with standard parameters of steam at 400 °C and 4 MPa. While the upper limit can be achieved by using condensing turbines in units with higher processing capacity.

The efficiency of the power production can be increased by reducing the pressure behind the turbine or increasing the parameters of steam at the turbine entry (boiler output). However, higher values of steam will lead to more risks of high-temperature corrosion [88].

4.2. Characteristics of the CTRSU

The Central of Municipal Solid Waste Treatment (CTRSU) is a WtE plant with energy recovery for electricity production, operated by the company Valorsul, located in the metropolitan area of Lisbon, Portugal. It consists of an incineration plant for mass burning of solid waste with 3 incineration lines installed, each with a capacity of processing 28 $\mathrm{t/h}$ of MSW [94].

CTRSU is equipped with 3 boilers, each producing around 66 $\mathrm{t/h}$ (420 ℃, 52.8 bar) of steam [95]. The boilers are connected to a turbogenerator with a condensing turbine with a rated power of 50 MW to produce electricity. The annual electricity production is approximately 350 GWh, and a small fraction is used for internal consumption of the plant, while most of it is injected into the Portuguese national electricity grid [96].

The CTRSU is the main unit of the Valorsul in terms of energy production and economic revenues. In 2019, 316 GWh of the 361 GWh of electricity produced was exported to the national grid. While in 2020, the revenues from the CTRSU electricity sales represented about 41% of the total revenues of the company [97].

Like many other incineration WtE systems with energy recovery, CTRSU follows 5 main operation stages: Reception of the unsorted MSW, combustion, electrical energy production, flue gas treatment, and ash residue treatment.

Electricity Production

The heat produced in the combustion is used in the boilers to generate steam at a high temperature that is then applied to the turbogenerator for electrical energy production. Natural gas is utilised to start up the combustion and on occasions when the minimum temperature of 850 ℃ needs to be maintained inside the combustion chamber.

The water circulated in the boilers unit is previously demineralised to avoid corrosions in the walls of the unit. Despite the water circulation system being a closed loop, there are still some losses that occur through purging and other loss factors; therefore, some water is injected according to the necessity into the water storage tank that feeds into the boiler to replenish for losses, around 6 to 7 $\mathrm{m^3/h}$ [94].

Because of the proximity of the plant installations to the Tagus River, water for cooling down the condenser is obtained directly from the river with an open circuit. Filters are used to avoid the entrance of undesired particles into the engine unit.

The system of electricity production from CTRSU uses a steam flowrate of about 198 $\mathrm{t/h}$ for the turbogenerator. The gross power production is estimated at 587 $\mathrm{kWh/t}$ of MSW, from which 89 $\mathrm{kWh/t}$ is for internal consumption [95].

5. Scenarios for Hydrogen Production in CTRSU

The alkaline and the SOEC electrolysis technologies were targeted as the most desirable candidates for hydrogen production in CTRSU since the alkaline is currently the most established and mature technology for water electrolysis in the market and the SOEC would seem to be well fitting as the WtE plant already produces both electricity and high-temperature steam. Hence, to evaluate the feasibility of Hydrogen production, two scenarios were defined and both technologies will be assessed inside each scenario;

1. **Alkaline and SOEC hydrogen production using the total energy from the plant;**
2. **Alkaline and SOEC hydrogen production using one-third of the total energy from the plant.**

To execute the analysis of hydrogen production in both scenarios, some initial values were acquired from the company Valorsul based on numbers from the year 2019. The data from the year 2019 was preferred instead of the year 2020, because the production data for 2020 was rather atypical due to the pandemic situation that affected the regular consumption trend of citizens in the region of operation of the CTRSU, resulting in a lower level of energy production [97].

In both scenarios, it is assumed an injection of the gas into the grid with regular demand, however, a 24h buffer storage is considered necessary to maintain a regular supply.

The costs related to power supply, installation, the general balance of the plant and others are assumed to be included in the CAPEX for the electrolyser system as indicated in [98].

5.1. Scenario 1: Hydrogen Production Using the Total Energy from CTRSU

In this first scenario, the possibility of converting the entire energy production into hydrogen fuel is considered.

Table 3 – Energy production data at CTRSU from the year 2019 *[97]*.

Parameter	**Value**	**Unit**
Power Produced	316,375	MWh
Steam Produced	1,710,959	tonnes
Annual Plant Availability (h_a)	8,410	hours

Scenario 1: Alkaline Electrolysis Case

Considering the large scale of production to be considered in this case, a NEL electrolyser A3880 is chosen for reference for the calculations.

The A series of electrolysers from NEL are amongst the most energy efficient in the world [99], with different projects at a large scale around the world, such as the Green H_2 for Fuelling in AZ & CA for Demo plus 28 Stations Network, USA [100] and Norway (Notodden) Atmospheric Alkaline Water Electrolysers [101].

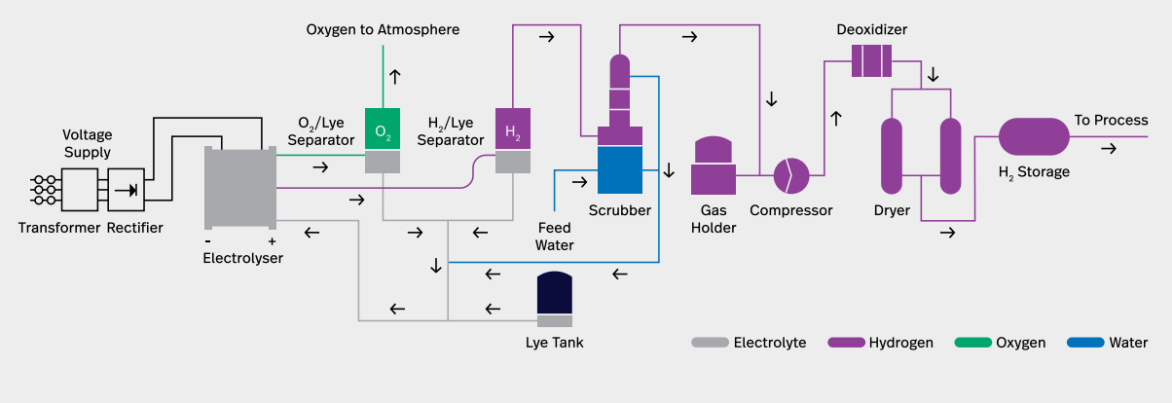

Figure 33 - Process flowchart of A3880 electrolysis system *[99]*.

The electrolyser systems in general operate with DC power, hence at the initial stage of the process, AC power must be converted to DC, which implies some energy losses. Scrubbing for filtration of the gas and compression for storage are also other operations that contribute to the energy consumption of the system level being slightly higher than the consumption at the stack level.

Figure 34 – 3D Plant set up of A3880 *[99]*.

The A series electrolysers feature a cell stack power consumption of down to 3.8 $\mathrm{kWh/Nm^3}$of hydrogen gas produced, up to 2.2 MW per stack. Each of the stacks can produce up to 485 $\mathrm{Nm^3/h}$ of hydrogen or just over 1 tonne per day [99].

The key specifications of the electrolysis system can be found in Table 4.

Table 4 - Key specifications of the A3880 *[99]*.

Specifications	**A3880**
Capacity Range per Unit	2 400 - 3 880 $\mathrm{Nm^3/h}$
DC Power Consumption at Stack Level	3.8-4.4 $\mathrm{kWh/Nm^3}$
H_2 Purity	99.9 ± 0.1%
O_2 Purity	99.5 ± 0.2%
Delivery Pressure	1–200 bar(g)
Electrolyte	25% KOH Aqueous Solution
Ambient Temperature	5-35°C

Based on technical data from other electrolyser systems with similar values to A3880, such as the SUNFIRE-HYLINK ALKALINE [102], for the calculations, the AC power consumption at the system level was assumed to be 4.7 $\mathrm{kWh/Nm^3}$.

The size of the electrolysis system required for the case scenario is determined by equation (7), which estimates the $\mathrm{H_2}$ production capacity rate $\mathrm{Nm^3\ (of\ H_2)/h}$.

$$\mathrm{H_2\ (Nm^3/h)} = \frac{\text{Available Power (kWh)}}{\text{System Consumption Rate (kWh/Nm}^3\text{)} \times \mathrm{h_a(h)}} \tag{7}$$

The $\mathrm{H_2}$ production capacity rate can also be estimated in $\mathrm{kg(of\ H_2)/h}$ by adopting the system consumption rate in $\mathrm{kWh/kg}$, (see equation (8)).

$$\mathrm{H_2\ (kg/h)} = \frac{\text{Available Power (kWh)}}{\text{System Consumption Rate (kWh/kg)} \times \mathrm{h_a(h)}} \tag{8}$$

In the same manner, the $\mathrm{O_2}$ production in the electrolysis system can also be estimated by the stoichiometric of $\mathrm{H_2O}$. For each 2 mol of $\mathrm{H_2}$ produced during the splitting of water one mol of $\mathrm{O_2}$ is produced. And for 1kg of $\mathrm{H_2}$, there is 8kg of $\mathrm{O_2}$.

$$\mathrm{2H_2(g) + O_2(g) \rightarrow H_2O(l)} \tag{9}$$

Additionally, the potable water that is to be fed into the electrolysis system is to be demineralised, and, it is assumed that the electrolysis plant includes a water treatment system with reverse osmosis that requires 1.2 to 2 $\mathrm{L/Nm^3}$ [13 to 17 L/kg of $\mathrm{H_2}$] (varies depending on potable water quality) to produce approximately 0.8 $\mathrm{L/Nm^3}$ of demineralised water for the electrolysis process [103]. Therefore, the potable water consumption rate is taken as 2 of $\mathrm{L/Nm^3}$ of $\mathrm{H_2}$, considering the worst scenario possible of potable water quality.

Having the demineralised water consumption rate, it is also possible to estimate the KOH rate per $\mathrm{H_2}$, considering the density of KOH to be 2040 $\mathrm{kg/m^3}$ [104], and the density of $\mathrm{H_2}$ at NTP (0.0837 $\mathrm{kg/m^3}$).

Table 5 - Production and consumption rates.

$\mathrm{H_2}$ Production	$8\,000\ \mathrm{Nm^3/h}$
	$670.35\ \mathrm{kg/h}$
$\mathrm{O_2}$ Production	$4\,000\ \mathrm{Nm^3/h}$
	$5326.68\ \mathrm{kg/h}$
Potable Water Consumption	$2\ \mathrm{L/Nm^3(H_2)}$
	$0.02388\ \mathrm{m^3/kg(H_2)}$
KOH Consumption	$4.87\ \mathrm{kg(KOH)/kg(H_2)}$

The A3880 would therefore be scaled up to a 17 stacks modular system to cover the $\mathrm{H_2}$ production rate. Since each stack is rated at 485 $\mathrm{Nm^3/h}$ and 2.2 MW, the system capacity range per unit is 8245 $\mathrm{Nm^3/h}$, 37.4 MW.

CAPEX and OPEX for the A3880 are not available. Hence, values were estimated based on values presented in different literature, such as [66] and [98]. CAPEX and OPEX data were obtained from a report from IRENA [98] that presents comprehensive information about a 20 MW alkaline system. Subsequently, the value of the electrolyser CAPEX was scaled for a 37.4 MW system using Figure 23. Furthermore, the CAPEX for compression of $\mathrm{H_2}$ before storage had to be calculated separately.

The power $\mathrm{P(kW)}$ required to compress $\mathrm{H_2}$ from $\mathrm{p_{in}} = 1\ \mathrm{bar}$, atmospheric pressure at electrolysis delivery to $\mathrm{p_{out}} = 200\ \mathrm{bar}$ is computed with the equation (10) from [105].

$$\mathrm{P(kW)} = \mathrm{Q} \times \frac{\mathrm{ZTR}}{\mathrm{M_{H_2}} \times \eta_{\mathrm{comp}}} \times \frac{\mathrm{N}\gamma}{\gamma - 1} \times \left[\left(\frac{\mathrm{p_{out}}}{\mathrm{p_{in}}} \right)^{\frac{\gamma - 1}{\mathrm{N}\gamma}} - 1 \right] \tag{10}$$

Where Q is the flow rate in $\mathrm{kg/s}$, Z the compressibility factor (set at 1 as an approximation), T the temperature at the inlet (293.15 K), R the ideal gas constant (8.314 $\mathrm{J/K.mol}$), $\mathrm{M_{H_2}}$ the hydrogen molecular mass, η_{comp} the compressor efficiency (set at 75%), N the number of compressor stages and γ the isentropic coefficient (1.4). After computing, the compression power, the compressor CAPEX can be calculated with the equation

$$\mathrm{CAPEX_{compressor}}\,(€) = 0.84 \times 15\,000\ \times \left(\frac{\mathrm{P(kW)}}{10\ \mathrm{kW}}\right)^{0.9} \quad (11)$$

Table 6 shows the complete information regarding the unit CAPEX and OPEX established for the alkaline case in scenario 1.

Table 6 - Capital and operational costs rates for scenario 1: alkaline case.

Equipment	**Costs**
Electrolyser system	
CAPEX [€/kW]	550
OPEX [% of electrolyser CAPEX/YEAR]	2 [98]
CAPEX stack replacement [€/kW]	340 [98]
Potable Water [$€/m^3$]	3.26 [106]
KOH [€/kg]	0.475 [107]
H_2 Compressor	
CAPEX [€/kW]	694.45
OPEX [% of compressor CAPEX/YEAR]	3 [17]
H_2 Storage	
CAPEX [€/kg]	225 [17]
OPEX [% of storage CAPEX/YEAR]	0.5 [17]

In Table 7, there are presented the CAPEX and OPEX calculated according to the size of the electrolysis system.

Table 7 - CAPEX and OPEX for the A3880 system with 17 stack modules.

Equipment	**Costs**
Electrolyser system	
CAPEX [€]	20,570,000
OPEX [€/YEAR]	411,400
CAPEX stack replacement [€]	12,716,000
Potable Water [€/kg(H_2)]	0.0778488
KOH [€/kg(H_2)]	2.313972
H_2 Compressor	
CAPEX [€]	2,684,713.872
OPEX [€/YEAR]	80,541.416
H_2 Storage	
CAPEX [€]	3,728,894.47
OPEX [€/YEAR]	18,644.47

Scenario 1: SOEC Case

For the high temperature of water electrolysis case, a Topsoe electrolyser system (SOEC 100 MW SOEC 32,000 $\mathrm{Nm^3/h}$) [108] is considered as reference. Topsoe is a compact stack built mainly from abundant, low-cost ceramic materials enclosed within a metal housing, and offers Industry-leading efficiency.

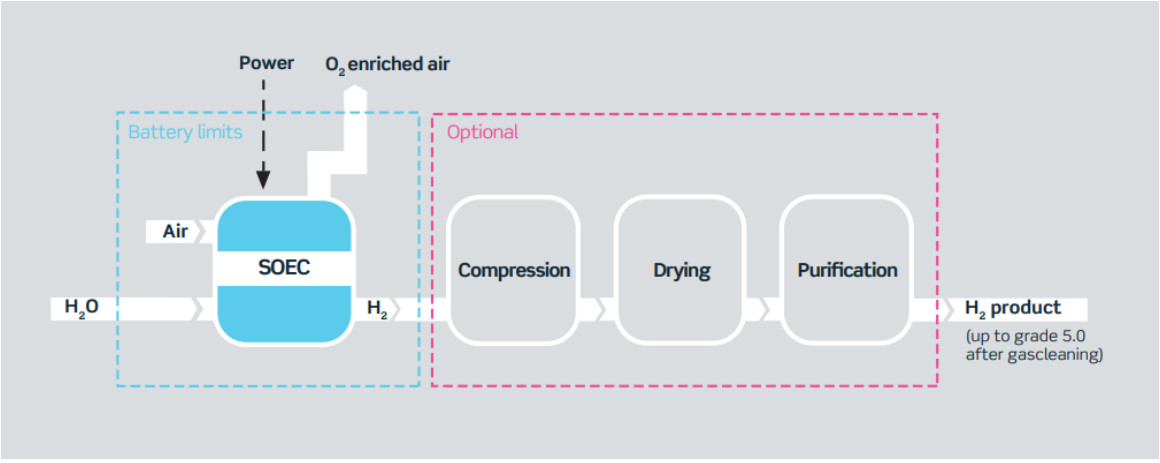

Figure 35 - Topsoe SOEC unit process model *[108]*.

The key specifications of the Topsoe SOEC system electrolysis system can be found in Table 8.

Based on the same reason as in the alkaline case (Scenario 1: Alkaline Electrolysis Case), the AC power consumption at the system level is estimated to be 3.4 $\mathrm{kWh/Nm^3}$.

Table 8 - Key specifications of the Topsoe SOEC electrolyser system *[108]*.

Specifications	**Topsoe**
Capacity Range per Unit	32,000 $\mathrm{Nm^3/h}$
Power consumption rating	100 MW
DC Power Consumption at Stack Level	3.1 $\mathrm{kWh/Nm^3}$
H_2O (Steam) consumption	27,000 kg/h
H_2 Purity	Up to 99.999% (dry basis after gas cleaning)
Delivery Pressure	2 bar(g)
Delivery temperature	Ambient

The Topsoe SOEC capacity range proved to be oversized for the CTRSU plant energy specifications because, with the energy available at CTRSU, the H_2 production capacity range would not be more than 12,000 $\mathrm{Nm^3/h}$. Hence, the SOEC was scaled down by a factor of 3, which gives the characteristics in Table 9.

Table 9 – SOEC system characteristics sized according to CTRSU energy specifications.

Specifications	**Topsoe**
Capacity Range per Unit	10,666.66 $\mathrm{Nm^3/h}$
Power Consumption Rating	33.3 MW
AC Power Consumption at System Level	3.4 $\mathrm{kWh/Nm^3}$
H_2O (Steam) Consumption Flowrate	9,000 kg/h

SOEC electrolysis utilised both electricity and steam as inputs, therefore, a fraction of the steam generated by the boiler will be deviated from entering the turbogenerator, to be applied to the electrolysis simultaneously with the electricity produced with the remaining fraction that entered the turbogenerator. This implies that the total electricity available for electrolysis will be reduced compared to the alkaline case.

Knowing the steam flow rate required, it is possible to estimate the annual amount of steam required by multiplying by the plant's annual availability hours. The steam required per year is then computed as a percentage of the total amount of steam available in the year 2019. This process is represented in equation (12).

$$\text{Steam Input (\%)} = \frac{\text{Steam Consumption Flowrate (kg/h)} \times \mathrm{h_a\ (h)}}{\text{Steam Produced (kg)}} \quad (12)$$

The power input is then deduced from the remained percentage of steam not used as direct input for electrolysis which is converted into electricity.

$$\text{Power Input (kWh)} = [100\% - \text{Steam Input (\%)}] \times \text{Power Produced}_{2019}\ \text{(kWh)} \quad (13)$$

Table 10 - Steam and energy usage ratio for SOEC.

Steam and Energy Usage Ratio			
Steam to SOEC	4.42%	**Steam to SOEC**	75,690 tonnes
Steam to Electricity	95.58%	**Electricity to SOEC**	302.4 GWh
Electricity/Steam Ratio	$4\ \text{kWh/kg}(H_2O)$		

The production rates of hydrogen and oxygen are estimated using both the power consumption rate and steam flow rate of the SOEC system, combined with the amounts of electrical power and steam available for input.

Table 11 - Production rates for scenario 1, SOEC case.

H_2 Production	$10{,}574.91\ \text{Nm}^3/\text{h}$
	$885.67\ \text{kg/h}$
O_2 Production	$5287.46\ \text{Nm}^3/\text{h}$
	$7{,}037.60\ \text{kg/h}$

CAPEX and OPEX for the Topsoe electrolysis are not available, hence, the values are obtained from academic literature and reports. Likewise, the power $P(kW)$ required to compress H_2 from $p_{in} = 2\ \text{bar}$, delivery pressure from the Topsoe electrolyser unit to $p_{out} = 200\ \text{bar}$ is computed with the equation (10) from [105]. And the compressor CAPEX is equally obtained from equation (11).

Table 12 - Capital and operational costs rates for scenario 1: SOEC case.

Equipment	**Costs**
Electrolyser system	
CAPEX [€/kW]	2,500 [109]
OPEX [% of electrolyser CAPEX/YEAR]	3 [110]
CAPEX stack replacement [€/kW]	340 [98]
H_2 Compressor	
CAPEX [€/kW]	693.58
OPEX [% of compressor CAPEX/YEAR]	3 [17]
H_2 Storage	
CAPEX [€/kg]	225 [17]
OPEX [% of storage CAPEX/YEAR]	0.5 [17]

In Table 13, there are presented the CAPEX and OPEX calculated according to the size of the SOEC electrolysis system adapted to the energy specifications of the CTRSU.

Table 13 - CAPEX and OPEX for the Topsoe SOEC.

Equipment	**Costs**
Electrolyser system	
CAPEX [€]	83,333,333.33
OPEX [€/YEAR]	2,500,000
CAPEX stack replacement [€]	11,333,333.33
H_2 Compressor	
CAPEX [€]	2,715,322.526
OPEX [€/YEAR]	81,459.67
H_2 Storage	
CAPEX [€]	4,824,120.603
OPEX [€/YEAR]	24,120.603

5.2. Scenario 2: Hydrogen Production Using One-third of Total Energy from CTRSU

In this scenario, only one-third of the initial values of power and steam produced at CTRSU are considered for hydrogen production. But the annual plant availability time remains constant.

Table 14 – Energy values for scenario 2.

Parameter	**Initial value**	**One third value**	**Unit**
Power Produced	316,375	105,458.3	MWh
Steam Produced	1,710,959	570,319.6	tonnes
Annual Plant Availability (h_a)	8,410		hours

Scenario 2: Alkaline Electrolysis Case

For this case, the A3880 is chosen again, although the capacity of the electrolysis plant unit must be adjusted to a certain extent to meet the production rates of this scenario.

The production rates are calculated based on equations (7) and (8). While the consumption rates remain unchanging.

Table 15 - Production and consumption rates for scenario 2: alkaline case.

H_2 Production	$2{,}668\ Nm^3/h$
	$223.45\ kg/h$
O_2 Production	$1{,}334\ Nm^3/h$
	$1{,}775.56\ kg/h$
Potable Water Consumption	$2\ L/Nm^3(H_2)$
	$0.02388\ m^3/kg(H_2)$
KOH Consumption	$4.87\ kg(KOH)/kg(H_2)$

Based on production rates from Table 15 the A3880 is then scaled to a 6 stacks modular system to cover the H_2 production rate. Since each stack is rated at 485 Nm^3/h and 2.2 MW, the system capacity range per unit is 2910 Nm^3/h, 13.2 MW.

CAPEX and OPEX are estimated based on the rates presented in Table 6, with two exceptions:

- Since the size of the electrolyser system CAPEX rate is now smaller (13.2 MW) than in Scenario 1: Alkaline Electrolysis Case, the value of CAPEX per unit of power is estimated to be 575 €/kW, based on Figure 23.
- The Compressor CAPEX per unit had to be recalculated using equations (10) and (11) since the hydrogen flowrate Q takes a smaller value compared to scenario 1.

Table 16 - CAPEX and OPEX for the A3880 system with 6 stack modules.

Equipment	**Costs**
Electrolyser system	
CAPEX [€]	7,590,000
OPEX [€/YEAR]	151,800
CAPEX stack replacement [€]	4,488,000
Potable Water [€/kg(H_2)]	0.0778488
KOH [€/kg(H_2)]	2.313972
H_2 Compressor	
CAPEX [€]	1,051,550.424
OPEX [€/YEAR]	31,546.51
H_2 Storage	
CAPEX [€]	1,316,080.402
OPEX [€/YEAR]	6,580.402

Scenario 2: SOEC case

For the high temperature of water electrolysis case of scenario 2, a SUNFIRE-HYLINK SOEC system [111] is considered as a reference. The electrolyser follows a modular system design. One system produces 750 Nm³/h hydrogen with an AC power consumption of 3.6 kWh/Nm³.

SUNFIRE-HYLINK SOEC is pointed to be implemented in a few projects on small scale (less than 3 MW), such as the MULTIPLHY project, which consists of a SOEC electrolyser that will supply renewable hydrogen to Neste's refinery in Rotterdam as a replacement for hydrogen produced from fossil natural gas, and the GRINHY 2.0 to produce renewable, high-purity hydrogen that will be used for annealing processes in Salzgitter's integrated steelwork as a replacement for hydrogen produced from natural gas [111].

Figure 36 - SUNFIRE-HYLINK SOEC representation *[111]*.

SUNFIRE-HYLINK SOEC is chosen in this case scenario because the production rate is expected to be much lower compared to scenario 1: SOEC case. Since the technical data available for the SUNFIRE-HYLINK SOEC is estimated for relatively small production capacity rates, it is assumed that scaling the SUNFIRE-HYLINK SOEC will provide more accurate estimations in terms of power consumption and steam flowrate requirements than the Topsoe unit applied in the latter scenario.

Table 17 - Key specifications of the SUNFIRE-HYLINK SOEC electrolyser system *[111]*.

Specifications	**SUNFIRE-HYLINK**
Capacity Range per Unit	750 $\mathrm{Nm^3/h}$
Power consumption rating	2.68 MW
DC Power Consumption at Stack Level	3.3 $\mathrm{kWh/Nm^3}$
AC Power Consumption at System Level	3.6 $\mathrm{kWh/Nm^3}$
H_2O (Steam) consumption	860 kg/h
H_2 Purity	99.99 %
Delivery Pressure	0 bar(g)
Delivery temperature	Ambient

After calculations, the SUNFIRE-HYLINK SOEC capacity range was found to be undersized for the CTRSU plant energy specifications, as with one-third of the total energy available at CTRSU, the H_2 production capacity range would be around 3,500 $\mathrm{Nm^3/h}$. Hence, the SOEC was scaled up by a factor of 5, which gives the characteristics in Table 18.

Table 18 – SOEC system characteristics sized according to CTRSU energy specifications.

Specifications	**SUNFIRE-HYLINK**
Capacity Range per Unit	3,750 $\mathrm{Nm^3/h}$
Power Consumption Rating	13.4 MW
AC Power Consumption at System Level	3.6 $\mathrm{kWh/Nm^3}$
H_2O (Steam) Consumption Flowrate	4,300 kg/h

The steam and power input percentages for the high-temperature electrolysis with SUNFIRE-HYLINK SOEC were estimated by applying equations (12) and (13) to attain the values in Table 19.

Table 19 - Steam and energy usage ratio for SOEC, scenario 2.

Steam and Energy Usage Ratio			
Steam to SOEC	6.34%	**Steam to SOEC**	36,163 tonnes
Steam to Electricity	93.66%	**Electricity to SOEC**	98.8 GWh
Electricity/Steam Ratio	$2.73\ \mathrm{kWh/kg(H_2O)}$		

Therefore, production rates of hydrogen and oxygen can be estimated using both the power consumption rate and steam flow rate of the SOEC system, combined with the amounts of electrical power and steam available for input.

Table 20 - Production rates for scenario 2, SOEC case.

H_2 Production	$3262.37\ \mathrm{Nm^3/h}$
	$273.2\ \mathrm{kg/h}$
O_2 Production	$1631.18\ \mathrm{Nm^3/h}$
	$2{,}171.10\ \mathrm{kg/h}$

CAPEX and OPEX for scenario 2: SOEC case is estimated based on the rates presented in Table 12, considering the two exceptions mentioned previously in 0. The CAPEX for the electrolyser system is now estimated at the rate of 2750 €/kW.

Table 21 - CAPEX and OPEX for the SUNFIRE-HYLINK SOEC.

Equipment	**Costs**
Electrolyser system	
CAPEX [€]	36,850,000
OPEX [€/YEAR]	1,105,500
CAPEX stack replacement [€]	4,556,000
H_2 Compressor	
CAPEX [€]	1,321,157.376
OPEX [€/YEAR]	39,634.72
H_2 Storage	
CAPEX [€]	1,695,979.90
OPEX [€/YEAR]	8479.90

5.3. Oxygen Selling Option

In both scenarios presented in the previous sections, it is seen that oxygen is also produced in large amounts (0.5 m^3 per m^3 of hydrogen or 8 kg for every kg of hydrogen), which could be economically advantageous if sold instead of being freely released into the atmosphere. Despite having the largest share of the global industrial gas market (26%) [21], the potential for selling oxygen is esteemed to be low, except in cases where the oxygen produced in the plant can be used onsite [112]. The location of the production plant is critical for the potential sale of oxygen, as is the balance of supply and demand. If the oxygen demand is not as high as the supply of the plant, large amounts of oxygen will be wasted, and capturing it may not be economically feasible [112]. Nonetheless, oxygen capture will be considered in both cases (alkaline and SOEC) for scenarios 1 and 2.

A 24h buffer storage approach is considered as in the hydrogen production scenarios with a pipeline system for direct injection. Liquefaction and storage in tanks are assumed because of the large production rates, with the possibility to sell to local industry or for medical applications (high purity).

The estimations for CAPEX and OPEX for Oxygen liquefaction and storage are mostly based on the work present in [17].

Table 22 - Capital and operational costs rates for O_2 liquefaction and storage.

Equipment	**Costs**
O_2 Liquefaction	
CAPEX $[€/\mathrm{kW}_{\mathrm{electrolyser}}]$	125 [17]
OPEX [% of Liquefaction CAPEX/YEAR]	3 [17]
O_2 Storage	
CAPEX $[€/\mathrm{m}^3{}_{\mathrm{liquid\ O_2}}]$	453 [113]
OPEX [% of Storage CAPEX/YEAR]	3 [17]

In [17] there is the assumption that 65,280 $\mathrm{kg}_{\mathrm{O_2}} \approx 57\ \mathrm{m}^3$ of liquid $\mathrm{O_2}$, which is an approximation confirmed in [114]. This rate was therefore assumed for the liquefaction of $\mathrm{O_2}$ calculations throughout this study.

The price of oxygen varies in the literature and is determined by its form (gaseous/liquid) and end-use application. The price per tonne was claimed to range from 24.5 €/tonne to values of 250 €/tonne in Finland for medical use (liquid oxygen) [17]. However, the cost of oxygen for industrial applications is 100 €/tonne.

6. Results and Discussion

6.1. Hydrogen Production Cost

Initially, the specific cost of hydrogen production (C_{H_2}) is calculated for all scenarios and cases, as a function of the variation in the electricity prices. Oxygen selling is also considered for the calculations. The formula for the specific cost of hydrogen production is described below in equation (14), adapted from [17].

$$C_{H_2} = \varepsilon_{electrolyser} \times \left(p_{elect} + \frac{OPEX_{H_2}}{P.h_a}\right) + \varepsilon_{compressor}.p_{elect} + \varepsilon_{H_2O} + \varepsilon_{KOH} \quad (14)$$

Where $\varepsilon_{electrolyzer}$ represents the power consumption of the electrolyser at the system level $[kWh/kg_{H2}]$; p_{elect} the electricity price $[€/kWh]$; $OPEX_{H_2}$ the electrolyser system, compressor and H_2 storage OPEX $[€/year]$; P the electrolyser system power rating $[kW]$; h_a the annual plant availability hours $[h]$; $\varepsilon_{compressor}$ the specific power consumption of the compressor $\left[kWh/kg_{H_2}\right]$ (0.93 [17]); ε_{H_2O} the water cost per kg of produced H_2 $[€/kg_{H_2}]$; ε_{KOH} the KOH cost per kg of produced H_2.

For the SOEC case ε_{H_2O} and ε_{KOH} are considered zero, as water is replaced by the steam already existent at the WtE plant and KOH is not needed.

When oxygen selling is introduced, the specific cost of oxygen production (C_{O_2}) is also calculated considering the OPEX of O_2 liquefier and storage $[€/year]$ ($OPEX_{O_2}$), and ε_{liq} the liquefier power consumption $\left[kWh/kg_{O_2}\right]$ ($\varepsilon_{liq} = 0.52$ [17]).

$$C_{O_2} = \varepsilon_{electrolyser} \times \left(p_{elect} + \frac{OPEX_{O_2}}{P.h}\right) + 8 \times \varepsilon_{liq}.p_{elect} - 8 \times p_{O_2} \quad (15)$$

Therefore, the total specific cost of hydrogen with the impact of oxygen (C_{H_2/O_2}) is estimated by equation (16). Where p_{O_2} is the selling price of oxygen, considered as 100 €/tonne (for industrial applications).

$$C_{H_2/O_2} = C_{H_2} + C_{O_2} \quad (16)$$

In both scenarios of hydrogen production, it is assumed that all capital investment costs for the hydrogen plant are achieved in year zero, and the hydrogen production activities start in year one,

hence, when calculating production costs of hydrogen, CAPEX values are not included in the equations (14) and (15).

Scenario 1

After applying equations (14) were (16), the results presented below were obtained, considering both hydrogen production cost and hydrogen production cost with the selling of oxygen.

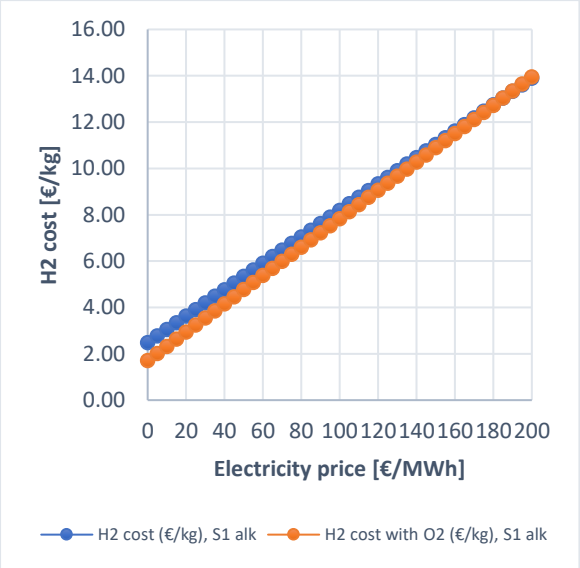

Figure a) Alkaline

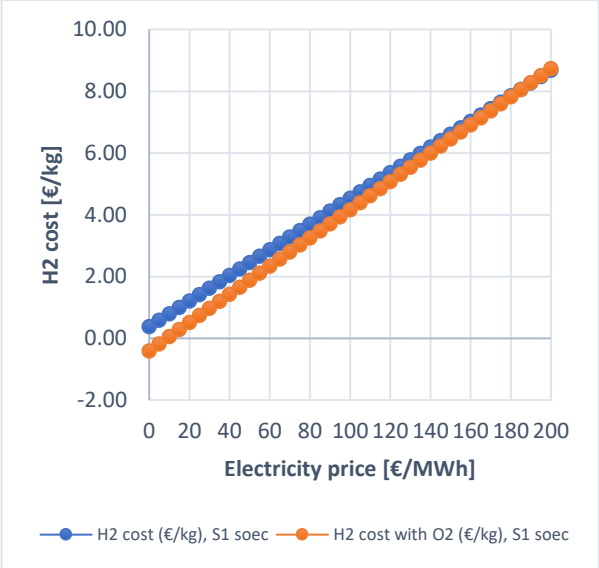

Figure b) SOEC

Figure 37 - Hydrogen production costs, scenario 1: a) alkaline case; b) SOEC case

In Figure 37, it is observed that the costs increase together with the electricity prices, and H_2 cost with oxygen selling is lower than H_2 cost without oxygen selling, however, the latter tends to become cheaper when electricity prices are high.

In the SOEC case, H_2 cost with oxygen selling is negative at very low prices of electricity because the oxygen selling revenue is higher than the cost of hydrogen production. This does not happen in the alkaline case because the cost of hydrogen production is higher than SOEC since additional feedstocks are required (potable water and KOH).

Scenario 2

In scenario 2, since hydrogen is being produced with one-third of electricity and the remaining two-thirds is being directly exported to the grid, the revenue of the electricity selling is deducted from the cost of hydrogen production (see equation (17)).

$$C_{H_{2\,\text{scenario 2}}} = C_{H_2} - \lambda \times p_{\text{elect}} \tag{17}$$

Where λ $[\mathrm{kWh/kg_{H_2}}]$ is the ratio of exported electricity per kg of produced $\mathrm{H_2}$, calculated with equation (18).

$$\lambda = \frac{\frac{2}{3} \times \text{total produced power(kWh)}}{\mathrm{H_2}\ \text{Production rate(kg/h)} \times \text{Plant availability(h)}} \tag{18}$$

The results of the cost of hydrogen production can be found in the two following figures below.

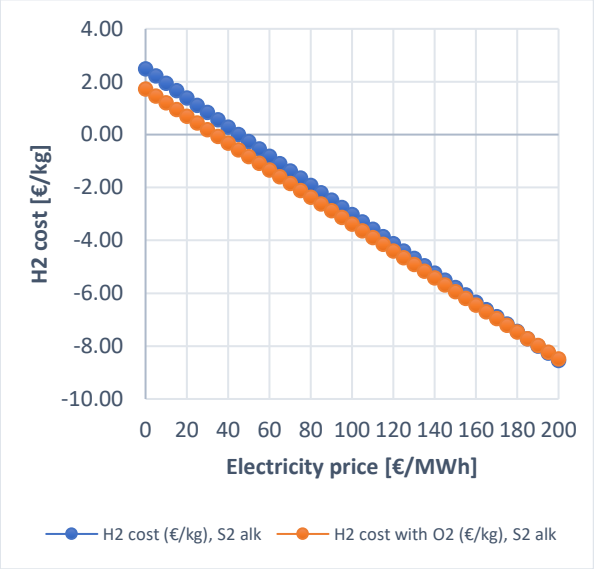

Figure a)

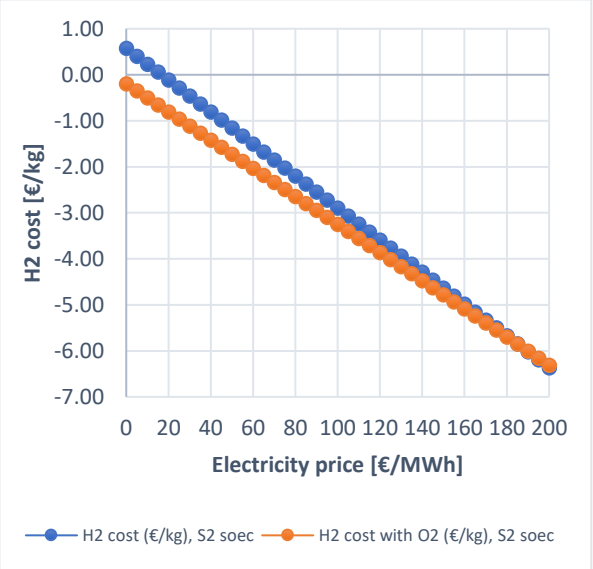

Figure b)

Figure 38 - Hydrogen production costs, scenario 2: a) alkaline case; b) soec case.

Comparison of Production Costs

Like the scenario 1, $\mathrm{H_2}$ cost with oxygen selling is negative at very low prices of electricity, contrary to $\mathrm{H_2}$ cost without oxygen selling that tends to become cheaper at high electricity prices. However, the greatest difference is the fact that in scenario 2 the costs decrease as the electricity price increases because the selling of the remaining two-thirds of electricity is deducted from the hydrogen costs.

In scenario 2, SOEC is initially the cheapest technology at low electricity prices but alkaline seems to take over at high prices. This only happens because λ is greater for the alkaline case as the plant has a lower $\mathrm{H_2}$ Production rate compared to the SOEC case which causes the alkaline case to have more direct electricity selling revenues than the SOEC case. Essentially, SOEC remains the cheaper technology as seen in scenario 1, and scenario 2 when the electricity prices are low (close to zero).

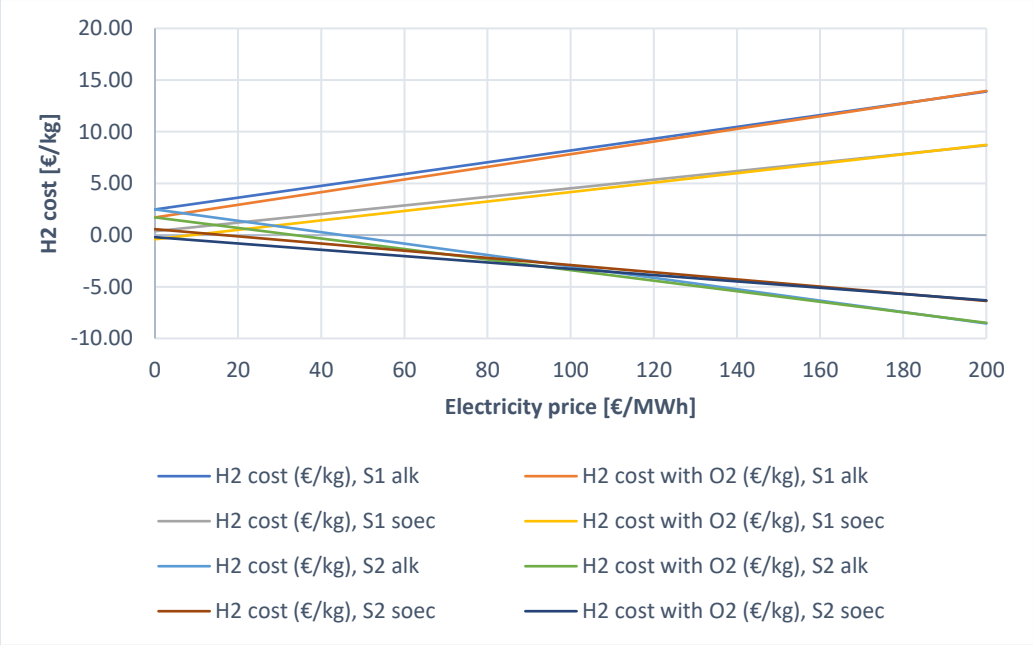

Figure 39 - Hydrogen production costs in all scenario cases.

Overall, scenario 1 with alkaline electrolysis is generally the most expensive option, and scenario 2 with alkaline technology is the cheapest, although the second cheapest, scenario 2 with SOEC, is not very far behind.

6.2. Selling Profits

Three different contexts are considered to analyse the profits:

1) Sale of hydrogen and oxygen.

$$\text{Profit} = Q_{H_2}\left[p_{H_2} + 8 \times p_{O_2} - \left(C_{H_2/O_2}\right)\right] \tag{19}$$

Q_{H_2} is the quantity of hydrogen produced in a year $[\text{kg}]$.

2) Sale of hydrogen only. Oxygen is released into the atmosphere.

$$\text{Profit} = Q_{H_2}\left[p_{H_2} - C_{H_2}\right] \tag{20}$$

3) Sale of all electricity to the grid. Without H_2 and O_2 production.

$$\text{Profit} = \text{total produced power(kWh)} \times p_{\text{elect}} \tag{21}$$

The selling price for green hydrogen may vary between 3 to 8 €/kg [115]. For all calculations, hydrogen selling price (p_{H_2}) is taken to be 8 €/kg.

Scenario 1

For the alkaline case, selling hydrogen and oxygen shows to be more profitable than selling hydrogen only. The hydrogen profits decrease as the specific hydrogen costs increase, and the hydrogen profits start to turn negative as the costs approach p_{H_2}.

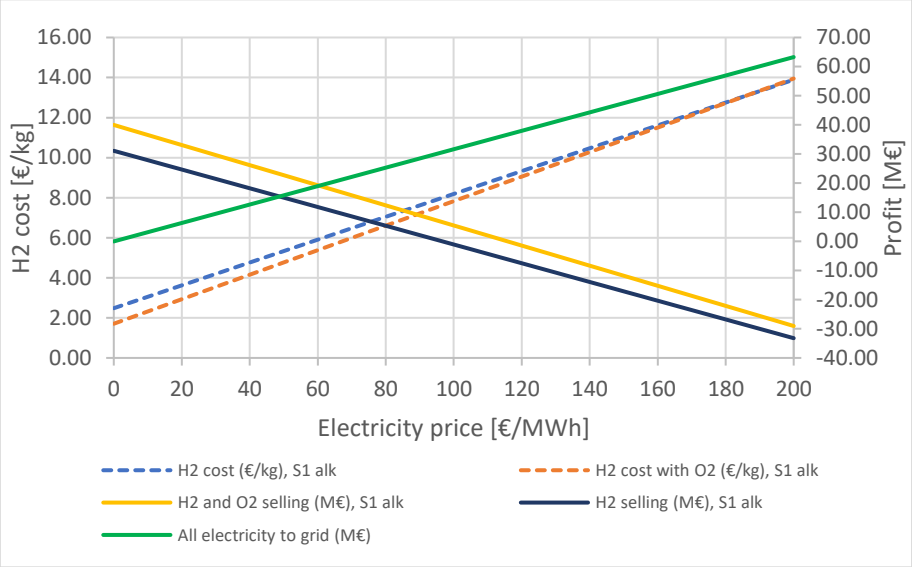

Figure 40 - Profits and specific costs of hydrogen production, scenario 1: alkaline case.

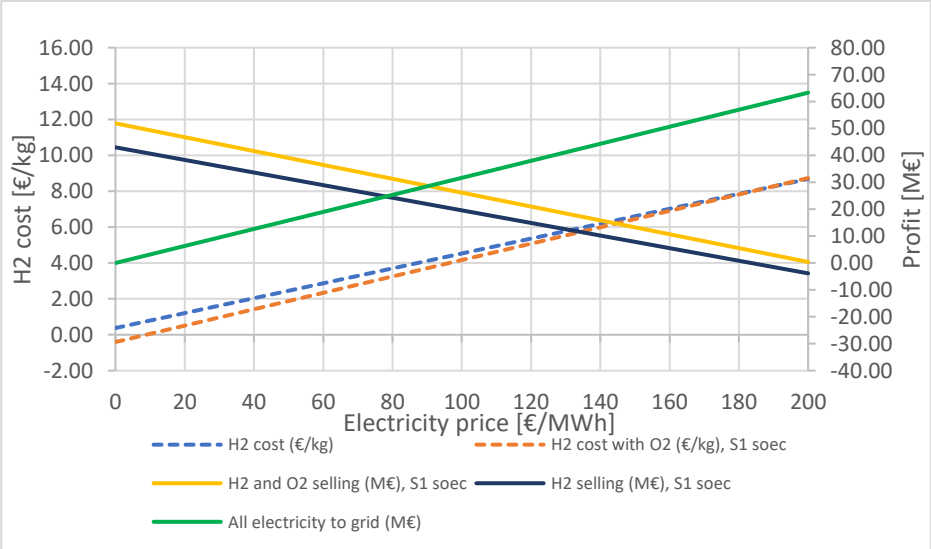

Figure 41 - Profits and specific costs of hydrogen production, scenario 1: SOEC case.

On the other hand, selling all electricity is more profitable than selling H_2 only, when the electricity price is above 50 €/MWh and more profitable than selling H_2 and O_2 when the electricity price is above 60 €/MWh.

For the SOEC case, the trends are similar to the alkaline case. But in this case, selling all electricity is more profitable than selling H_2 only when the electricity price is above approximately 80 €/MWh and more profitable than selling H_2 and O_2 when the electricity price is above 90 €/MWh.

Scenario 2

In scenario 2, the profit increase together with the electricity prices because the production costs are decreasing since the electricity selling of the remaining two-thirds of the total electricity is discounted in the hydrogen production costs.

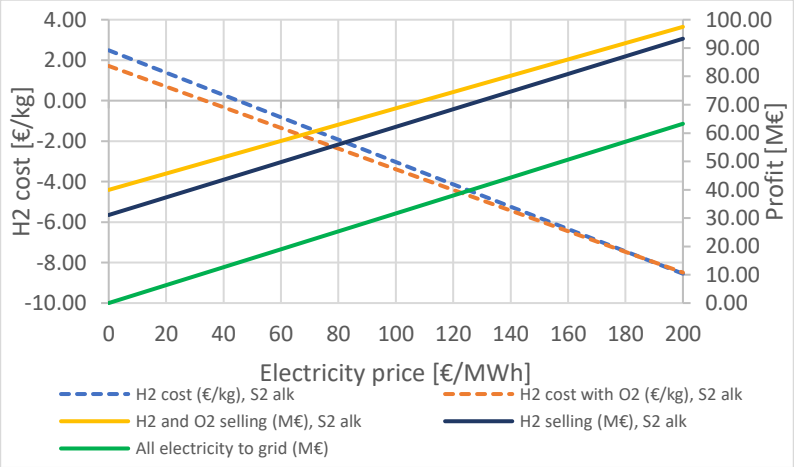

Figure 42 - Profits and specific costs of hydrogen production, scenario 1: alkaline case

In scenario 2, it is always more advantageous to produce and sell either H_2 only, or H_2 and O_2, than to sell all electricity to the grid. In general, scenario 2, shows higher profitability than scenario 1.

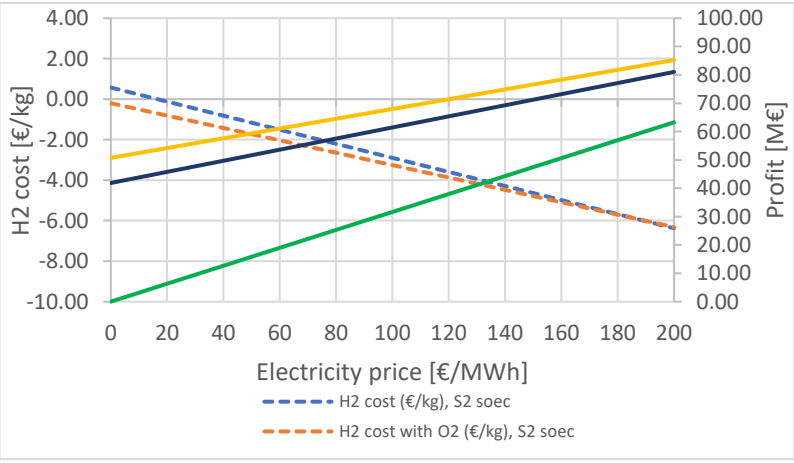

Figure 43 - Profits and specific costs of hydrogen production, scenario 2: SOEC case

Comparison of Profits

The graphs of the profits point that scenario 2 leads to the most profitable results. In this scenario, Selling H_2 and O_2 from SOEC is most profitable when the electricity price is below 100 €/MWh; beyond this price, it is more profitable to sell H_2 and O_2 from alkaline electrolysis. Selling H_2 only is also more profitable than in scenario 1.

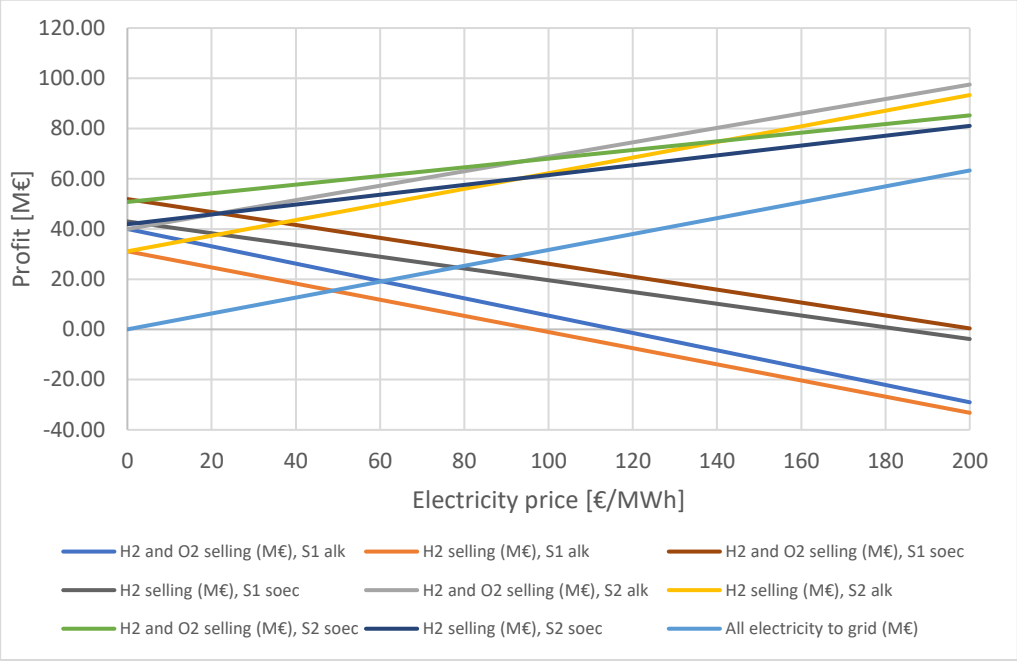

Figure 44 - Comparison of Profits between the two scenarios.

Nonetheless, when the electricity price is absolutely zero, selling H_2 and O_2 from SOEC in either scenario is equally the most profitable, however, profitability in scenario 1 will have a decreasing trend as electricity prices increase.

6.3. Economic Feasibility of the Project

To Analyse the economic feasibility of the H_2 production at CTRSU, the following economic and financial indicators are considered: Levelised cost of H_2 (LCOH), Net Present Value (NPV), and the Internal Rate of Return (IRR).

- **LCOH** measures the average net present cost of hydrogen production over the lifetime of the generating plant. It can be estimated with the formula in equation (22).

$$\mathrm{LCOH}[€/\mathrm{kg}] = \frac{\alpha \times \mathrm{CAPEX_{Total}} + \mathrm{OPEX_{Total}}}{\mathrm{H_2\ rate} \times \mathrm{h_a}} + \mathrm{C_{H_2}} \quad (22)$$

Where,

$$\alpha = \frac{r(1+r)^n}{(1+r)^n - 1} \tag{23}$$

For calculating the LCOH H_2 rate is the hydrogen production rate of the electrolyser system $[kg/h]$. while r the discount rate $[\%]$, and n the estimated hydrogen plant lifetime $[years]$, taken to be 10% and 20 years respectively for all calculations.

The project would be considered economically feasible when $LCOH \geq p_{H_2}$

- **NPV** is used to analyse the profitability of a project. Being defined as the difference between the discounted incomes and the discounted outcomes, called the cash flow over the lifetime of the project.

$$NPV[€] = \frac{CF}{\alpha} - CAPEX_{Total} \tag{24}$$

Where CF stands for cash-flow and $CAPEX_{Total}$ is the total investment in year zero.

In Portugal, the corporate tax, called IRC (Imposto sobre o Rendimento de Pessoas Coletivas) is 21% [17]. This tax is imposed on companies over their profits. This is amount is deducted from the cash-flow for the relevant calculations of NPV.

When $NPV > 0$, the project is considered economically profitable, the investment is recovered, the minimum rate of return of capital is achieved and a surplus is achieved.

When $NPV = 0$, the project is feasible, the investment is recovered and the minimum rate of return of capital is achieved.

When $NPWhen\ NPV < 0$, the project is not economically profitable.

- **IRR** is the discount rate that turns the NPV equal to zero. It also shows the real rate of return of the project. A project is considered profitable if IRR is higher than the discount of the initial rate, r.

$$IRR^{(k+1)} = \frac{CF}{CAPEX_{Total}} \times \frac{\left(1 + IRR^{(k)}\right)^n - 1}{(1 + IRR^{(k)})^n} \tag{25}$$

LCOH

Scenario 1

As expected, the LCOH results follow a similar trend to the production costs per unit of H_2, with a growing trend together with the increase of electricity prices. For the alkaline case, the LCOH reaches the selling price of hydrogen (8 €/kg) when electricity is around 80 €/MWh, while this interception happens for the SOEC case when the electricity price is approximately 135 €/MWh.

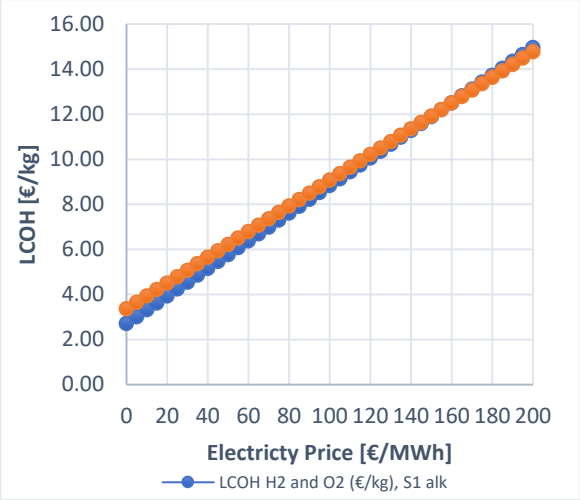

Figure a) Alkaline

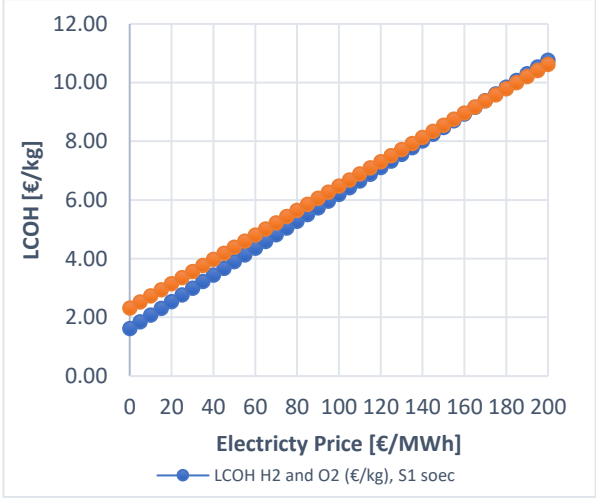

Figure b) SOEC

Figure 45 – LCOH scenario 1: a) alkaline case; b) SOEC case

Scenario 2

In scenario 2, LCOH is expectedly decreasing as electricity prices increase. In both technology cases, LCOH is always lower than the hydrogen selling price (Figure 46), meaning the project would always be feasible.

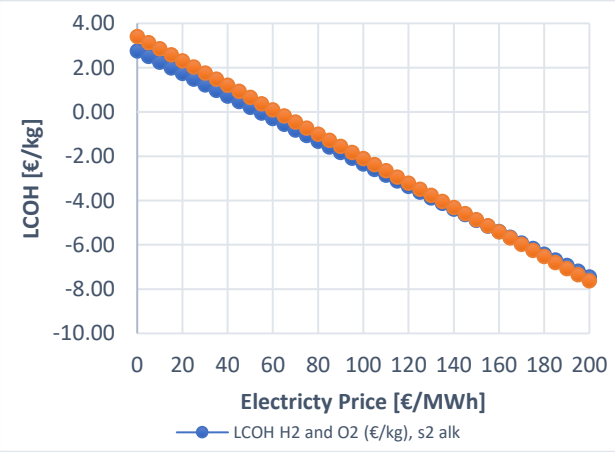

Figure a) Alkaline

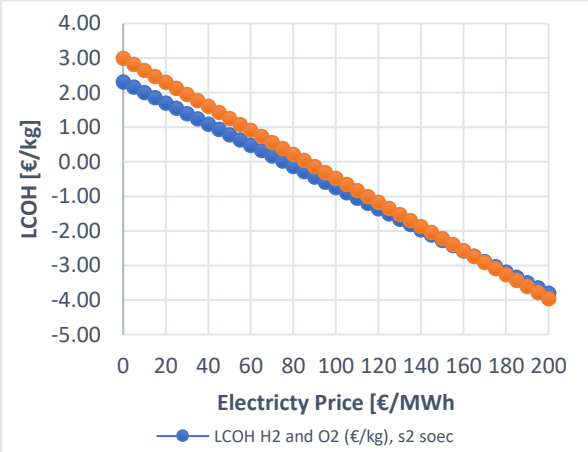

Figure b) SOEC

Figure 46 – LCOH scenario 2: a) alkaline case; b) SOEC case.

LCOH: Scenario 1 vs Scenario 2

Figure 47 demonstrates that scenario 2 has the cheapest options, and all below the selling price of hydrogen. This implies that the average cost of producing hydrogen can be recovered.

In scenario 1, for alkaline technology, the project would be feasible only when the electricity price is lower than approximately 80 €/MWh, while SOEC remains feasible up to roughly 135 €/MWh.

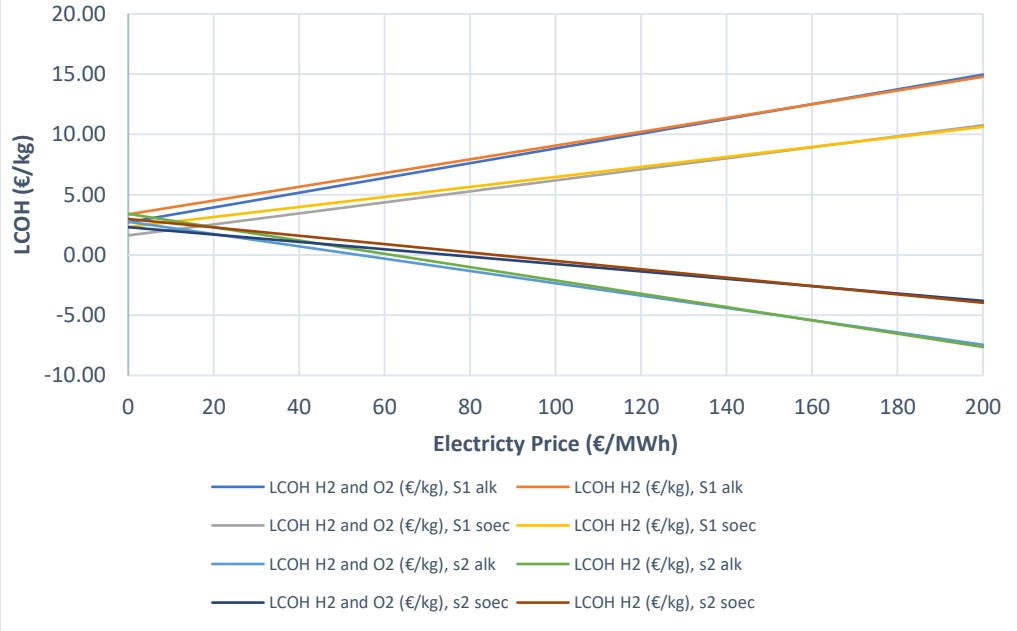

Figure 47 – LCOH curves from all scenarios and cases.

Nevertheless, in any case, LCOH with H_2 and O_2 is always slightly cheaper than solely producing H_2.

NPV

Scenario 1

Figure 48 shows that NPV has a downward trend. The project can be considered economically feasible at the points where NPV has a positive value. It is expected that NPV turn negative as it approximates the point where LCOH becomes lower than the hydrogen selling price. This can be observed in Figure 48.

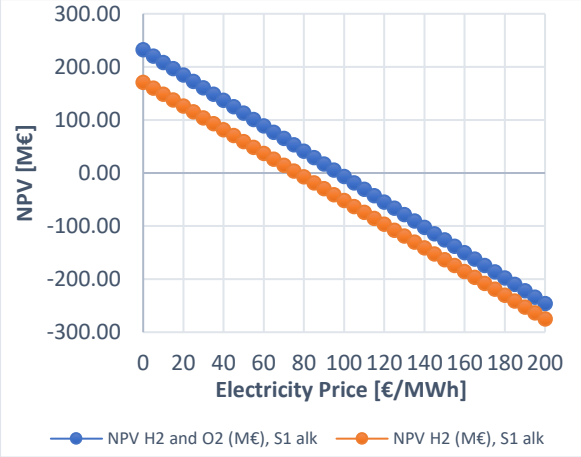

Figure a) Alkaline

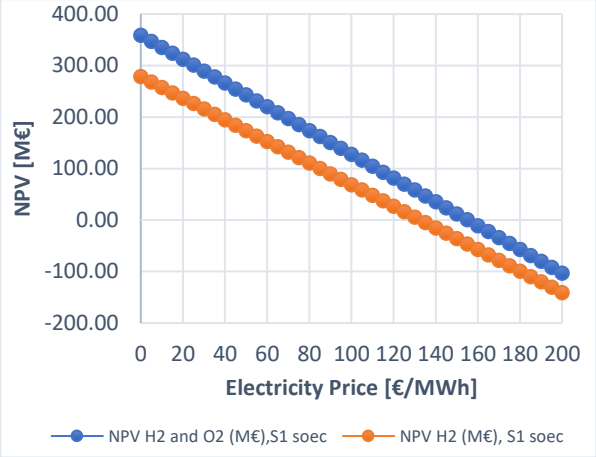

Figure b) SOEC

Figure 48 – NPV scenario 1: a) alkaline case; b) SOEC case.

Scenario 2

Since NPV would turn negative at the point where LCOH is becoming lower than the hydrogen selling price, and scenario 2 of shows that LCOH is always lower than the hydrogen selling price, it is, therefore, coherent that the project will always be profitable as shown in Figure 49.

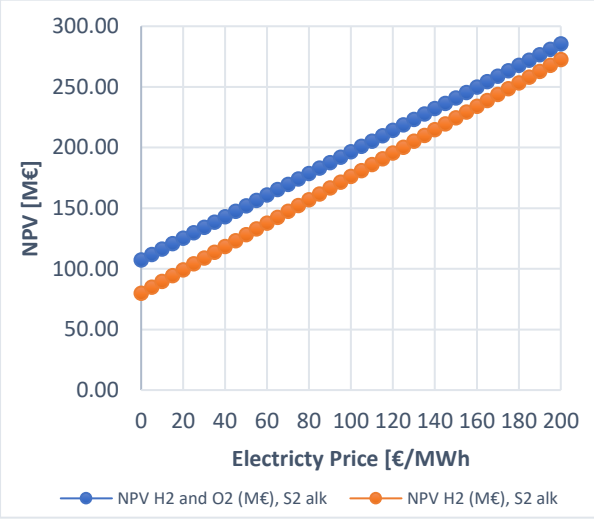

Figure a) Alkaline

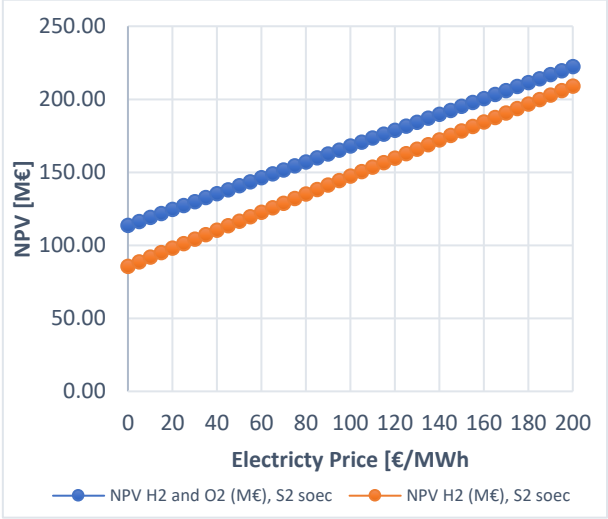

Figure b) SOEC

Figure 49 - NPV scenario 2: a) alkaline case; b) SOEC case.

NPV: Scenario 1 vs Scenario 2

As estimated by the LCOH, Figure 50 indicates that all cases in scenario 2 are always economically profitable since their curves remain increasingly positive along all electricity prices. Alkaline technology produces more profitability in this scenario, followed by SOEC.

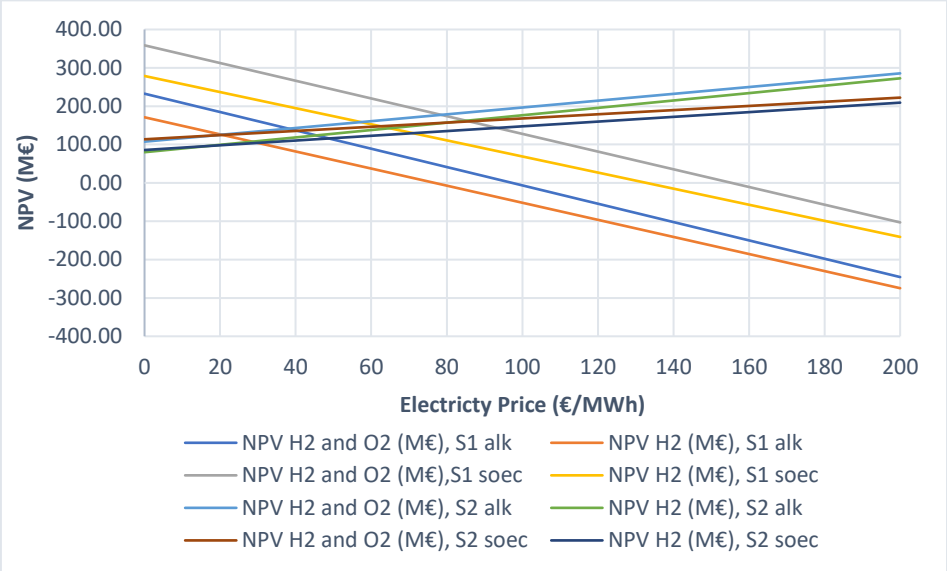

Figure 50 – NPV from all scenarios and cases.

Nevertheless, scenario 1 is the most profitable option when the electricity price is at least up to 20 €/MWh, where selling H_2 only from alkaline stops being profitable, being overtaken by SOEC from scenario 2.

Selling H_2 and O_2 from alkaline of scenario, 1 will be profitable until the electricity price is below 40 €/MWh, after this price both cases from scenario 2 become more profitable.

Utilising SOEC for producing and selling H_2 only is profitable until the electricity price is below 60 €/MWh, beyond this point, all cases in scenario 2 become more profitable. While producing and selling H_2 and O_2 from SOEC in the scenario is profitable until 80 €/MWh.

Conclusively, Figure 50 shows that, in all individual cases from both scenarios, producing and selling H_2 and O_2 is always more profitable than H_2 only.

IRR

Scenario 1

The IRR value is close to the initial discount rate, r, as the electricity price is near 80 €/MWh for alkaline. In the SOEC case, IRR is close to r near 110 €/MWh for H_2 selling option, while for H_2 and O_2 selling, it occurs when the price is close to 135 €/MWh.

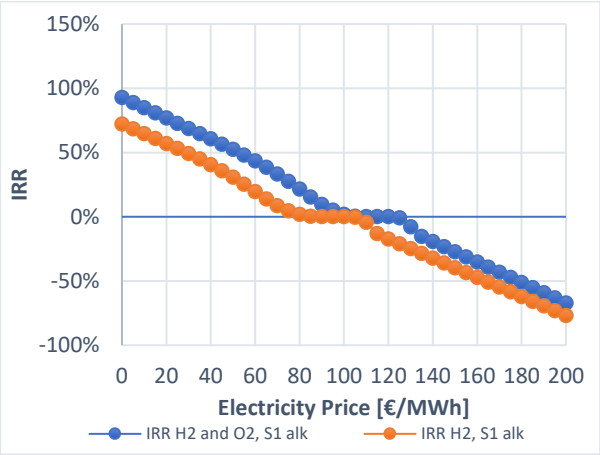

Figure a) Alkaline

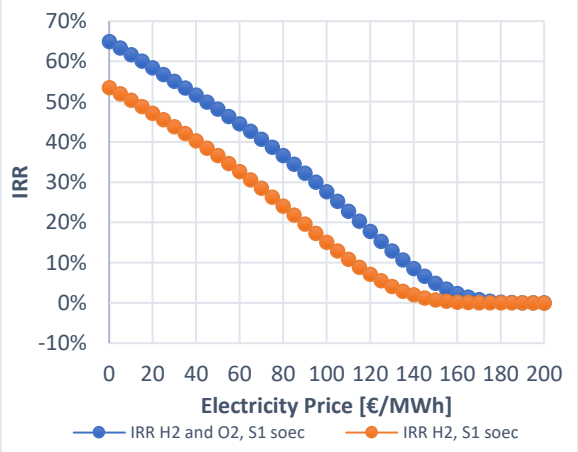

Figure b) Alkaline

Figure 51 – IRR scenario 1: a) alkaline case; b) SOEC case.

Scenario 2

In scenario 2, IRR in both cases is represented by positive growing curves (Figure 52), since the projects become more profitable as the electricity prices increase.

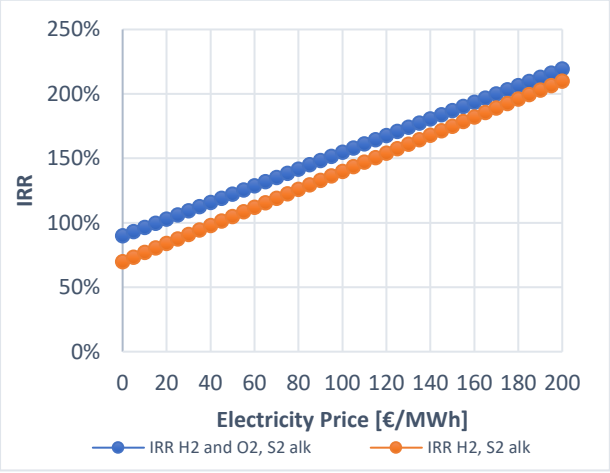

Figure a) Alkaline

Figure b) SOEC

Figure 52 – IRR scenario 2: a) alkaline case; b) SOEC case.

IRR: Scenario 1 vs Scenario 2

Figure 53 shows that alkaline electrolysis technology in scenario 2 gives the two the highest internal return rate, in which selling H_2 and O_2 gives a marginally higher return rate than producing and selling only H_2. Likewise, the SOEC technology case has the two second-highest IRR in scenario 2.

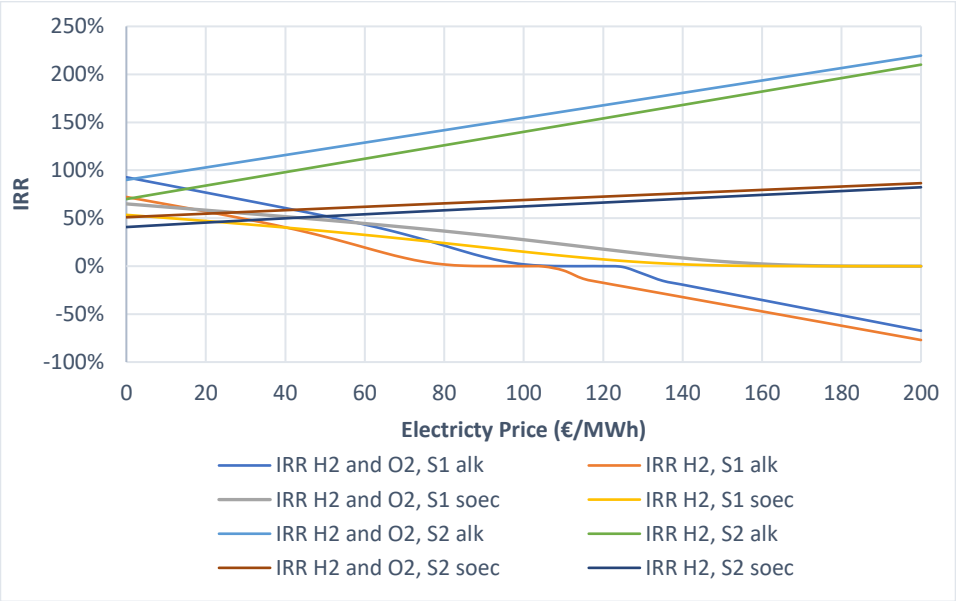

Figure 53 – Comparison of all IRR values.

As expected, in scenario 2, all IRRs are always higher than the initial discount rate, r, ensuring the profitability of the options.

7. Concluding Remarks

Three water electrolysis technologies were studied, namely alkaline water electrolysis, proton exchange membrane (PEM), and solid oxide electrolysis cell (SOEC). Both alkaline and SOEC technologies were studied in the context of the problem proposed due to the maturity of the alkaline technology and the appealing characteristics of the SOEC since steam and electricity are already produced at the CTRSU.

Initially, a literature review of the economic aspects of the technologies was conducted by investigating the CAPEX values currently reported in different bibliographies and their associated costs. Besides CAPEX, the current state of development of the three technologies is also reviewed. In the review, it was found that a CAPEX of 750 €/kW for Alkaline systems is currently achievable for a single stack, 2.13 MW system. While for SOEC, it is estimated to be at 3000 – 5000 €/kW for the year 2020.

Furthermore, the current levels of MSW generated by Portugal residents were found to be stabilising in the last 3 years up to 2020. In Portugal, around 325 GWh of electricity was produced from the conversion of MSW into energy in 2020, meanwhile, CTRSU alone exported about 316 GWh of electricity into the national grid in 2020.

In face of the fluctuation of electricity prices in the MIBEL, the analysis in this work is done taking into account the variation of prices from 0 to 200 €/MWh for two scenarios. In scenario 1, the entire energy produced from the WtE at CTRSU is applied for electrolysis (316.4 GWh and 1,710,959 tonnes of steam) meanwhile in scenario 2, only one-third of the energy produced (105.5 GWh and 570,316,6 tonnes of steam) is used for electrolysis, as the remaining two-thirds is injected into the national grid. Both scenarios are assessed with the alkaline and SOEC technologies. The energy production values for the year 2019 from CTRSU are considered for the calculations since the values of MSW and energy production are regular and unaffected by the pandemic situation. Additionally, oxygen capturing and sales are also introduced into the analysis of hydrogen production.

Specific hydrogen production costs are calculated in both scenarios. Scenario 2 is the cheapest way to produce hydrogen, mostly because the remaining two-thirds of electricity sold into the grid is discounted in the specific production cost of hydrogen.

Producing hydrogen in scenario 1 is more profitable than selling all the electricity to the grid when the electricity price is lower than 90 €/MWh. However, producing hydrogen in scenario 2 is always

more profitable than selling all electricity to the grid. Furthermore, applying the LCOH calculations, it is perceived that scenario 2 is generally the cheapest in average cost and is always feasible despite the electricity prices, assuming a hydrogen selling price of 8 €/kg.

On the other hand, NPV curves point out that scenario 1 is the most profitable option when the electricity price is at least below 20 €/MWh. SOEC for hydrogen with oxygen capture in scenario 1 can be the most profitable option when the electricity price is zero, but the profit level drop rather quickly as the electricity price rises, becoming less profitable than alkaline for hydrogen with oxygen capture in scenario 2 at 80 €/MWh. From 90 €/MWh onwards is more profitable to apply any case of scenario 2 than any case from scenario 1.

In the IRR analysis, it is evident that scenario 2 has a higher rate of return than the discount rate ($r = 10\%$) along all electricity prices. In this scenario, alkaline technology always has a higher return rate than SOEC. Scenario 1 produces a decreasing rate of return, making the project only when electricity prices are considerably low.

Overall, the results indicate that converting one-third of the total electricity into hydrogen gives the lowest production costs since these costs are reduced and profits per kg of hydrogen are increased through the selling of the remaining fraction of the electricity. Alternatively, when the electricity price is close to zero, it is more convenient to convert all the energy into hydrogen.

Finally, it was observed that in all cases and scenarios, the LCOH decreases and NPV for hydrogen is increased as an oxygen capturing option is included. However, this fact may not be realistic if the oxygen end-use application site is out of reach of the plant location since other economic factors would need to be considered, such as bigger storage capacity, transportation and/or distribution systems.

7.1. Remarks for the Future

First of all, it is important to state that the results obtained in this study require a careful evaluation of the company Valorsul, responsible for the WtE plant with energy recovery at CTRSU, which is the entity that proposed the current topic in analysis. Due to the time constraints imposed for this study and the respective presentation of the report with results, it was not possible to carry out the necessary evaluation and subsequent validation with Valorsul. This step remains an open remark to be achieved in near future.

Additionally, the next few points can also be considered to enrich the current study:

- Apply a sensibility study to the economic feasibility by considering different discount rate values, and varying the operating hours of the hydrogen plant as well as the hydrogen selling prices.
- Assess more in-depth the hydrogen market in Portugal to understand the current or potential demand and selling prices
- Analyse more deeply the storage options, their costs and potential implications in the final results.
- Study other promising and commercially available water electrolysis technologies such as PEM.

References

[1] S. Kaza, L. Yao, P. Bhada-Tata and F. Van Woerden, What a Waste 2.0: A Global Snapshot of Solid Waste Management to 2050, Washington, DC: World Bank Group, 2018.

[2] V. Garcilasso, M. Dos Santos and L. Caio, Tecnologias de produção e uso de biogás e biometano: Part. I Biogás; Part. II Biometano, São Paulo: IEE-USP, Brasil, 2018.

[3] C. Mukherjee, J. Denney, E. Mbonimpa, J. Slagley and R. Bhowmik, "A review on municipal solid waste-to-energy trends in the USA," *Renewable and Sustainable Energy Reviews,* vol. 119, p. 109512, 2020.

[4] K. Moustakas, M. Rehan, M. Loizidou, A. Nizami and M. Naqvi, "Energy and resource recovery through integrated sustainable waste management," *Applied Energy,* vol. 261, p. 114372, 2020.

[5] V. A. F. de Campos, V. B. Silva, J. S. Cardoso, P. S. Brito, C. E. Tuna and J. L. Silveira, "A review of waste management in Brazil and Portugal: Waste-to-energy as pathway for sustainable development," *Renewable Energy,* vol. 178, pp. 802-820, 2021.

[6] UNEP, Global Waste Management Outlook, 2015.

[7] European Parliament, "DIRECTIVE 2010/75/EU OF THE EUROPEAN PARLIAMENT AND OF THE COUNCIL of 24 November 2010 on industrial emissions (integrated pollution prevention and control)," Council of the European Union, Brussels, 2010.

[8] European Commission, "European Commission: Environment," [Online]. Available: https://environment.ec.europa.eu/topics/waste-and-recycling/waste-framework-directive_en. [Accessed 17 July 2022].

[9] N. Scarlat, F. Fahl and J.-F. Dallemand, "Status and Opportunities for Energy Recovery from Municipal Solid Waste in Europe," *Waste and Biomass Valorization,* vol. 10, p. 2425–2444, 2019.

[10] M. Margallo, R. Aldaco, A. Irabien, V. Carrillo, M. Fischer, B. A. and F. P., "Life cycle assessment modelling of waste-to-energy incineration in Spain and Portugal," *Waste Management & Research,* vol. 32, no. 6, pp. 492-499, 2014.

[11] S. Xará, M. F. Almeida and C. Costa, "ENERGY FROM WASTE IN PORTUGAL: the state of the

art," 2008.

[12] APA, "WASTE: MUNICIPAL WASTE PRODUCTION AND MANAGEMENT," 2021. [Online]. Available: https://rea.apambiente.pt/content/municipal-waste-production-and-management?language=en. [Accessed 17 July 2020].

[13] IEA, "Renewables," International Energy Agency, 2021. [Online]. Available: https://www.iea.org/fuels-and-technologies/renewables. [Accessed 17 July 2020].

[14] EDP, "Mibel: how does iberic energy market works?," [Online]. Available: https://www.edp.com/en/edp-stories/mibel-how-does-iberic-energy-market-works. [Accessed 17 July 2020].

[15] MIBEL, "Market today," 2022. [Online]. Available: https://www.omip.pt/en/plazo-hoy. [Accessed 17 July 2022].

[16] M. Aneke and M. Wang, "Energy storage technologies and real life applications – A state of the art review," *Applied Energy,* vol. 179, pp. 350-377, 2016.

[17] T. R. Lucas, A. F. Ferreira and R. S. Pereira, "Hydrogen production from the WindFloat Atlantic offshore wind farm: A techno-economic analysis," 2021.

[18] International Energy Agency, "Technology Roadmap - Hydrogen and Fuel Cells," 2015.

[19] U.S. Department of Energy, "Office of Energy Efficiency & Renewable Energy," [Online]. Available: https://www.energy.gov/eere/fuelcells/h2scale. [Accessed 17 August 2021].

[20] A. Godula-Jopek, Hydrogen Production: by Electrolysis, Berlin: John Wiley & Sons, Incorporated, 2015.

[21] M. Lappalainen, "Techno-economic feasibility of hydrogen production via polymer membrane electrolyte electrolysis for future Power-to-X systems," Tampere, Finland, 2019.

[22] Ordin and P. M., "Safety Standard for Hydrogen and Hydrogen Systems: Guidelines for Hydrogen System Design, Materials Selection, Operations, Storage and Transportation," Office of Safety and Mission Assurance, NASA, Washington, DC, 1997.

[23] SHELL, "SHELL HYDROGEN STUDY," Shell Deutschland Oil GmbH, Hamburg, 2017.

[24] A. Keçebaş, M. Kayfeci and M. Bayat, "Electrochemical hydrogen generation," in *Solar*

Hydrogen Production: Processes, Systems and Technologies, Elsevier Inc., 2019, pp. 299-317.

[25] EERE, "HYDROGEN AND FUEL CELL TECHNOLOGIES OFFICE," Office of ENERGY EFFICIENCY & RENEWABLE ENERGY, [Online]. Available: https://www.energy.gov/eere/fuelcells/hydrogen-production-electrolysis. [Accessed 8 May 2022].

[26] C. Hussy, PtX Hub, 2022. [Online]. Available: https://ptx-hub.org/water-electrolysis-explained/. [Accessed 8 May 2022].

[27] E. Zoulias, E. Varkaraki, N. Lymberopoulos, C. Christodoulou and G. Karagiorgis, "A REVIEW ON WATER ELECTROLYSIS," *TCJST,* vol. 4, pp. 41-71, January 2004.

[28] J. Chi and H. Yu, "Water electrolysis based on renewable energy for hydrogen production," *Chinese Journal of Catalysis,* vol. 39, no. 3, pp. 390-394, 2018.

[29] Y. Guo, G. Li, J. Zhou and Y. Liu, "Comparison between hydrogen production by alkaline water electrolysis and hydrogen production by PEM electrolysis," *IOP Conference Series: Earth and Environmental Science,* vol. 371, no. 4, 2019.

[30] G. Gahleitner, "Hydrogen from renewable electricity: An international review of power-to-gas pilot plants for stationary applications," *International Journal of Hydrogen Energy,* vol. 38, no. 5, pp. 2039-2061, 2013.

[31] A. Đukić and M. Firak, "Hydrogen production using alkaline electrolyzer and photovoltaic (PV) module," *International Journal of Hydrogen Energy,* vol. 36, no. 13, pp. 7799-7806, 2011.

[32] J. Brauns and T. Turek, "Alkaline Water Electrolysis Powered by Renewable," *processes,* vol. 8, no. 2, p. 248, 2020.

[33] R. L. LeRoy, C. T. Bowen and D. J. LeRoy, "The Thermodynamics of Aqueous Water Electrolysis," *Journal of The Electrochemical Society,* vol. 127, no. 9, p. 1954, 1980.

[34] P. Haug, M. Koj and T. Turek, "Influence of process conditions on gas purity in alkaline water electrolysis," *International Journal of Hydrogen Energy,* vol. 42, no. 15, pp. 9406-9418, 2017.

[35] P. Haug, B. Kreitz, M. Koj and T. Turek, "Process modelling of an alkaline water electrolyzer," *International Journal of Hydrogen Energy,* vol. 42, no. 24, pp. 15689-15707, 2017.

[36] S. Grigoriev, V. Porembsky and V. Fateev, "Pure hydrogen production by PEM electrolysis for

hydrogen energy," *International Journal of Hydrogen Energy,* vol. 31, no. 2, pp. 171-175, 2006.

[37] M. Carmo, D. L. Fritz, J. Mergel and D. Stolten, "A comprehensive review on PEM water electrolysis," *International Journal of Hydrogen Energy,* vol. 38, no. 12, pp. 4901-4934, 2013.

[38] A. Ursua, L. M. Gandia and P. Sanchis, "Hydrogen Production From Water Electrolysis: Current Status and Future Trends," *Proceedings of the IEEE,* vol. 100, no. 2, pp. 410 - 426, 2012.

[39] S. Grigoriev, V. Porembsky and V. Fateev, "Pure hydrogen production by PEM electrolysis for hydrogen energy," *International Journal of Hydrogen Energy,* vol. 31, no. 2, pp. 171-175, 2006.

[40] M. Seitz, H. von Storch, A. Nechache and D. Bauer, "Techno economic design of a solid oxide electrolysis system with solar thermal steam supply and thermal energy storage for the generation of renewable hydrogen," *International Journal of Hydrogen Energy,* vol. 42, no. 42, pp. 26192-26202, 2017.

[41] A. Nechache and S. Hody, "Alternative and innovative solid oxide electrolysis cell materials: A short review," *Renewable and Sustainable Energy,* vol. 149, p. 111322, 2021.

[42] L. Bi, S. Boulfrad and E. Traversa, "Steam electrolysis by solid oxide electrolysis cells (SOECs) with proton-conducting oxides," *Chemical Society Reviews,* vol. 43, no. 24, pp. 8255-8270, 2014.

[43] H. Safaei and M. J. Aziz, "Thermodynamic Analysis of Three Compressed Air Energy Storage Systems: Conventional, Adiabatic, and Hydrogen-Fueled," *Energies,* vol. 10, no. 7, p. 1020, 2017.

[44] A. Kade, "ILK Dresden," [Online]. Available: https://www.ilkdresden.de/en/project/hydrogen-test-area-at-ilk-dresden/.

[45] S. Niaz, T. Manzoor and A. H. Pandith, "Hydrogen storage: Materials, methods and perspectives," *Renewable and Sustainable Energy Reviews,* vol. 50, pp. 457-469, 2015.

[46] J. Andersson and S. Grönkvist, "Large-scale storage of hydrogen," *International Journal of Hydrogen Energy,* vol. 44, no. 23, pp. 11901-11919, 2019.

[47] V. Tietze, S. Luhr and D. Stolten, "Bulk Storage Vessels for Compressed and Liquid Hydrogen," in *Hydrogen Science and Engineering : Materials, Processes, Systems and Technology*, 2016, pp. 659-690.

[48] H. Barthelemy, M. Weber and F. Barbier, “Hydrogen storage: recent improvements and industrial perspectives,” *International Journal of Hydrogen Energy,* vol. 42, no. 11, pp. 7254-7262, 2017.

[49] F. Crotogino, “Larger Scale Hydrogen Storage,” in *Storing Energy: With Special Reference to Renewable Energy Sources*, 2016, pp. 411-429.

[50] E. Wolf, “Large-scale hydrogen energy storage,” in *Electrochemical Energy Storage for Renewable Sources and Grid Balancing*, 2015, pp. 129-142.

[51] A. Witkowski, A. Rusin, M. Majkut and K. Stolecka, “Comprehensive analysis of hydrogen compression and pipeline transportation from thermodynamics and safety aspects,” *Energy,* vol. 141, pp. 2508-2518, 2015.

[52] T. Q. Hua and R. K. Ahluwalia, “Alane hydrogen storage for automotive fuel cells – Off-board regeneration processes and efficiencies,” *International Journal of Hydrogen Energy,* vol. 36, no. 23, pp. 15259-15265, 2011.

[53] S. Satyapal, J. Petrovic, C. Read, G. Thomas and G. Ordaz, “The U.S. Department of Energy's National Hydrogen Storage Project: Progress towards meeting hydrogen-powered vehicle requirements,” *Catalysis Today,* vol. 120, no. 3-4, pp. 246-256, 2007.

[54] Y. Li and R. T. Yang, “Significantly Enhanced Hydrogen Storage in Metal−Organic Frameworks via Spillover,” *Journal of the American Chemical Society,* vol. 128, no. 3, p. 726–727, 2006.

[55] A. Godula-Jopek, W. Jehle and J. Wellnitz, “Storage of pure hydrogen in different states,” *Hydrogen storage technologies,* pp. 97 - 170, 2012.

[56] U. Cardella, L. Decker and H. Klein, “Roadmap to economically viable hydrogen liquefaction,” *International Journal of Hydrogen Energy,* vol. 42, no. 19, pp. 13329-13338, 2017.

[57] G. Valenti, “Hydrogen liquefaction and liquid hydrogen storage,” in *Compendium of Hydrogen Energy*, 2016, pp. 27-51.

[58] A. Kuendig, K. Loehlein, G. Kramer and J. Huijsmans, “Large scale hydrogen liquefaction in combination with LNG re-gasification,” in *16th world hydrogen energy conference*, 2006.

[59] M. Hirscher and K. Hirose, Handbook of Hydrogen Storage: New Materials for Future Energy Storage, Weinheim Wiley-VCH-Verl, 2010.

[60] Á. Berenguer-Murcia and J. P. C.-A. D. Marco-Lozar, “Hydrogen Storage in Porous Materials: Status, Milestones, and Challenges,” *The Chemical Record,* vol. 18, no. 7-8, pp. 900-912, 2018.

[61] L. O. K. Klebanoff, L. Simpson, K. O’Malley and N. Stetson, “Accelerating the Understanding and Development of Hydrogen Storage Materials: A Review of the Five-Year Efforts of the Three DOE Hydrogen Storage Materials Centers of Excellence,” *Metallurgical and Materials Transactions E,* vol. 1, pp. 81-117, 2014.

[62] L. Blankenship and R. Mokaya, “Cigarette butt-derived carbons have ultra-high surface area and unprecedented hydrogen storage capacity,” *Energy & Environmental Science,* vol. 10, pp. 2552-2562, 2017.

[63] P. García-Holley, B. Schweitzer, T. Islamoglu, Y. Liu, L. Lin, S. Rodriguez, M. Weston, J. Hupp, D. Gómez-Gualdrón, T. Yildirim and O. Farha, “Benchmark study of hydrogen storage in metal–organic frameworks under temperature and pressure swing conditions,” *ACS Energy Letters,* vol. 3, no. 3, pp. 748-754, 2018.

[64] B. Sakintuna, F. Lamari-Darkrim and M. Hirscher, “Metal hydride materials for solid hydrogen storage: a review,” *International Journal of Hydrogen Energy,* vol. 32, no. 9, pp. 1121-1140, 2007.

[65] J. Von Colbe, J. Ares, J. Barale, M. Baricco, C. Buckley, G. Capurso, N. Gallandat, D. Grant, M. Guzik, I. Jacob and E. Jensen, “Application of hydrides in hydrogen storage and compression: Achievements, outlook and perspectives,” *International Journal of Hydrogen Energy,* vol. 44, no. 15, pp. 7780-7808, 2019.

[66] J. Proost, “State-of-the art CAPEX data for water electrolysers, and their impact on renewable hydrogen price settings,” *International Journal of Hydrogen Energy,* vol. 44, no. 9, pp. 4406-4413, 2019.

[67] E. Anderson, “MW Electrolysis Scale Up,” in *DOE Electrolytic Hydrogen Production Workshop*, Golden, CO, 2014.

[68] ISPT, “Gigawatt green hydrogen plant: State-of-the-art design and total installed capital costs,” Institute for Sustainable Process Technology , Amersfoort, Netherlands, 2020.

[69] O. Schmidt, A. Gambhir, I. Staffell, A. Staffell, J. Nelson and S. Few, “Future cost and performance of water electrolysis: An expert elicitation study,” *International Journal of*

Hydrogen Energy, vol. 42, no. 52, pp. 30470-30492, 2017.

[70] M. G. McKellar, E. A. Harvego and A. M. Gandrik, "System Evaluation and Economic Analysis of a HTGR Powered High-Temperature Electrolysis Hydrogen Production Plant," Prague, Czech Republic, 2010.

[71] R. Navarro, R. Guil and J. Fierro, "Introduction to hydrogen production," in *Compendium of Hydrogen Energy: Hydrogen Production and Purification*, V. Subramani, A. Basile and T. N. Veziroğlu, Eds., Woodhead Publishing, 2015, pp. 21-61.

[72] P. Millet and S. Grigoriev, "Chapter 2 - Water Electrolysis Technologies," in *Renewable Hydrogen Technologies: Production, Purification, Storage, Applications and Safety*, L. M. Gandía, G. Arzamendi and P. M. Diéguez, Eds., Elsevier Science, 2013, pp. 19-41.

[73] A. Rahim, A. S. Tijani and S. H. S. Kamarudin, "An overview of polymer electrolyte membrane electrolyzer for hydrogen production: Modeling and mass transport," *Journal of Power Sources,* vol. 309, pp. 56-65, 2016.

[74] C. N. C. Hitam and A. A. Jalil, "A review on biohydrogen production through photo-fermentation of lignocellulosic biomass," *Biomass Conversion and Biorefinery,* 2020.

[75] Y. Ying and S. M. M. Kamarudin, "Silica-related membranes in fuel cell applications: An overview," *International Journal of Hydrogen Energy,* vol. 43, no. 33, pp. 16068-16084, 2018.

[76] X. Sun, S. C. Simonsen, T. Norby and A. Chatzitakis, "Composite Membranes for High Temperature PEM Fuel Cells and Electrolysers: A Critical Review," *Membranes,* vol. 6, no. 7, p. 83, 2019.

[77] Y. Zhang, A. Lundblad, P. E. Campana and J. Yan, "Comparative study of battery storage and hydrogen storage to increase photovoltaic self-sufficiency in a residential building of Sweden," *Energy Procedia,* vol. 103, pp. 268-273, 2016.

[78] E. Fabbri, A. Habereder, K. Waltar, R. Kötz and T. J. Schmidt, "Developments and perspectives of oxide-based catalysts for the oxygen evolution reaction," *Catalysis Science & Technology,* vol. 4, p. 3800–3821, 2014.

[79] K. E. Ayers, E. B. Anderson, C. Capuano, B. Carter, L. Dalton, G. Hanlon, J. Manco and M. Niedzwiecki, "Research Advances towards Low Cost, High Efficiency PEM Electrolysis," *The*

Electrochemical Society, vol. 33, no. 1, 2010.

[80] N. Danilovic, K. E. Ayers, C. Capuano, J. N. Renner, L. Wiles and M. Pertoso, "Challenges in Going from Laboratory to Megawatt Scale PEM Electrolysis," *The Electrochemical Society,* vol. 75, no. 14, 2016.

[81] R. Maric and H. Yu, "Proton Exchange Membrane Water Electrolysis as a Promising Technology for Hydrogen Production and Energy Storage," 2018.

[82] O. Posdziech, K. Schwarze and J. Brabandt, "Efficient hydrogen production for industry and electricity storage via high-temperature electrolysis," *International Journal of Hydrogen Energy,* vol. 44, no. 35, pp. 19089-19101, 2019.

[83] F. R. Bianchi and B. Bosio, "Operating Principles, Performance and Technology Readiness Level of Reversible Solid Oxide Cells," *Sustainability,* vol. 13, no. 9, p. 4777, 2021.

[84] P. Prabhakaran, D. Giannopoulos, W. Köppel, U. Mukherjee, G. Remesh, F. Graf, D. Trimis, T. Kolb and M. Founti, "Cost optimisation and life cycle analysis of SOEC based Power to Gas systems used for seasonal energy storage in decentral systems," *Journal of Energy Storage,* vol. 26, p. 100987, 2019.

[85] J. Mermelstein, C. Cannova, M. Cruz and B. Anderson, "Field Demonstration of a Novel Reversible SOFC System for Islanded Microgrid Energy Storage," *The Electrochemical Society,* vol. 78, no. 1, p. 2907–2912, 2017.

[86] World Energy Council, "World Energy Resources: Waste to Energy," 2013.

[87] Eurostat, "eurostat Statistics Explained," 10 December 2021. [Online]. Available: https://ec.europa.eu/eurostat/statistics-explained/index.php?title=File:Municipal_waste_treatment,_EU,_1995-2020_(kg_per_capita).png. [Accessed 03 July 2022].

[88] A. Tabasová, J. Kropáč, V. Kermes, A. Nemet and P. Stehlík, "Waste-to-energy technologies: Impact on environment," *Energy,* vol. 44, no. 1, pp. 146-155, 2012.

[89] C. Fushan, S. Haiyan and L. Xiaoping, "Intital analysis on main points of generation projects by municipal wastes in feasibility study," *Kezaisheng Nengyuan/Renewable Energy Resources,* vol. 31, no. 4, pp. 123-128, 2013.

[90] Z. Xin-gang, J. Gui-wu, L. Ang and L. Yun, "Technology, cost, a performance of waste-to-energy incineration industry in China," *Technology, cost, a performance of waste-to-energy incineration industry in China,* vol. 55, pp. 115-130, 2016.

[91] J. Oral, J. Sikula, R. Puchyr, Z. Hajny, P. Stehlik and L. Bebar, "Processing of waste from pulp and paper plant," *Journal of Cleaner Production,* vol. 13, no. 5, pp. 509-515, 2005.

[92] UNEP, "CCET guideline series on intermediate municipal solid waste treatment technologies: Waste-to-Energy Incineration," United Nations Environment Programme, 2020.

[93] Z. Jegla, L. Bébar, M. Pavlas, J. Kropác and P. Stehlík, "Secondary combustion chamber with inbuilt heat transfer area-thermal model for improved waste-to-energy systems modelling," *Chemical Engineering Transactions,* vol. 21, 2010.

[94] S. G. Furtado, F. J. M.-H. dos Santos and R. J. R. Laia, "Análise do sistema de tratamento de efluentes gasosos de," ISEL, Lisbon, 2014.

[95] Valorsul, "A Combustão," Valorsul, 2022. [Online]. Available: http://www.valorsul.pt/pt/seccao/areas-de-negocio/valorizacao-energetica/a-combustao. [Accessed 20 July 2022].

[96] V. S. R. Tavares, J. M. D. J. de Melo and M. d. G. M. Martinho, "Análise de Ciclo de Vida dos RU em Destino Final. Caso de Estudo: Aterros e Incineradoras de Portugal," 2013.

[97] Valorsul, "Relatório e contas 2020," 2021.

[98] IRENA, "Hydrogen from Renewable Power: Technology Outlook for the Energy Transition," 2018.

[99] NEL, "Atmospheric Alkaline Electrolyser," NEL , [Online]. Available: https://nelhydrogen.com/product/atmospheric-alkaline-electrolyser-a-series/. [Accessed 21 July 2022].

[100] NEL, "Green H2 for a Sustainable Integrated Economy," 2020.

[101] NEL, "Renewable Hydrogen from Electrolysis: How do we get to a relevant scale?," 2018.

[102] SUNFIRE, "RENEWABLE HYDROGEN FOR ALL APPLICATIONS: SUNFIRE-HYLINK ALKALINE".

[103] Cummins, "HySTAT®: ALKALINE ELECTROLYZERS," 2021.

[104] National Center for Biotechnology Information, “PubChem Compound Summary for CID 14797, Potassium hydroxide,” 2022.

[105] T. R. Lucas, A. F. Ferreira, B. S. Pereira and M. Alves, “Hydrogen production from the WindFloat Atlantic offshore wind farm: A techno-economic analysis,” *Applied Energy,* vol. 310, p. 118481, 2022.

[106] EPAL, “www.epal.pt,” EPAL, 2022. [Online]. Available: https://www.epal.pt/EPAL/menu/clientes/tarif%C3%A1rio/%C3%A1gua. [Accessed 23 July 2022].

[107] PHARMACOMPASS, “Potassium Hydroxide,” 2016. [Online]. Available: https://www.pharmacompass.com/price/potassium-hydroxide. [Accessed 22 July 2022].

[108] TOPSOE, 2021. [Online]. Available: https://www.topsoe.com/processes/green-hydrogen. [Accessed 23 July 2022].

[109] L. Wang, M. Chen, R. Küngas, T.-E. Lin, S. Diethelm, F. Maréchal and J. Van herle, “Power-to-fuels via solid-oxide electrolyzer: Operating window and techno-economics,” *Renewable and Sustainable Energy Reviews,* vol. 110, pp. 174-187, 2019.

[110] EU, “FUEL CELLS AND HYDROGEN JOINT UNDERTAKING (FCH JU): Multi - Annual Work Plan 2014 - 2020,” 2014.

[111] Sunfire GmbH, “RENEWABLE HYDROGEN FOR INDUSTRIAL APPLICATIONS: SUNFIRE-HYLINK SOEC,” 2021.

[112] C. van Leeuwen and A. Zauner, “Innovative large-scale energy storage technologies and Power-to-Gas concepts after optimisation,” 2018.

[113] [Online]. Available: https://www.alibaba.com/product-detail/30m3-liquid-oxygen-hold-up-vessel_62517830815.html. [Accessed 09 July 2022].

[114] “Universal Industrial Gases, Inc,” [Online]. Available: http://www.uigi.com/o2_conv.html. [Accessed 09 July 2022].

[115] PwC, “The green hydrogen economy: Predicting the decarbonisation agenda of tomorrow,” [Online]. Available: https://www.pwc.com/gx/en/industries/energy-utilities-resources/future-energy/green-hydrogen-cost.html. [Accessed 27 July 2022].

[116] S. M. Saba, M. Müller, M. Robinius and D. Stolten, “The investment costs of electrolysis – A comparison of cost studies from the past 30 years,” *International Journal of Hydrogen Energy,* vol. 43, no. 3, pp. 1209-1223, 2018.

[117] L. Schlapbach and A. Züttel, “Hydrogen-storage materials for mobile applications,” *Materials for Sustainable Energy,* pp. 265-270, 2010.

[118] G. Sandrock, “A panoramic overview of hydrogen storage alloys from a gas reaction point of view,” *Journal of Alloys and Compounds,* vol. 293–295, pp. 877-888, 1999.

[119] G. Liuzzo, N. Verdone and M. Bravi, “The benefits of flue gas recirculation in waste incineration,” *Waste Management,* vol. 27, no. 1, pp. 106-116, 2007.